

©[2011]

Fei Song

ALL RIGHTS RESERVED

Chemical Characterization of Urban Air pollutants in Precipitation, Aerosols and Gas-
Phases in Northeast New Jersey in the US East Coast

by

Fei Song

A Dissertation submitted to the
Graduate School – Newark
Rutgers, The State University of New Jersey
in partial fulfillment of the requirements

for the degree of

Doctor of Philosophy

Graduate Program in

written under the direction of

Professor Yuan Gao

and approved by

Newark, New Jersey

May, 2011

ABSTRACT OF THE DISSERTATION

Chemical Characterization of Urban Air pollutants in Precipitation, Aerosols and Gas-Phases in Northeast New Jersey in the US East Coast

By Fei Song

Dissertation Director:

Dr. Yuan Gao

To chemically characterize urban air pollution in the US east coast, precipitation for water-soluble inorganic/organic ions and trace metals, aerosols for trace metals, and gas-phase samples for NO_x , O_3 and NO_3 were studied in northeast New Jersey metropolitan areas from 2006 to 2008. Precipitation and aerosols were collected by automatic wet-only precipitation collector and MOUDI (Multi-Orifice Uniform Deposit Impactor), respectively, while gaseous pollutants were measured by O_3/NO_x analyzers.

Results showed that sulfate (SO_4^{2-}) and ammonium (NH_4^+) are the most dominant ions controlling the precipitation acidity (pH 3.8 ~ 6.4). Acetate (CH_3COO^-) and formate (HCOO^-) are the major water-soluble organic acid species in the region. The elements Al, Zn and Fe are dominant in the mass of the trace metals measured. Major sources for pollutants in precipitation were identified as: (1) nitrogen-enriched soil, (2) secondary pollution processes, (3) marine sources, (4) incineration, (5) oil combustion, and (6) malonate-vanadium-enriched sources. About half of the precipitation events were characterized by mixed sources.

For the size distributions of aerosol particles collected during this study, the total

aerosol mass showed a typical bimodal distribution with two peaks around 0.32-0.56 μm and 3.2-5.6 μm . Typical crustal trace metals (Fe, Cu, Mn and Sc) had coarse particulate accumulation mode and their enrichment factors showed tilted normal distributions pattern peaking at 1.0-1.8 μm , while the other trace metals had fine particulate accumulation mode and their enrichment factor showed monotonic decline patterns with overwhelmingly high peaks in the size range of 0.18-0.32 μm . Three major traffic related sources for trace metals were identified: (1) brake wear and fuel combustion, (2) primary fuel combustion, and (3) tire abrasion and fuel combustion.

Results from the gas-phase measurements showed significant diurnal and weekday/weekend variations in the O_3 concentrations, with higher concentrations being found during the daytime and on weekends. The 24-h diurnal variations of O_3 and NO_x showed a typical four-periods pattern: (1) morning NO_x peak, (2) mid-day O_3 formation, (3) afternoon NO_x accumulation, and (4) nighttime balancing. NO_x and O_3 showed negative correlations indicating possible VOC-sensitive characteristics while no obvious influence of HNO_3 on O_3 was observed.

ACKNOWLEDGEMENTS

First and foremost, I would like to thank my advisor Dr. Yuan Gao for providing me the opportunity to resume my PhD research and finally complete my PhD thesis at Rutgers University. I will never find the words to thank her for all her contributions of time, ideas, and mentoring and I much regret the fact that I will have little chance to pay her back for all her personal dedications. With her enthusiasm, her inspirations and her great effects to guide me to get everything planed and done in right way and in right time, she helped me to qualify myself for a PhD candidate as much as possible. In every sense, none of my PhD research work would have been possible without her. I am also thankful for the excellent example she has provided as a devoted, loyal, persistent and successful professional.

Many thanks must go to our department graduate director Dr. Alexander Gates and department administrative assistant Ms. Liz Morrin. Dr. Gates has been always very supportive whenever we need him. I could always learn something from him. Each time after talking with him I would usually become more positive. I also appreciate his dedication of his time and knowledge to my PhD research as one of my committee members. Liz is the one who makes my life at Rutgers-Newark much easier and usually the one who first comes to my mind when I need help. I would also like to thank her for her trust and I would not forget the last conversation with her before I temporarily left Rutgers-Newark in 2009.

It is an honor for me to also have Dr. Evert Jan Elzinga (Rutgers - Newark) and Dr. Xiaoguang Meng (Stevens Institute of Technology) as my dissertation committee

members. Thanks for their professional comments and suggestions to improve my work. I really appreciate the time they dedicated from their busy schedules. Their long-term professional experiences, diverse knowledge and humble attitudes made them fantastic committee members for my PhD research.

I would like to thank many people who have taught me the knowledge of Chemistry, Environment Science, Instrumental Analysis, Biology, Geology, Statistics, Programming et al., including Dr. Liping Wei and Dr. Joseph W. Bozzelli at NJIT, Dr. Gary L. Taghon and Dr. Lisa Rodenburg at Rutgers-New Brunswick. I would also like to thank Dr. Andreas Vassiliou, a Rutgers-Newark emeritus professor, who has taught us how to teach undergraduates geology labs.

I want to thank present and past members of our “Air Group” at Rutgers-Newark. I thank Yunliang Zhao, Rafael Jusino-Atresino, Lili Xia, Lu Wang, Christopher Thuman and Dawn Semple for the help with sampling, chemistry determinations, and discussions. Without them, my research work would not be carried out so smoothly and efficiently. It was such a good time staying together with them on the isolated coastal Rutgers Marine Field Station in Tuckerton, NJ, on the roof of Bradley Hall on our campus, at the road side of I95, and in the crowded Rutgers Marine Science ICPMS lab.

I am always very grateful that all faculties and graduate students in the Earth and Environmental Science Department of Rutgers- Newark are so friendly and very helpful all the time. With them, my PhD life has more joys and funs in both teaching and doing research. I am especially grateful to Chi Zhang, Jincai Ma, Sweeta Chauhan, Mehrez Elwaseif, Kisa Mwakanyamale and James Nolan. Special thanks go to Dr. Lee Slater, our

new Graduate program director, who helped creat the department PhD handbook and who is right there ready for any procedure questions.

I received a lot help from other institutions/departments for samplings and chemistry analysis. Here I want to thank Dr. Jinyong Shin and Dr. Francisco Artigas from the New Jersey Meadowlands Commission, Mr. Roland Hagan and Dr. Kenneth W. Able from the Rutgers University Marine Field Station for their generous help for the aerosol samplings. And Thanks to Mr. Paul Field from the Rutgers Inorganic Analytical Laboratory and the technicians from NJIT Material Characterization Laboratories for their great help in the ICPMS instrument determinations.

Lastly, my tones of thanks must go to my family. Thanks to my wonderful parents Yuanfa Song and Zhuyu Shao who raised me and taught me with unreserved loves. Thanks to my excellent sister Xiaofang Song for always supporting every decision I made. Thanks to my wife Yi Xu for everything she did for me since we first met nine years ago. It's her who has companied me through every stop of my PhD journey. And my loved son, Aiden Song, who brings me countless joys and happiness. I could not describe how grateful I am to have him.

Table of Contents

Chapter 1. Chemical Characteristics of Precipitation at Metropolitan Newark in the US East Coast.....	1
1.1. Introduction.....	4
1.2. Materials and Methods	6
1.2.1. Sampling.....	6
1.2.2. Chemical Analyses.....	6
1.2.3. Data Analysis	7
1.3. Result and Discussion.....	8
1.3.1. Mass Concentrations	8
1.3.2. Acidity and Acid-Alkaline Equilibrium.....	11
1.3.3. Enrichment Factor Analysis.....	13
1.3.4. Factor Analysis.....	14
1.3.5. Cluster analysis	16
1.4. Conclusions.....	18
1.5. References.....	20
 Chapter 2. Size Distributions of Trace Elements Associated with Ambient Particular Matter in the Affinity of Highways in the New Jersey-New York Metropolitan Area on the US East Coast	 44
2.1. Introduction.....	47

2.2. Methods	50
2.2.1. Sampling	50
2.2.2. Chemical Determination	50
2.2.3. Data Processing	51
2.3. Results.....	52
2.3.1. Concentrations and Seasonal Variations	52
2.3.2. Trace Metal Enrichment Factors	53
2.4. Discussions	54
2.4.1. Mass Size Distributions of Particulate Matter	54
2.4.2. Mass Size Distributions of Trace Metals.....	56
2.4.3. Enrichment Factor Size Distributions of Trace Metals	58
2.4.4. Trace Metal Sources Identification.....	59
2.4.5. Weather Influence on Trace Metal Concentrations and Size Distributions	62
2.5. Conclusions.....	63
2.6. References.....	66
Chapter 3. Relationships among the Springtime Ground-level NO_x, O₃ and NO₃	
in the Vicinity of Highways in the US East Coast.....	87
3.1. Introduction.....	89
3.2. Method.....	91
3.2.1. Sampling.....	91

3.2.2. Chemical determinations	92
3.2.3. Data processing.....	93
3.3. Results and Discussions.....	93
3.3.1. Overall Concentrations and 24-hour Variations Characteristics	93
3.3.1.1. Concentrations.....	93
3.3.1.2. 24-hour Variations.....	95
3.3.2. Weekday/Weekend and Diurnal Variation.....	96
3.3.3. Weather Influences on Concentrations	98
3.3.3.1. Daily Concentrations.....	98
3.3.3.2. Diurnal Variations	99
3.3.4. Correlations between NO _x and O ₃	100
3.3.5. Correlations between NO _x and OX.....	101
3.3.6. Relationships between NO ₃ and O ₃	103
3.3.7. Multi-Regression analysis of the NO _x -O ₃ -NO ₃ system	103
3.4. Conclusions.....	104
3.5. References.....	107
Chapter 4. Conclusions	128
4.1. Conclusions of the three studies	129
4.1.1. Pollution Sources	129
4.1.2. Temporal Variation Patterns.....	130

4.1.3. Size Distribution Characteristics of Aerosol Mass and Associated Trace Metals.....	130
4.1.4. Others.....	131
4.2. Recommendation for future research.....	132
Appendices	134
I-1. Sampling information, precipitation amount and pH.....	136
I-2. Inorganic ions concentrations data (ppm).....	138
I-3. Organic acids concentrations data (ppm).....	140
I-4. Trace metals concentrations data (ppb).....	142
II-1. Air concentrations (ng m^{-3}) of trace metals from the 1 st set of winter intensive sampling (12/11/2007-12/14/2007).....	145
II-2. Air concentrations (ng m^{-3}) of trace metals from the 2 nd set of winter intensive sampling (12/14/2007-12/18/2007).....	145
II-3. Air concentrations (ng m^{-3}) of trace metals from the 3 rd set of winter intensive sampling (12/18/2007-12/21/2007).....	146
II-4. Air concentrations (ng m^{-3}) of trace metals from the 4 th set of winter intensive sampling (1/29/2008-2/1/2008).....	146
II-5. Air concentrations (ng m^{-3}) of trace metals from the 5 th set of winter intensive sampling (2/21/2008-2/14/2008).....	147
II-6. Air concentrations (ng m^{-3}) of trace metals from the 6 th set of winter intensive sampling (2/24/2008-2/27/2008).....	147

II-7. Air concentrations (ng m^{-3}) of trace metals from the 1 st set of summer intensive sampling (7/3/2008-7/7/2008).....	148
II-8. Air concentrations (ng m^{-3}) of trace metals from the 2 nd set of summer intensive sampling (7/7/2008-7/11/2008).....	148
II-9. Air concentrations (ng m^{-3}) of trace metals from the 3 rd set of summer intensive sampling (7/11/2008-7/15/2008).....	149
II-10. Air concentrations (ng m^{-3}) of trace metals from the 4 th set of summer intensive sampling (7/15/2008-7/19/2008).....	149
II-11. Air concentrations (ng m^{-3}) of trace metals from the 5 th set of summer intensive sampling (7/19/2008-7/23/2008).....	150
III-1. NO_x - O_3 sampling weather data.....	152
III-2. Ground level NO_x - O_3 concentration data (ppm).....	155

List of Tables

Chapter 1

Table 1. 1 Summary of major anions, cations concentrations and pH in precipitation (ppm).....	28
Table 1. 2 Summary of Trace Metals concentrations in precipitation (ppb).....	29
Table 1. 3 Concentrations of selected organic acids in precipitation at Newark (ppm)....	30
Table 1. 4 Summary of Fractional Acidity and Neutralization factors of NH_4^+ , Ca^{2+} and Mg^{2+}	31
Table 1. 5 Summary of Enrichment Factors.....	32
Table 1. 6 Varimax Rotated Factor Loadings.....	33
Table 1. 7 Scores of selected clusters model and seasonal distribution of precipitation events.....	34

Chapter 2

Table 2. 1 Summary of meteorological parameters during the sampling period.	73
Table 2. 2 Summary of trace metal concentrations and the relative standard variations. .	74
Table 2. 3 Crustal enrichment factors of trace metals in fine, coarse and all particles.	75
Table 2. 4 Similarity levels of size distributions in/between different seasons (Centroid Linkage Method).	76
Table 2. 5 Size distributions of trace metals by cluster analysis.....	77
Table 2. 6 Factor Analysis Result of trace metals concentrations.....	78
Table 2. 7 Identified Clusters of MOUDI sampling events and their dominant factors. ..	79
Table 2. 8 Correlations between weather parameters and trace metal concentrations.....	80

Chapter 3

Table 3. 1 Ground level concentrations of NO, NO ₂ , O ₃ , HNO ₃ and NO ₃ ⁻	113
Table 3. 2 Weekday/weekend and diurnal differences of NO _x , O ₃ and NO ₃	114
Table 3. 3 Pearson correlations efficient among NO _x , O ₃ , NO ₃ and selected weather parameters.....	115
Table 3. 4 Descriptive data of NO _x , O ₃ , NO ₃ under different weather conditions	116
Table 3. 5 Rotated Factor Loadings for the factor analysis of NO _x , NO ₃ and O ₃	117
Table 3. 6 Cluster analysis results with respect to NO _x , NO ₃ and O ₃	118

List of Figures

Chapter 1

Figure 1. 1 Map of sampling location	35
Figure 1. 2 Electric charge equilibrium between total anions and total cations.....	36
Figure 1. 3 Pie charts of Anions, Cations, Trace Metals and Organic Acid, shown in (a), (b), (c), (d) respectively	37
Figure 1. 4 Dilution effect of Precipitation volume on total anions (a), total cations (b), trace metals (c) and Organic Acid (d)..	38
Figure 1. 5 Histogram of pH.	39
Figure 1. 6 Correlations between major cations NH_4^+ , Ca^{2+} and major anions NO_3^- and SO_4^{2-}	40
Figure 1. 7 Correlations between Cl^- and Na^+ , K^+ in precipitation.....	41
Figure 1. 8 Examples of the air mass back-trajectories for each cluster of the precipitation with height of 20m, 500m and 2000m.	42
Figure 1. 9 Examples of the wind speed and wind directions in precipitation periods....	43

Chapter 2

Figure 2. 1 Map of sampling location.	81
Figure 2. 2 The mass size distribution of particles in winter and summer.....	82
Figure 2. 3 The mass size distribution trace metals in two groups: (I) Coarse Particle Accumulation and (II) Fine Particle Accumulation.	83
Figure 2. 4 The mass size distributions of the 6 identified clusters of trace metals in atmosphere (In the figure labels, W means winter while S means summer)...84	
Figure 2. 5 The EF size distributions of the trace metal in three different clusters: (a)	

Cluster 1, (b) Cluster 2, (c) Cluster 3 and (d) Comparison of the average patterns of the three clusters.....	85
Figure 2. 6 Back-Trajectories of air mass using NOAA HYSPLIT Model with arriving height 5 m and duration 48 hours: (a). Cluster 1 (Sampling set #9 as example), (b). Cluster 2 (Sampling set #4 as example), (c). Cluster 3 (Sampling set #5 as example), (d). Cluster 4 (Sampling set #6 as example). For each sampling period (3- 4days), a total of 24 Back-Trajectories were calculated with same interval (3-4 hours).	86

Chapter 3

Figure 3. 1 Study sampling site map.....	119
Figure 3. 2 Box-whisker plot of daily averaged NO, NO ₂ , NO _x and O ₃ concentrations in whole spring monitoring period.....	120
Figure 3. 3 Time series of weekly averaged NO _x , O ₃ and NO ₃ concentrations in spring (Feb. 26th -May 20 th 2007)	121
Figure 3. 4 The 24-h temporal variations of hourly averaged NO _x and O ₃	122
Figure 3. 5 The 24-h temporal variations of hourly averaged NO _x and O ₃ concentrations in weekdays (a) and weekends (b).....	123
Figure 3. 6 The 24-h temporal variations of NO _x and O ₃ in Clear days (a), Cloudy days (b) and Rainy days (c).....	124
Figure 3. 7 Correlations between daytime averaged NO _x and O ₃ in weekdays (a), weekends (c), and between nighttime averaged NO _x and O ₃ in weekdays (b) and weekends (d).....	125
Figure 3. 8 Correlations between NO _x and NO ₂ /NO _x ratio.....	126

Figure 3. 9 Correlations between daytime averaged NO_x and O_3 in weekdays (a),
weekends (c), and between nighttime averaged NO_x and O_3 in weekdays
(b) and weekends (d)..... 127

**Chapter 1 . Chemical Characteristics of Precipitation at
Metropolitan Newark in the US East Coast***

** This work has been published and could be referenced as “ Song, F., and Y. Gao, Chemical characteristic of precipitation at metropolitan Newark in the US East Coast, Atmospheric Environment. 43. 4903-4913. 2009 ”.*

Abstract

To investigate the chemical characteristics of precipitation in the polluted coastal atmosphere, a total of 46 samples were collected using a wet-only automatic precipitation collector from September 2006 to October 2007 at metropolitan Newark, New Jersey in the US East Coast. Samples were analyzed by ion chromatography for the concentrations of major inorganic ions (Cl^- , NO_3^- , SO_4^{2-} , F^- , NH_4^+ , Ca^{2+} , Mg^{2+} , Na^+ , K^+) and organic acid species (CH_3COO^- , HCOO^- , $\text{CH}_2(\text{COO})_2^{2-}$, $\text{C}_2\text{O}_4^{2-}$). Selected trace metals (Sb, Pb, Al, V, Fe, Cr, Co, Ni, Cu, Zn, Cd) in samples were determined by ICPMS. Mass concentration results show that SO_4^{2-} is the most dominant anion accounting for 50.5% of the total anions, controlling the acidity of the precipitation. NH_4^+ accounts for 48.6% of the total cations, dominating the precipitation neutralization. CH_3COO^- and HCOO^- are the two dominant water-soluble organic acid species, accounting for 42.0% and 40.2% of the total organic acids analyzed respectively. Al, Zn and Fe are the three major trace metals in precipitation, accounting for 33.6%, 26.8%, and 25.2% of the total metals. The pH values in precipitation ranged from 3.8 to 6.4, indicating an acidic nature. Enrichment Factor (EF) Analysis showed that Na^+ , Cl^- , Mg^{2+} and K^+ in the precipitation are primarily of marine origin, while most of the Fe, Co and Al are from crust sources. Pb, V, Cr, Ni are moderately enriched with EFs ranging 43 - 414, while Zn, Sb, Cu, Cd and F^- are highly enriched with EFs > 700, indicating significant anthropogenic influences. Factor analysis suggests 6 major sources contributing to the observed composition of precipitation at this location: (1) nitrogen-enriched soil, (2) secondary pollution processes, (3) marine sources, (4) incineration, (5) oil combustion, and (6) malonate-vanadium-enriched sources. To further explore the source-precipitation event relationships and seasonality, cluster

analysis was performed and all precipitation events were grouped into 6 clusters. Results show that about half of the precipitation events were characterized by mixed sources. Significant influences of nitrogen-enriched soil and marine sources were associated with precipitation events in spring and autumn, while secondary pollution processes, incineration and oil combustion contributed greatly in summer.

Key Words: Precipitation, Trace Metals, Anions and Cations, Urban, Enrichment Factor, Factor Analysis, Cluster Analysis.

1.1. Introduction

Precipitation plays important roles in carrying chemical species from the atmosphere to the surface (Goncalves *et al.*, 2000; Lara *et al.*, 2001) and thus can bring potential adverse effects to the terrestrial and marine aquatic ecosystems (Kim, 2000). One of the consequent effects is “acid rain”, common in North America (Heuer *et al.*, 2000; Ito *et al.*, 2002), which harmfully affects human health, damages buildings, and acidifies aquatic systems. On the other hand, precipitation is episodic in nature and many dissolved chemicals in precipitation can also serve as the sources of nutrients to enhance biological activities and stimulate marine primary production (Pearls, 1985; Spanos *et al.*, 2002). Characterization of precipitation is critically important to better understand its effects, develop control strategies and protect the environment.

The chemical characteristics of precipitation can be affected by many environment impacts, including anthropogenic emissions (Lara *et al.*, 2001), sea spray and terrestrial dust (Safai *et al.*, 2004; Das *et al.*, 2005). In precipitation, the major inorganic ions NO_3^- and SO_4^{2-} can be transformed from their precursor gases, such as SO_2 and NO_x emitted from pollution sources (Seinfeld and Pandis, 2006). NH_4^+ primarily comes from fertilizers used in agriculture, biomass burning, livestock breeding and even natural activities (Topcu *et al.*, 2002; Hu *et al.*, 2003; Migliavacca *et al.*, 2005). Other major elements Cl^- , Mg^{2+} , K^+ and Na^+ originate mainly from natural sources such as sea spray, rock and soil re-suspension and forest fires (Đorđević *et al.*, 2005). Trace metals in precipitation are strongly affected by anthropogenic pollution sources (Nriagu and Pacyna, 1988), except Fe, Al and Mn which originate mainly from the earth's crust. Organic acid species mainly come from direct anthropogenic emissions, biogenic

emission and in situ production from precursors in the troposphere. (G. Brooks et al., 2006 and references therein)

The acidity of precipitation, a measure of active H^+ concentration, is controlled by the balance between acidification and neutralization processes. NO_3^- and SO_4^{2-} are the two major ions contributing to the acidity of precipitation (Zunckel *et al.*, 2003; Migliavacca *et al.*, 2004). Organic acids, especially formate ($HCOO^-$) and acetate (CH_3COO^-), also contribute to the acidity of precipitation in both rural and urban areas (Keene and Galloway, 1984; Yu *et al.*, 1998; Pena *et al.*, 2002). About 16-35% of the total acidity was contributed by organic acids in North America (Keene *et al.*, 1983). The neutralization of the acidity is mainly caused by Ca^{2+} (Saxena *et al.*, 1996; Basak and Alagha, 2004) and NH_4^+ (Zunckel *et al.*, 2003). With high rates of anthropogenic emissions in the US East Coast, acid rain has been observed as a common feature in the region. However, few studies on detailed precipitation chemistry have been conducted recently in this region.

To characterize precipitation chemistry in this region, a one-year precipitation sampling was carried out at Newark, New Jersey, with the following objectives: (1) identifying the chemical characteristics of precipitation in this area; (2) investigating the factors controlling the acidity of the precipitation; and (3) identifying the relative contributions of different sources of chemical species in precipitation. The results of this work will fill the data gap of precipitation chemistry for this geographic region and help better understand the major processes and sources that control precipitation composition. This study can also provide important insights into the linkages between urban air pollution and its potential influence on human health and aquatic ecosystems.

1.2. Materials and Methods

1.2.1. Sampling

Event-based precipitation sampling was conducted in Newark (40°44'N, 74°10'W), New Jersey in the US East Coast (Fig. 1.1) from September 2006 to October 2007. Located on the US East Coast, Newark is the largest metropolitan center of the state, adjacent to New York City and the Atlantic Ocean. The composition of precipitation in this area could be influenced by both continental and marine sources. An automatic wet only precipitation sampler (Type B1C, M.I.C Company, Canada) was set on the roof of a building of ~ 20m height on the Rutgers University campus in downtown Newark for sample collection. Before sampling, clean techniques for the sampler and bottles cleaning were used, following the procedures by Kim *et al.*, (2000). After each sampling, samples were kept in a freezer until analysis. A total of 46 samples were collected during the study period. The precipitation volume and other weather parameters for this sampling site were obtained from a nearby weather station at Newark Museum (www.wunderground.com).

1.2.2. Chemical Analyses

The major inorganic ions and organic acid species in the precipitation were measured using ion chromatography (ICS-2000, Dionex) in the Atmosphere Chemistry Lab of Rutgers University at Newark. The major inorganic ions include Cl^- , NO_3^- , SO_4^{2-} , F^- , NH_4^+ , Ca^{2+} , Mg^{2+} , Na^+ , K^+ , and organic acid ions include Acetate, Formate, Malonate ($\text{CH}_2(\text{COO})_2^{2-}$) and Oxalate ($\text{C}_2\text{O}_4^{2-}$). Samples were first taken out from the freezer and thawed overnight at room temperature, and then were filtered by PTFE syringe filter (0.45 μm). Samples were injected into the IC system via automated sampler (AS40,

Dionex) using 0.5ml vials. An AS11 analytical column (2_250mm2, Dionex), KOH eluent generator cartridge (EGC II KOH, Dionex) and 25 μ l sample loop were employed for the determinations of anions, while for cations, a CS12A analytical column (2_250mm2, Dionex), MSA generator cartridge (EGC II MSA, Dionex) and 25 μ l sample loop were used. The detection limit of the method is below 0.01ppm, and the precision of the analysis is \sim 1%. Detailed information of the method is given in Zhao and Gao (2008). Strong linear correlations existed between the two electrically charged groups of anions and cations with a slope of \sim 1.00 ($R^2 = 0.875$) (Fig. 1.2), suggesting that good electric charge equilibrium existed between the two groups. Therefore the sampling and determination methods in the study are reliable (Rastogi and Sarin, 2005).

Selected trace metals including Sb, Pb, Al, V, Fe, Cr, Co, Ni, Cu, Zn and Cd were determined using High Resolution Inductively Coupled Plasma Mass Spectrometry (HR-ICP-MS) (Finnigan™ ELEMENT2, Thermo Scientific) in the Institute of Marine and Coastal Science at Rutgers University. Before determination, samples were filtered using the same procedure as indicated above and then acidified to \sim 4% acidity by adding nitric acid (Optima A460-500, Fisher Scientific). The detection limits for all trace metals are less than 1ppt and the precision of the method is \sim 2%. More information on the ICPMS methods can be found at <http://marine.rutgers.edu/>.

1.2.3. Data Analysis

Enrichment Factor Analysis, Factor Analysis and Cluster Analysis were employed to explore the possible sources affecting the chemical characteristics of precipitation. Enrichment Factor distinguishes the relative contributions of crustal or marine sources from other sources (Chabas and Lefevre, 2000; Okay *et al.*, 2002). Factor analysis was

used for further identifying the more detailed information of all possible major sources. In this study, Factor Analysis was carried out using SAS 9.1 with principle components analysis and Varimax Rotations. Based on the sources information from Enrichment Factor Analysis and Factor Analysis, precipitation events were then grouped and characterized separately by Cluster Analysis to explore the source-precipitation event relationships and seasonality, using SAS 9.1 according to the Ward's method (Ward, 1963). This method is appropriate for the quantitative variables, since it takes the Cluster Analysis as a variance problem instead of using distance matrix or association measures. After analysis, each cluster was realized in a multivariate distribution.

1.3. Result and Discussion

1.3.1. Mass Concentrations

Fig. 1.3a shows that SO_4^{2-} is the most predominant anion, accounting for 50.5% of the total anion mass, followed by NO_3^- (24.6%), organic acid (13.8%), Cl^- (10.6%), and F^- (0.5%). The mass contribution of organic acid species to the total anions from this study is similar to the results of Keene *et al.* (1983) for North America. For cations (Fig. 1.3b), NH_4^+ and Na^+ are the dominant contributors to the total cation mass, accounting for 48.6% and 27.9% respectively, followed by Ca^{2+} (13.5%), K^+ (5.50%) and Mg^{2+} (4.50%). The high percentage of NH_4^+ , which is mainly non-crust originated, indicates a high anthropogenic contribution to the study area. This could also be confirmed by the relatively low concentration of the crust-originated element calcium (Table 1.1). Besides, the high mass percentage of Na^+ may reflect the significant influence of marine sources. For trace metals, the contributions of Al (33.6%), Zn (26.8%) and Fe (25.2%) are overwhelmingly high compared with other trace metals (Fig. 1.3c), suggesting a mixed

influence of crust soil and anthropogenic emissions. Other trace metals including Cu, Pb, Ni, Sb, and V contributed about 13.8% of the total trace metal mass, while the percentage contributions of Cr and Cd were small. Similar to the observations in other regions (Injuk and van Grieken, 1995; Herut *et al.*, 2001; Hou *et al.*, 2005), the abundance sequence of $Zn > Fe > Cu$ was also observed in the study. For organic acid species, the VWA concentrations of acetate and formic acid are 0.21ppm and 0.20ppm, respectively (Table 1.3), together contributing to 82.2% of the total organic anions (Fig. 1.3d), and this result is consistent with the data from other urban regions (Keene and Galloway, 1984; Yu *et al.*, 1998; Pena *et al.*, 2002). Oxalate and malonate are the additional organic acidic species in precipitation observed in the area of this study.

Concentration dilution effects caused by high precipitation rate were observed for total anions, total cations and total trace metals, but not for total organic acid. Fig. 1.4 shows that the concentrations of inorganic anions, major cations and total trace metals decreased exponentially with increasing precipitation rates, while no obvious relationships were found between total organic species and precipitation rates. This could also be confirmed by the fact that event-averaged concentrations are higher than VWA concentrations (Tables 1.1 & 1.2). The observed exponential relationships could be attributed to the below-cloud raindrop scavenging effect (Goncalves *et al.*, 2000; Pelicho *et al.*, 2006). For organic acids, however, such a raindrop scavenging effect was not found, indicating that the in-cloud processes may play more important roles than that of the scavenging effect (Goncalves *et al.*, 2002).

Tables 1.1, 1.2 and 1.3 summarize the Volume Weighted Average (VWA) concentrations of chemical species in precipitation measured at Newark along with the

comparisons at other locations. The concentrations of NO_3^- , NH_4^+ at Newark are comparable to other regions, especially the US East Coast regions such as the Adirondacks, NY and Great Bay, NJ. The concentrations of SO_4^{2-} , Ca^{2+} , Mg^{2+} and K^+ from this study are lower than other sites worldwide such as the Central Mediterranean, Northern Jordan, and Italy etc. The trace metals at Newark are generally of lower concentrations compared with other regions (Pike and Moran, 2001; Al-Momani, 2003; Deboudt *et al.*, 2004), and their concentrations varied tremendously with time during the sampling period. Such variations could be caused by many factors including transport patterns, different source strength and weather conditions. The concentrations of organic acid species in this study show the levels similar to those in other regions, such as southern California (G. Brooks *et al.*, 2006), except for the fact that malonate has much higher concentrations even exceeding oxalate at the Newark site, which did not appear in previous studies of both precipitation and aerosols (Huang *et al.*, 2005; Zhao and Gao, 2008).

Obvious but different seasonality was found for all the chemicals studied in the event averaged concentrations of the precipitation. For major anions and cations, as shown in Table 1.1, the SO_4^{2-} and NH_4^+ concentrations were observed highest in summer, even though more precipitation happened in summer, indicating the possible much higher emissions. While Na^+ , Cl^- and NO_3^- were of much higher concentrations in winter and Ca^{2+} concentrations were higher in spring compared with other reasons. For trace metals, more than half of them (Sb, Pb, Co, Zn, Cd) were of higher concentrations in spring (Table 1.2). Al, Fe and Ni were more concentrated in precipitation of summer while for the other trace metals V and Cr, their highest concentrations happened in winter. Finally,

all the organic acid in the study were of highest concentrations in summer, indicating their consistent and strong seasonality, as shown in Table 1.3.

1.3.2. Acidity and Acid-Alkaline Equilibrium

The acidity in precipitation found in this study is much higher than in other regions worldwide, showing significant “acid rain” characteristics. The pH values of the precipitation shown in Table 1.1 and Fig. 1.5 ranged between 3.8 and 6.4, averaging (VWA) at 4.6, lower than the typical pH of natural water (5.6) at equilibrium with only atmospheric CO₂ (Seinfeld and Pandis, 2006). However, the low pH in precipitation observed at Newark is consistent with the low pH reported by Ayres and Gao (2007) and Gao (2002) at Tuckerton in southern New Jersey, suggesting that acid rain is a common feature in this region.

The acidity in precipitation at Newark was mainly caused by H₂SO₄, with HNO₃ and organic acids as major additional contributors. As shown in Table 1.4, SO₄²⁻ contributed more than half of the acidity (64% of the total), while NO₃⁻ and organic acid contribute 22% and 14% of the total acidity, respectively. This finding is consistent with the conclusions of Kaya and Tuncel (1997) and similar to the work by Keene *et al* (1986) who predicted that organic acid may account for ~15% of the total acidity for North America. Compared with other regions, the H₂SO₄ contribution to the acidity is higher (Al-Momani *et al.*, 1995; Tuncer *et al.*, 2001) while HNO₃ contribution is lower (Migliavacca *et al.*, 2005) in this study area, indicating reduced NO_x emission. These results suggest that the source strength of each contributing acidic species varies, contributing differently to the precipitation acidity at this location.

To better understand the precipitation acidity, Fractional Acidity (FA)

(Balasubramanian *et al.*, 2001) was used to measure the acid neutralization capacity in precipitation. We modified the original FA method by adding an organic acid component, given in Equation (1-1). The Neutralization Factor (NF) was used to measure the contribution of the total alkaline species to the neutralization according to Possanzini *et al.* (1988) as shown in Equation (1-2):

$$FA = \frac{[H^+]}{[SO_4^{2-}] + [NO_3^-] + [Organic\ Acid]} \quad (1-1)$$

$$NF_{xi} = \frac{[xi]}{[NO_3^-] + [SO_4^{2-}] + [Organic\ Acid]} \quad (1-2)$$

The calculated FA in precipitation was 0.47 at Newark, indicating that 47% of acidity still had not been neutralized. The neutralization in precipitation was mainly caused by NH_4^+ (72%), while Ca^{2+} and Mg^{2+} together contributed about 17% (Table 1.4). These results support the conclusion that neutralization in precipitation was primarily caused by anthropogenic NH_3 (Zunckel *et al.*, 2003) and airborne dust $CaCO_3$ (Saxena *et al.*, 1996; Glavas and Moschonas, 2002; Al-Momani, 2003). However, compared with the higher $CaCO_3$ contribution relative to NH_3 found in other studies (Samara *et al.*, 1992), the contribution of NH_3 in the study is much higher than $CaCO_3$, indicating significant anthropogenic NH_3 emission.

Major species that influence the precipitation acidity and its neutralization are NO_3^- , SO_4^{2-} , NH_4^+ and Ca^{2+} , confirmed by the strong linear correlations between NO_3^- , SO_4^{2-} and NH_4^+ , Ca^{2+} (Fig. 1.6). The high contributions of NH_4NO_3 and $(NH_4)_2SO_4$ could be explained by the fact that they are the two common fertilizers used in soil. Part of such fertilizers could be decomposed and converted to NH_3 , which will neutralize the acidity (Al-Momani *et al.*, 1995; Saxena *et al.*, 1996). They may also become airborne by wind and then form NH_4NO_3 and $(NH_4)_2SO_4$ aerosols (Seinfeld and Pandis, 2006). Besides,

emissions from fossil fuel combustion could also contribute to the NH₃ production (Ugucione *et al.*, 2002). Previous studies suggest that ammonium salts produced from reaction with NH₃ are the most important acidity-controlling chemicals (Langford *et al.*, 1992; Lee and Atkins, 1994).

1.3.3. Enrichment Factor Analysis

Enrichment Factors (EFs), a first-step source estimator of chemical components in precipitation (Chabas and Lefevre, 2000; Okay *et al.*, 2002), was employed in this study to explore the possible sources: anthropogenic, marine or crust origins. For seawater EFs, Na was used as a reference element (Keene *et al.*, 1986); while Al was selected as a reference to crust sources. The EFs were calculated via following equations:

$$EF_{Seawater}(xi) = \frac{(xi/Na)_{precipitation}}{(xi/Na)_{seawater}} \quad (1-3)$$

$$EF_{Crust}(xi) = \frac{(xi/Al)_{precipitation}}{(xi/Al)_{crust}} \quad (1-4)$$

In these equations, the ratios (xi/Na)_{Seawater} are taken from Keene *et al.* (1986), and (xi/Al)_{Crust} are taken from Weaver and Tamey (1984), and Taylor and McLennan (1985). Based on the rules of Poissant *et al.* (1994), EFs between 1 and 10 suggest the major influence of marine or soil sources; when EFs range between 10-500, moderate enrichments are indicated, while when EFs are over 500, extreme enrichments exist.

As shown in Table 1.5, the EF_{Seawater} for Na⁺, Cl⁻, Mg²⁺ and K⁺ ranged from 1 to 10, suggesting a marine origin, mainly sea salt aerosols emitted from seawater (Zunckel *et al.*, 2003; Migliavacca *et al.*, 2004). This conclusion is further confirmed by strong correlations between Cl⁻ and Na⁺ and between Cl⁻ and K⁺ (Fig. 1.7). The Ca²⁺ ion is moderately enriched compared with both seawater and crustal sources, with its EF_{Seawater}, EF_{crustal} being 28.4 and 51.2 respectively, suggesting that Ca²⁺ in precipitation may

mainly derived from both the marine and crustal sources, especially the marine source. Meanwhile the anthropogenic sources could also contribute and thus lead to the moderate enrichment factors.

For trace elements in precipitation measured at this location, the crustal EFs calculations show that Fe, Co and Al mainly originate from crust sources. The elements Ca^{2+} , K^+ , Na^+ , Mg^{2+} , Pb, V, Cr, Ni are moderately enriched, with EFs being from 43 (V) to 414 (Pb). Apparently the moderate enrichment of Ca^{2+} , Na^+ , K^+ and Mg^{2+} is mainly caused by sea salt related sources, as indicated by their low EF_{Na} values. K^+ may also be emitted from forest fires and soil re-suspension (Đorđević *et al.*, 2005). Pb, V, Cr, Ni may come from high temperature combustion processes (Lindberg, 1982; Scudlark *et al.*, 1994) and traffic emissions (Al-Momani, 2003). The elements Sb, Cu, Zn, Cd, Cl^- and F^- are highly enriched, with EFs ranging from 714 (Cu) to more than 10^5 (Cl^-). For the most enriched Cl^- , in addition to the marine source, other anthropogenic sources may also contribute (Safai *et al.*, 2004; Migliavacca *et al.*, 2005). The highly enriched fluoride may originate from fertilizer production and coal-fired power plant emissions (Zunckel *et al.*, 2003; Migliavacca *et al.*, 2004), and Sb could be derived from fly ash generated during combustion processes (Velzen *et al.*, 1998). The high enrichment of Zn could be contributed by road traffic emissions (Steven *et al.*, 1997; Al-Momani, 2003) and hospital waste burning (Sanusi *et al.*, 1996). The extremely high enrichments of Cu and Cd are mainly caused by both lower and high temperature combustion processes, such as incineration (Pio *et al.*, 1996; Al-Momani, 2003).

1.3.4. Factor Analysis

To explore the correlations among observed variables and potential major sources

of chemical species in precipitation at this location, Factor Analysis was carried out. Six major factors were extracted from the 25 observed variables, with the prominent variables in bold (Table 1.6). The six factors together explain 83.9% of the total variations caused by all variables.

F1, with high loading of Al, Cr, Fe, Co, F⁻, NO₃⁻, NH₄⁺ and Ca²⁺, may represent a mixed source involving natural crustal material weathering and agricultural practices, considering that Fe, Al, Co are mainly of typical crust origin and NH₄NO₃ is a major component in fertilizers used in agriculture. F⁻ may also come from fertilizer industry related processes; Cr and Ca²⁺ probably came from crust sources or soil fertilization. F2 mainly consists of SO₄²⁻, NH₄⁺, H⁺ and three organic acids (acetate, formic acid and oxalate), representing the end-products of secondary reaction processes that control the alkalinity-acidity equilibrium. SO₄²⁻ and NH₄⁺ are the two major secondary pollutants controlling the alkalinity-acidity equilibrium. The association of the three organic acids with F2 indicates their important contribution to the acidity. NO₃⁻ is not associated with F2, suggesting that it may play less of a role in the alkalinity-acidity equilibrium. In contrast to the results of Avila and Alarco (1999) and Tang *et al.*, (2005), both alkaline and acidic secondary chemicals affecting the alkalinity-acidity equilibrium are included in F2, and in particular, NH₄⁺ is the dominant alkaline species in this study. F3 represents the marine source with high loading of Cl⁻, Mg²⁺, Na⁺, consistent with previous works (Lee *et al.*, 2000; Mihajlidi-Zelić *et al.*, 2006). F4 is characterized by the high contributions of Sb, Pb, Zn and Cd, attributed to possible fossil fuel burning and incineration processes (Scudlark *et al.*, 1994; Pio *et al.*, 1996; Al-Momani, 2003). F5 has high loadings of Ni and K⁺, representing oil combustion processes and biomass burning.

Ni is mainly from oil combustion processes (Lee and Duffield, 1977). For K^+ , it could be emitted from either oil combustion or biomass burning processes (Zunckel *et al.*, 2003; Khare *et al.*, 2004). F6 has malonate and vanadium as prominent variables, representing either natural or anthropogenic sources that are enriched with both species; this finding is unique at the site and may need further studies. The six factors could explain 23.9%, 19.2%, 14.6%, 12.0%, 7.7% and 6.5% of the total chemical composition variations, respectively (Table 1.6).

1.3.5. Cluster analysis

To characterize the source-precipitation event relationships as a function of the seasons, cluster analysis was carried out, using Ward's method to minimize the sum of the squares of any two hypothetical clusters that can be formed at each step (Ward, 1963) in order to emphasize the homogeneous nature of each cluster. This method is different from the cluster analysis commonly used in other studies that compute the square Euclidean distances between samples by K-mean clustering technique using chemicals' concentration data (Avila and Alarco, 1999; Gao and Anderson, 2001; Glavas and Moschonas, 2002). We used the 6 selected factors in cluster analysis instead of the original concentration data to reduce noise caused by errors in the original data.

All precipitation events were grouped into 6 clusters and their dominant influencing factors could be interpreted as: (1) well-mixed sources, (2) nitrogen-enriched soil, (3) marine sources, (4) secondary pollution processes, (5) incineration, oil combustion processes and (6) a combination of nitrogen-enriched soil and malonate-vanadium-enriched sources.

Different clusters of the precipitation events showed different air-mass

transportation patterns, as shown by the back-trajectory paths under NOAA HYSPLIT Model in Fig. 1.8. In the study, a 72 hours period of were selected for the back-trajectory considering the lifetime of the different secondary species (Wojcik and Chang, 1997). Usually for the precipitation events in cluster 3, which was interpreted as marine source, the air mass at the selected height of 20m, 500m and 2000m were mainly from the Atlantic Ocean, while for other precipitation events their air mass were mainly originated from the continent. The results of the back-trajectory shown in Fig. 1.8 supported well the result of cluster analysis and could indicate the potential geographic origins of the pollutants in the precipitation. In addition, the results of wind direction were found to influence the characteristic of precipitation (Fig. 1.9). For the precipitation in cluster 3, the corresponding wind direction were mainly east to south (Oct. 4, 2006 and Nov. 16, 2006 as examples), while for the other precipitation, the wind direction were mainly from east direction (Oct. 20, 2006 and Nov. 2, 2006 as examples). At last, Wind speed could not influence the chemical characteristic of the precipitation obviously.

After cluster analysis, the characteristics of precipitation during each season, with possible sources, are summarized in Table 1.7. About half of the precipitation events were classified into C1, indicating that mixed sources contribute greatly to precipitation events all year around. The other half of the precipitation events were controlled by specific sources in different seasons. Many events are grouped into C2 in springtime, which are associated with nitrogen-enriched soil sources. In summer, both C4 and C5 dominated the precipitation events associated with secondary pollution, incineration and oil combustion processes. In autumn, marine sources indicated by C3 influenced greatly the chemical characteristics of precipitation. In winter, mixed sources played the major role.

1.4. Conclusions

Results from this study on precipitation chemistry carried out during 2006-2007 in Newark, NJ lead to the following conclusions:

SO_4^{2-} and NH_4^+ are the two most dominant components of major ions in mass, accounting for 50.5% of the total anions and 48.6% of total cations, respectively. Al (33.6%), Zn (26.8%) and Fe (25.2%) are the three most abundant trace metals in precipitation. Organic acid mass in precipitation is predominately composed of acetate (42.0%) and formate (40.2%).

The precipitation at Newark showed an acidic nature, with VWA pH \sim 4.6. The acidity is caused mainly by SO_4^{2-} (64%), with NO_3^- (22%) and organic acid (14%) as additional acidity contributors. About 47% of the acidity was neutralized by NH_4^+ , Ca^{2+} and Mg^{2+} ; in particular NH_4^+ contributed as much as 72% of the total neutralization.

Marine, continental crust and anthropogenic sources showed significant influence on the chemical composition of precipitation at this location. Na^+ , Cl^- , Mg^{2+} and K^+ are primarily of marine origin and Fe, Co and Al are mainly from crust sources. Due to the anthropogenic influences, Pb, V, Cr, Ni are moderately enriched while Zn, Sb, Cu, Cd and F⁻ are highly enriched.

Based on factor analysis, six major sources were found to control the characteristics of precipitation: (1) nitrogen-enriched soil, (2) secondary pollution processes, (3) marine sources, (4) incineration processes, (5) oil combustion and (6) malonate-vanadium-enriched sources, together explaining \sim 83.9% of the variations of 25 variables.

The results of cluster analysis show that about half of the precipitation events

were controlled by mixed sources while for the rest of the precipitation events, their major sources showed obvious seasonality. In spring, nitrogen-enriched soil contributed much. During summer, secondary pollution, incineration and oil combustion showed great influences, while marine sources influenced the precipitation composition significantly during autumn. In winter, however, no specific sources controlled the characteristics of precipitation.

1.5. References

- Al-Momani, I. F., 2003. Trace elements in atmospheric precipitation at Northern Jordan measured by ICP-MS: acidity and possible sources. *Atmos. Environ* 37, 4507–4515.
- Al-Momani, I.F., Tuncel, S., Eler, U., Ortel, E., Sirin, G., Tuncel, G., 1995. Major ion composition of wet and dry deposition in the eastern Mediterranean basin. *Sci. Total Environ* 164, 75–85.
- Avila, A., Alarcon, M., 1999. Relationship between precipitation chemistry and meteorological situations at a rural site in NE Spain. *Atmos Environ* 33:1663–77.
- AYARS, J., Gao Y., 2007. Atmospheric nitrogen deposition to the Mullica River-Great Bay Estuary. *Marine Environmental Research* 64, 590-600.
- Balasubramanian, R., Victor, T., Chun, N., 2001. Chemical and statistical analysis of precipitation in Singapore. *Water, Air, and Soil Pollution* 130, 451–456.
- Basak, B., Alagha, O., 2004. The chemical composition of rainwater over Buyukcekmece Lake, Istanbul. *Atmos. Res* 71, 275–288.
- Chabas, A., Lefevre, R.A., 2000. Chemistry and microscopy of atmospheric particulates at Delos (Cyclades—Greece). *Atmos. Environ* 34, 225–238.
- Das, R., Das, S.N., Misra, V.N., 2005. Chemical composition of rainwater and dustfall at Bhubaneswar in the east coast of India. *Atmos. Environ* 39, 5908–5916.
- Dasch, J.M., Wolff, G., 1989. Trace inorganic species in precipitation and their potential use in source apportionment studies. *Water, Air, and Soil Pollution* 43, 401–412.
- Deboudt, K., Flament, P., Laure Bertho, M., 2004. Cd, Cu, Pb and Zn concentrations in atmospheric wet deposition at a coastal station in Western Europe. *Water, Air, and Soil Pollution* 151, 335–359.

- Dorđević, D., Mihajlidi-Zelić, A., Relić, D., 2005. Differentiation of the contribution of local resuspension from that of regional and remote sources on trace elements content in the atmospheric aerosol in the Mediterranean area. *Atmos Environ* 39: 6271–81.
- G. Brooks A. J., Kieber, R. J., Witt, M., Willey J. D., 2006. Rainwater monocarboxylic and dicarboxylic acid concentrations in southeastern North Carolina, USA, as a function of air-mass back-trajectory. *Atmos. Environ* 40, 1683-1693.
- Gao, Y., 2002. Atmospheric nitrogen deposition to Barnegat Bay. *Atmos. Environ* 36, 5783–5794.
- Gao Y., Anderson R. A., 2001. Characteristics of Chinese aerosols determined by individual-particle analysis. *Journal of Geophysical Research* 106, 18037–18045
- Glavas, S., Moschonas, N., 2002. Origin of observed acidic–alkaline rains in a wet-only precipitation study in a Mediterranean coastal site, Patras, Greece. *Atmos Environ* 36, 3089–99.
- Goncalves, F.L.T., Massambani, O., Beheng, K.D., Vautz, W., Schilling, M., Solci, M.C., Rocha, V., Klockow, D., 2000. Modelling and measurements of below cloud scavenging processes in the highly industrialized region of Cubatão-Brazil. *Atmos. Environ* 34, 4113–4120.
- Goncalves, F.L.T., Ramos, A.M., Freitas, S., Silva Dias, M.A., Massambani, O., 2002. In-cloud and below-cloud numerical simulation of scavenging processes at Serra do Mar region, SE Brazil. *Atmos. Environ* 36, 5245–5255.
- Heaton, R.W., Rahn, K.A., Lowenthal, D.H., 1990. Determination of trace elements, including regional traces, in Rhode Island precipitation. *Atmos. Environ* 24A (1),

147–153.

- Herut, B., Nimmo, M., Medway, A., Chester, R., Krom, M.D., 2001. Dry atmospheric inputs of trace metals at the Mediterranean coast of Israel (SE Mediterranean): sources and fluxes. *Atmos. Environ* 35, 803–813.
- Heuer, K., Tonnessen, K.A., Ingersill, G.P., 2000. Comparison of precipitation chemistry in the Central Rocky Mountains, Colorado, USA. *Atmos. Environ* 34, 1713–1722.
- Hou, H., Takamatsu, T., Koshikawa, M. K., Hosomi, M., 2005. Trace metals in bulk precipitation and throughfall in a suburban area of Japan. *Atmos. Environ* 39, 3583–3595.
- Hu, G.P., Balasubramanian, R., Wu, C.D., 2003. Chemical characterization of rainwater at Singapore. *Chemosphere* 51, 747–755.
- Huang, X., Hu, M., He, L., Tang, X., 2005. Chemical characterization of water-soluble organic acids in PM_{2.5} in Beijing, China. *Atmos. Environ* 39(16): 2819-2827.
- Huang, Y., Wang, Y., Zhang, L., 2008. Long-term trend of chemical composition of wet atmospheric precipitation during 1986-2006 at Shenzhen city, China, *Atmos. Environ.*, doi:10.1016/j. atmosenv.2007.12.063.
- Injuk, J., van Grieken, R.V., 1995. Atmospheric concentrations and deposition of heavy metals over the North Sea: a literature review. *Journal of Atmospheric Chemistry* 20, 179–212.
- Ito, M., Mitchell, M., Driscoll, C.T., 2002. Spatial patterns of precipitation quantity and chemistry and air temperature in the Adirondack region of New York. *Atmos. Environ* 36, 1051–1062.
- Kanellopoulou, E.A., 2001. Determination of heavy metals in wet deposition of Athens.

- Global Nest: The International Journal 3 (1), 45–50.
- Keene, W.C., Galloway, J.N., Holden, J.D., 1983. Measurement of weak organic acidity in precipitation from remote areas of the world. *J. Geophys. Res* 88, 5122–5130.
- Keene, W.C., Galloway, J.N., 1984. Organic acidity of precipitation of North America. *Atmos. Environ* 18, 2491–2497.
- Keene, W.C., Pszenny, A.P., Galloway, J.N., Hawley, M.E., 1986. Sea salt correction and interpretation of constituent ratios in marine precipitation. *J. Geophys. Res* 91, 6647–6658.
- Khare, P., Goel, A., Patel, D., Behari, J., 2004. Chemical characterization of rainwater at a developing urban habitat of Northern India. *Atmos. Res* 69, 135–145.
- Kim, G., Scudlark, J. R., Church, T. M., 2000. Atmospheric wet deposition of trace elements to Chesapeake and Delaware Bays. *Atmos. Environ* 34, 3437 – 3444.
- Langford, A. O., Fehsenfeld, F. C., Zachariassen, J., Schimel, D. S., 1992. Gaseous ammonia fluxes and background concentrations in terrestrial ecosystems in the United States. *Glob Biogeochem Cycles* 6, 459–483.
- Lara, L. B. L. S., Artaxo, P., Martinelli, L.A., Victoria, R.L., Camargo, P.B., Krusche, A., Ayres, G.P., Ferraz, E.S.B., Ballester, M.V., 2001. Chemical composition of rainwater and anthropogenic influences in the piracicaba river basin, Southeast Brazil. *Atmospheric Environment* 35, 4937–4945.
- Le Bolloch, O., Guerzoni, S., 1995. Acid and alkaline deposition in precipitation on the western coast of Sardinia, central Mediterranean (401N, 81E). *Water, Air, and soil pollution* 85, 2155–2160.
- Lee, R.E. Jr., Duffield, F.V., 1977. EPA's catalyst research program: environmental

- impact of sulfuric acid emissions. *J. Air Pollut. Control Assoc.* 27, 631-635.
- Lee, D. S., Atkins, D. H. F., 1994. Atmospheric ammonia emissions from agricultural waste combustion. *Geophys Res Lett* 21, 281–284.
- Lee, B.K., Hong, S.H., Lee, D.S., 2000. Chemical composition of precipitation and wet deposition of major ions on the Korean peninsula. *Atmos. Environ* 34, 563–575.
- Lindberg, S.E., 1982. Factors influencing trace metal, sulfate, and hydrogen ion concentration in rain. *Atmos. Environ* 16, 1701-1709.
- Migliavacca, D., Teixeira, E.C., Wiegand, F., Machado, A. C. M., Sanchez, J., 2005. Atmospheric precipitation and chemical composition of an urban site, Guaíba hydrographic basin, Brazil. *Atmos. Environ* 39, 1829–1844.
- Migliavacca, D., Teixeira, E. C., Pires, M., Fachel, J., 2004. Study of chemical elements in atmospheric precipitation in South Brazil. *Atmos. Environ* 38, 1641–1656.
- Mihajlidi-Zelić, A., Deršek-Timotić, I., Relić, D., Popović, A., Đorđević, D., 2006. Contribution of marine and continental aerosols to the content of major ions in the precipitation of the central Mediterranean. *Science of the Total Environment* 370, 441–451.
- Nriagu, J.O., Pacyna, J.M., 1988. Quantitative assessment o worldwide contamination of air, water, and soils by trace metals. *Nature* 333, 134-139.
- Okay, C., Akkoyunlu, B.O., Tayanc, M., 2002. Composition of wet deposition in Kaynarca, Turkey. *Environ. Pollut* 118, 401–410.
- Paerl, H.W., 1985. Enhancement of marine primary production by nitrogen enriched acid rain. *Nature* 315, 747–749.
- Pelicho, A. F., Martins, L. D., Nomi, S. N., Solci, M. C., 2006. Integrated and sequential

- bulk and wet-only samplings of atmospheric precipitation in Londrina, South Brazil (1998–2002). *Atmos. Environ* 40, 6827–6835.
- Pena, R.M., Garcia, S., Herrero, C., Losada, M., Vazquez, A., Lucas, T., 2002. Organic acids and aldehydes in rainwater in a northwest region of Spain. *Atmos. Environ* 36, 5277–5288.
- Pike, S.M., Moran, S.B., 2001. Trace elements in aerosol and precipitation at New Castle, NH, USA. *Atmos. Environ* 35, 3361–3366.
- Pio, C.A., Castro, L.M., Cerqueira, M.A., Santos, I.M., Belchior, F., Salgueiro, M.L., 1996. Source assessment of particulate air pollutants measured at the southwest European coast. *Atmos. Environ* 30 (19), 3309–3320.
- Poissant, L., Schmit, J.P., Beron, P., 1994. Trace inorganic elements in rainfall in the Montreal Island. *Atmos. Environ* 28, 339–346.
- Possanzini, M., Buttini, P., Dipalo, V., 1988. Characterization of a rural area in terms of dry and wet deposition. *Sci. Total Environ* 74, 111–120.
- Rastogi, N., Sarin, M.M., 2005. Chemical characteristics of individual rain events from a semi-arid region in India: three-year study. *Atmos. Environ* 39, 3313–3323.
- Taylor, S.R., McLennan, S.M., 1985. *The continental crust: Its composition and evolution*, Blackwell Sci. Publ., Oxford, 330.
- Safai, P.D., Rao, P.S.P., Momin, G.A., Ali, K., Chate, D.M., Praveen, P.S., 2004. Chemical composition of precipitation during 1984–2002 at Pune, India. *Atmos. Environ* 38, 1705–1714.
- Samara, C., Tsitouridou, R., Balafoutis, C., 1992. Chemical composition of rain in Thessaloniki, Greece, in relation meteorological conditions. *Atmos. Environ* 26B,

359–367.

- Sanusi, A., Wortham, H., Millet, M., Mirabel, P., 1996. Chemical composition of rainwater in eastern France. *Atmos. Environ* 30, 59–71.
- Saxena, A., Kulshrestha, U. C., Kumar, N., Kumari, K. M., Srivastava, S. S., 1996. Characterization of precipitation at Agra. *Atmos Environ* 30, 3405–12.
- Scudlark, J.R., Conko, K.M., Church, T.M., 1994. Atmospheric wet deposition of trace elements to Chesapeake Bay: CBAD study year 1 results. *Atmos. Environ* 28, 1487–1498.
- Seinfeld, J. H., Pandis, S. N., 2006. *Atmospheric Chemistry and Physics From Air Pollution to Climate Change*, John Wiley & Sons, Inc., Hoboken, New Jersey, 294–299, 336–337.
- Spanos, T., Simeonov, V., Andreev, G., 2002. Environmetric modeling of emission sources for dry and wet precipitation from an urban area. *Talanta* 58, 367–375.
- Steven, H.C., Mulawa, P.A., Balli, J., Donase, C., Weibel, A., Sagebiel, J.C., 1997. *Environmental Science and Technology* 31, 3405.
- Tang, A., Zhuang G., Wang Y., Yuan H., Sun Y., 2005. The chemistry of precipitation and its relation to aerosol in Beijing. *Atmos. Environ* 39, 3397–3406.
- Topcu, S., Incecik, S., Atimtay, A., 2002. Chemical composition of rainwater at EMEP station in Ankara, Turkey. *Atmospheric Research* 65, 77–92.
- Tuncer, B., Bayer, B., Yesilyurt, C., Tuncel, G., 2001. Ionic composition of precipitation at the central Anatolia, Turkey. *Atmos. Environ* 35, 5989–6002.
- Ugucione, C., Felix, E.P., Rocha, G.O., Cardoso, A.A., 2002. Daytime and nighttime removal processes of atmospheric NO₂ and NH₃ in Araraquara's region - SP.

- Ecletica Quimica* 27, 1–9.
- Velzen, D. V., Langenkamp, H., Herb, G., 1998. Antimony, its sources, applications and flow paths into urban and industrial waste: a review. *Waste Management & Research* 16(1), 32-40.
- Ward, J. H., 1963. Hierarchical grouping to optimize an objective function. *J. Am. Statist. Assoc.* 58, 236-244.
- Weaver, B.L., Tamey, J., 1984. Major and trace element composition of the continental lithosphere. *Physics and Chemistry of the Earth*, 39-68.
- Wojcik G.S. and Chang J.S., 1997. A re-evaluation of sulphur budgets, lifetimes, and scavenging ratios for eastern north America. *Journal of Atmospheric Chemistry* 26, 109–145.
- Yu, S., Gao, C., Cheng, Z., Cheng, X., Cheng, S., Xiao, J., Ye, W., 1998. An analysis of chemical composition of different rain types in ‘Minnan Golden Triangle’ region in the southeastern coast of China. *Atmos. Res.*, 47–48, 245–269.
- Zhao, Y., Gao, Y., 2008. Mass size distributions of water-soluble inorganic and organic ions in size-segregated aerosols over metropolitan Newark in the US east coast. *Atmos. Environ* , doi:10.1016/j.atmosenv.2008.01.032.
- Zunckel, M., Saizar, C., Zarauz, J., 2003. Rainwater composition in Northeast Uruguay. *Atmos Environ* 37, 1601–1611.

Table 1. 1 Summary of major anions, cations concentrations and pH in precipitation (ppm).

Chemicals	pH	Cl ⁻	F ⁻	NO ₃ ⁻	SO ₄ ²⁻	NH ₄ ⁺	Ca ²⁺	Mg ²⁺	K ⁺	Na ⁺
Minimum*	3.83	0.07	<0.00	0.32	0.37	0.02	0.04	<0.00	<0.00	0.03
Maximum*	6.36	3.35	0.13	4.23	8.92	1.73	1.67	0.28	0.18	2.04
Mean*	4.57	1.08	0.03	1.38	2.64	0.64	0.21	0.05	0.06	0.60
VWA*	4.60	0.38	0.02	0.89	1.83	0.44	0.12	0.04	0.05	0.25
SD*	0.45	0.71	0.04	0.98	1.90	0.41	0.26	0.06	0.04	0.44
Spring Mean*	4.84	0.44	0.04	1.3	2.00	0.66	0.37	0.05	0.07	0.26
Summer Mean*	4.34	0.36	0.01	1.5	3.66	0.72	0.18	0.03	0.06	0.14
Fall Mean*	4.56	0.89	0.04	1.21	2.37	0.53	0.15	0.08	0.07	0.59
Winter Mean*	4.67	1.06	0.03	1.75	1.75	0.63	0.13	0.04	0.07	0.62
Shenzhen, China^a	-	1.34	0.09	1.37	7.14	0.63	3.11	0.24	0.28	0.93
Adirondack, NY^b	6.62	0.08	-	1.40	3.54	0.19	0.14	0.02	0.01	0.04
Great Bay, NJ^c	4.32	9.47	-	2.33	2.88	0.42	-	-	-	2.07
Northern Jordan^d	-	1.31	-	4.68	5.97	0.27	4.33	0.75	0.43	1.15
Galilee, Israel^e	6.26	6.25	-	1.74	14.44	0.44	1.79	0.68	0.14	3.82
Singapore^f	-	0.78	-	1.04	5.64	0.31	0.87	0.19	0.15	0.71
Ankara, Turkey^g	-	0.72	-	1.81	4.61	1.56	2.86	0.23	0.38	0.36
Spain^h	-	1.01	-	1.28	4.43	0.41	2.30	0.24	0.16	0.51
Italyⁱ	-	11.42	-	1.80	8.65	0.45	2.81	1.87	0.66	5.79
Central-Mediterranean^j	-	4.90	-	2.97	12.75	0.79	5.91	1.42	0.85	5.42

*The study region; ^aHuang *et al.*, (2008); ^bIto *et al.*, (2002); ^cAyars and Gao, ^dAl-Momani, (2003); ^eHerut *et al.*, (2000); ^fBalasubramanian *et al.*, (2001); ^gTopcu *et al.*, (2002); ^hAvila and Alarcon, (1999); ⁱLe Bolloch and Guerzoni, (1995); ^jMihajlidi-Zelić *et al.*, (2006).

Table 1. 2 Summary of trace metals concentrations in precipitation (ppb).

Chemicals	Sb	Pb	Al	V	Cr	Fe	Co	Ni	Cu	Zn	Cd
Min*	0.06	0.03	0.90	0.02	<0.01	<0.01	<0.01	0.07	0.05	1.22	<0.01
Max*	2.10	1.97	31.68	0.69	0.33	43.20	0.11	1.51	64.32	16.95	0.21
Mean*	0.36	0.47	9.54	0.28	0.06	8.35	0.02	0.55	2.82	6.60	0.03
VWA*	0.27	0.39	6.09	0.24	0.07	4.57	0.01	0.45	1.15	4.86	0.02
SD*	0.36	0.45	8.50	0.18	0.06	10.52	0.03	0.28	56.46	4.40	0.04
Spring Mean*	0.55	0.53	9.58	0.20	0.06	7.25	0.03	0.37	1.86	8.61	0.04
Summer Mean*	0.32	0.48	11.45	0.27	0.05	11.48	0.02	0.70	1.45	7.25	0.03
Fall Mean*	0.27	0.39	7.50	0.33	0.03	5.42	0.02	0.52	1.20	4.59	0.02
Winter Mean*	0.29	0.51	9.86	0.39	0.07	10.19	0.03	0.62	1.13	6.31	0.01
Northern Jordan^a	0.16	2.57	382.00	4.21	0.77	92.00	-	2.62	3.08	6.52	0.42
Mediterranean^b	-	6.20	-	-	-	-	-	-	13.60	2.60	0.40
Athens^c	-	0.88	-	-	-	4.38	-	4.14	15.41	33.46	0.20
Western Europe^d	-	2.80	-	-	-	-	-	-	1.40	21.80	0.11
Western Massach^e	0.23	4.50	53.00	1.10	0.14	65.00	-	0.75	0.95	3.70	0.31
Rhode Island^f	0.05	-	71.00	0.80	-	38.00	-	-	-	4.50	-
New Castle, US^j	-	-	24.00	-	-	23.00	-	-	1.30	26.00	-
Montreal, Canada^h	0.25	-	18.00	-	-	91.00	-	-	4.00	28.00	-

*The study region; ^aAl-Momani, (2003); ^bMihajlidi-Zelić *et al.*, (2006); ^cKanellopoulou, (2001); ^dDeboudt *et al.*, (2004); ^eDasch and Wolff, (1989); ^fHeaton *et al.*, (1990); ^gPike and Moran, (2001); ^hPoissant *et al.*, (1994).

Table 1. 3 Concentrations of selected organic acids in precipitation at Newark (ppm).

Chemicals	Ac⁻	HCOO⁻	CH₂(COO)₂²⁻	C₂O₄²⁻
Minimum*	<0.01	<0.01	<0.01	<0.01
Maximum*	1.13	0.82	0.31	0.22
Mean*	0.25	0.22	0.03	0.06
VWA*	0.21	0.20	0.03	0.06
Spring Mean*	0.16	0.24	0.04	0.08
Summer Mean*	0.48	0.40	0.05	0.10
Fall Mean*	0.11	0.10	0.01	0.02
Winter Mean*	0.16	<0.01	0.04	0.02
SD*	0.27	0.23	0.06	0.06
California, USA^a	0.43	0.45	0.072	0.16

*This work; ^aG. Brooks et al., (2006).

Table 1. 4 Summary of Fractional Acidity and Neutralization factors of NH_4^+ , Ca^{2+} and Mg^{2+} .

	Contribution of acidic ions			FA	NF (NH_4^+)	NF (Ca^{2+})	NF (Mg^{2+})
	Organic Acid	Nitrate	Sulfate				
Range	0-0.32	0.13-0.50	0.46-0.80	0.023-0.65	0.14-1.76	0.028-1.48	0.0019-0.46
Average	0.12	0.26	0.62	0.42	0.80	0.15	0.070
VWA	0.14	0.22	0.64	0.47	0.72	0.10	0.070

Table 1. 5 Summary of Enrichment Factors.

	EF_{Seawater}	EF_{Crust}
Sb	73100	25300
Pb	1070000	414
Al	446000	1.00
V	12500	42.8
Cr	14500	49.0
Fe	197000	0.89
Co	5510	4.78
Ni	12700	136
Cu	6200	714
Zn	64500	1280
Cd	16300	3140
Cl⁻	1.42	107000
F⁻	1320	1170
Ca²⁺	28.4	51.2
Mg²⁺	1.48	44.8
K⁺	8.99	60.5
Na⁺	1.00	397

Table 1. 6 Varimax Rotated Factor Loadings.

	F1	F2	F3	F4	F5	F6
Sb	0.395	0.117	-0.205	0.759	0.017	-0.171
Pb	0.548	0.024	-0.183	0.683	0.078	-0.272
Al	0.825	0.341	-0.122	0.242	0.193	-0.038
V	0.243	0.212	-0.566	0.102	0.113	-0.51
Cr	0.77	0.17	-0.109	0.365	0.136	-0.241
Fe	0.766	0.347	-0.097	0.293	0.103	-0.267
Co	0.867	-0.021	0.013	0.187	0.024	-0.025
Ni	0.147	-0.011	-0.001	0.23	0.865	-0.271
Cu	0.486	-0.015	-0.111	0.528	0.474	-0.236
Zn	0.439	0.165	0.013	0.601	0.383	0.101
Cd	-0.01	0.029	0.023	0.845	0.147	0.196
CH ₃ COO ⁻	-0.05	0.86	0.204	0.074	-0.003	-0.293
Cl ⁻	0.053	-0.241	-0.942	0.077	0.02	-0.064
F ⁻	0.698	-0.379	-0.023	-0.297	0.074	0.082
HCOO ⁻	0.014	0.883	0.264	0.069	-0.068	-0.058
CH ₂ (COO) ₂ ²⁻	0.075	0.383	0.127	-0.052	0.128	-0.582
NO ₃ ⁻	0.753	0.423	-0.208	0.161	0.17	-0.245
C ₂ O ₄ ²⁻	0.235	0.827	0.191	0.021	-0.017	0.171
SO ₄ ²⁻	0.41	0.721	-0.176	0.074	0.269	-0.221
NH ₄ ⁺	0.603	0.609	-0.174	0.079	0.34	0.073
Ca ²⁺	0.749	0.371	-0.245	0.219	0.122	0.273
Mg ²⁺	0.156	-0.034	-0.941	0.051	0.084	0.171
K ⁺	0.276	0.243	-0.465	0.134	0.644	0.272
Na ⁺	0.056	-0.269	-0.939	0.047	0.033	-0.025
H ⁺	0.279	0.75	-0.011	0.074	0.129	-0.44
Eigen Values	5.97	4.81	3.65	2.99	1.93	1.63
%Variance	23.9%	19.2%	14.6%	12.0%	7.7%	6.5%

Table 1. 7 Scores of selected clusters model and seasonal distribution of precipitation events.

CLUSTER	Significant Factors included	*Precipitation events distribution			
		Spring	Summer	Autumn	Winter
C1	F1, F2, F3, F4, F5	3	7	9	3
C2	F1	4	1	-	-
C3	F3	-	-	5	-
C4	F2	-	4	-	-
C5	F4, F5	1	3	1	-
C6	F1, F6	-	-	-	1

*4 precipitation events with missing variables were not included



Figure 1. 1 Map of sampling location.

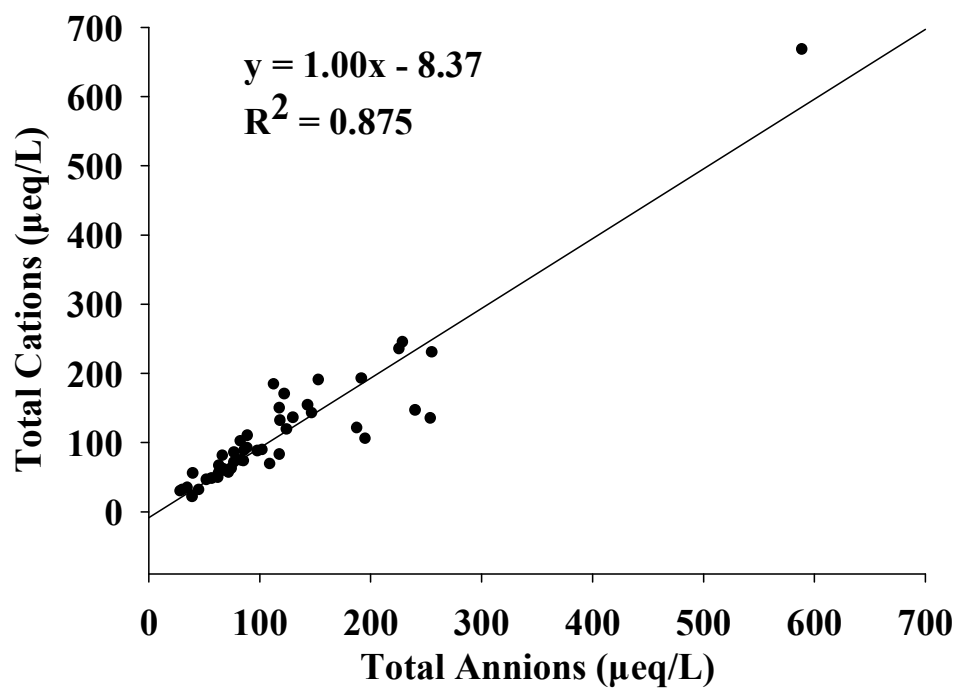


Figure 1. 2 Electric charge equilibrium between total anions and total cations.

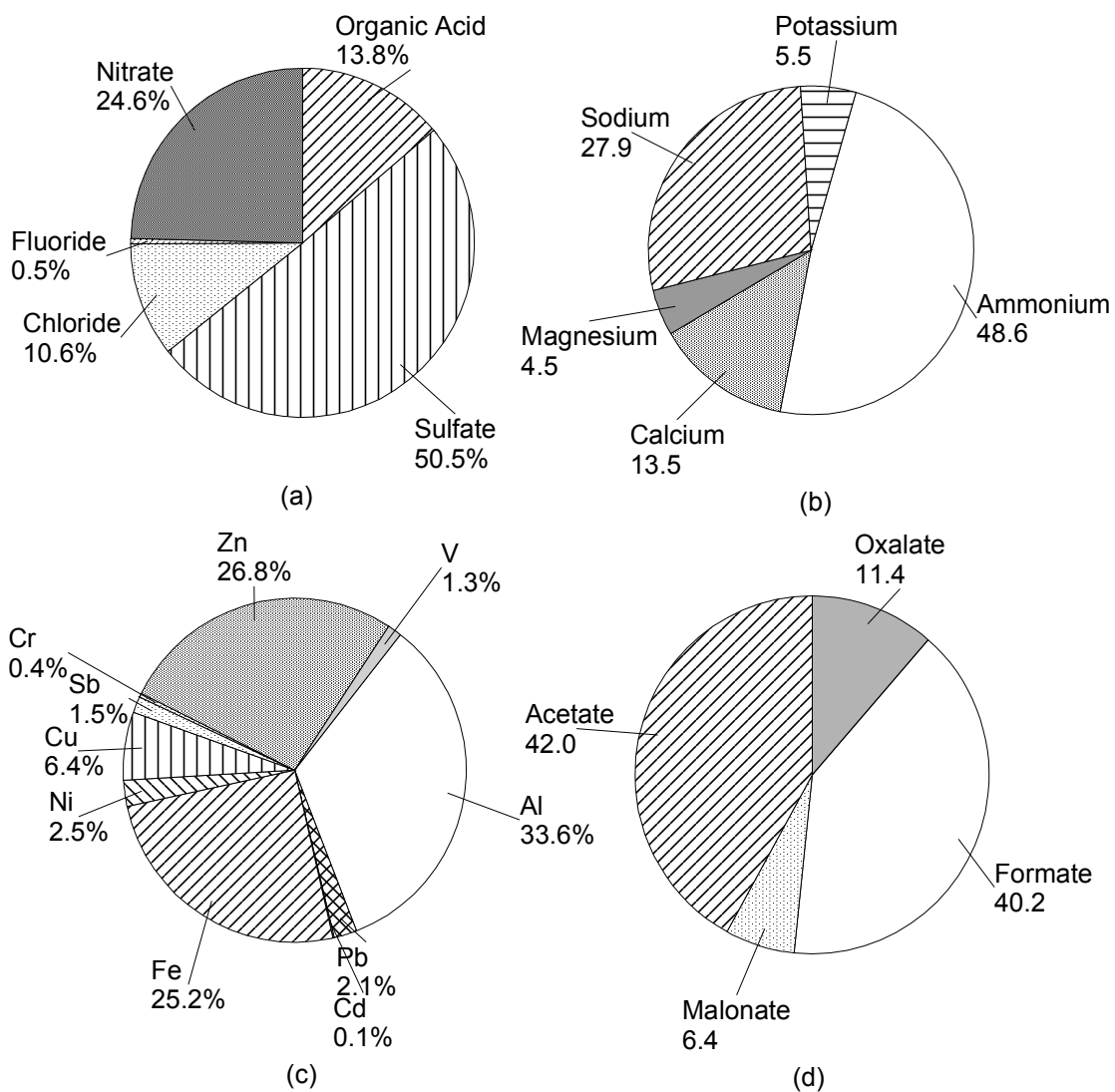


Figure 1. 3 Pie charts of Anions, Cations, Trace Metals and Organic Acid, shown in (a), (b), (c), (d) respectively.

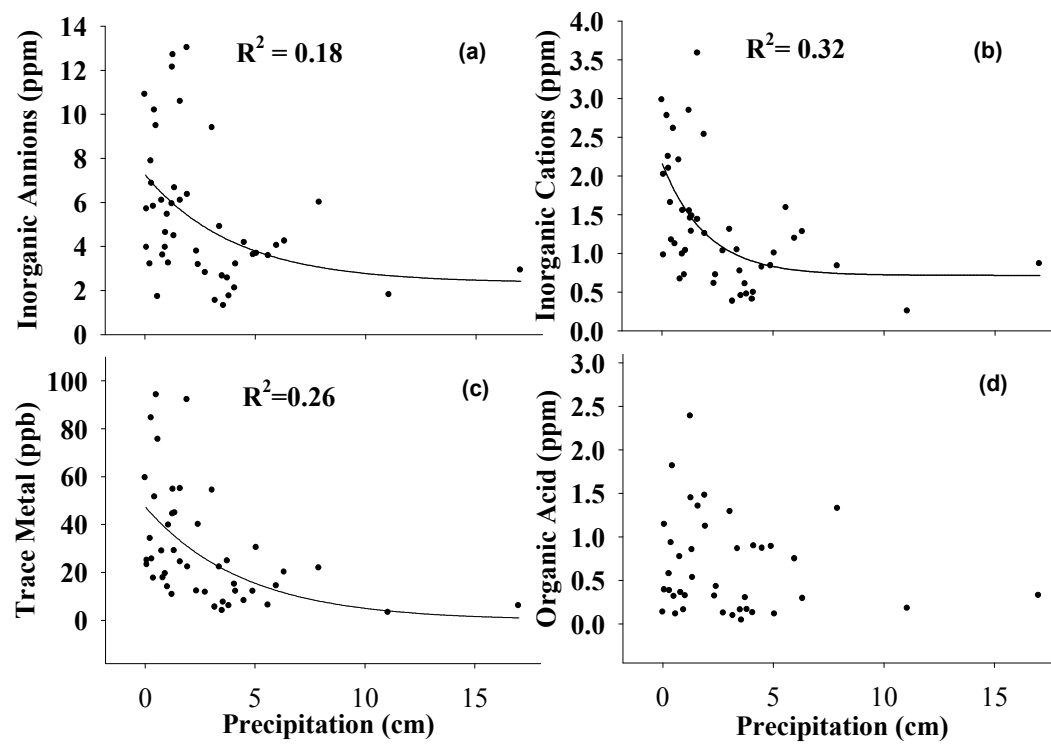


Figure 1. 4 Dilution effect of Precipitation volume on total anions (a), total cations (b), trace metals (c) and Organic Acid (d).

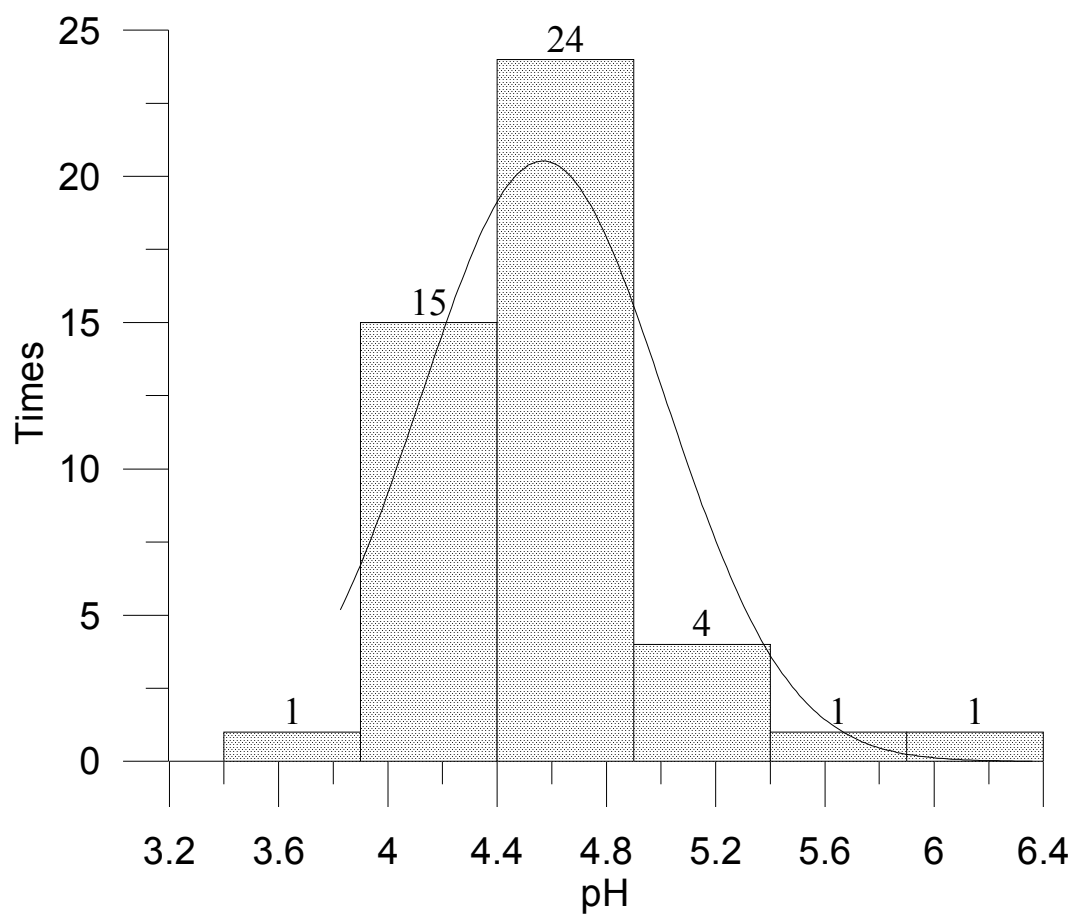


Figure 1. 5 Histogram of pH.

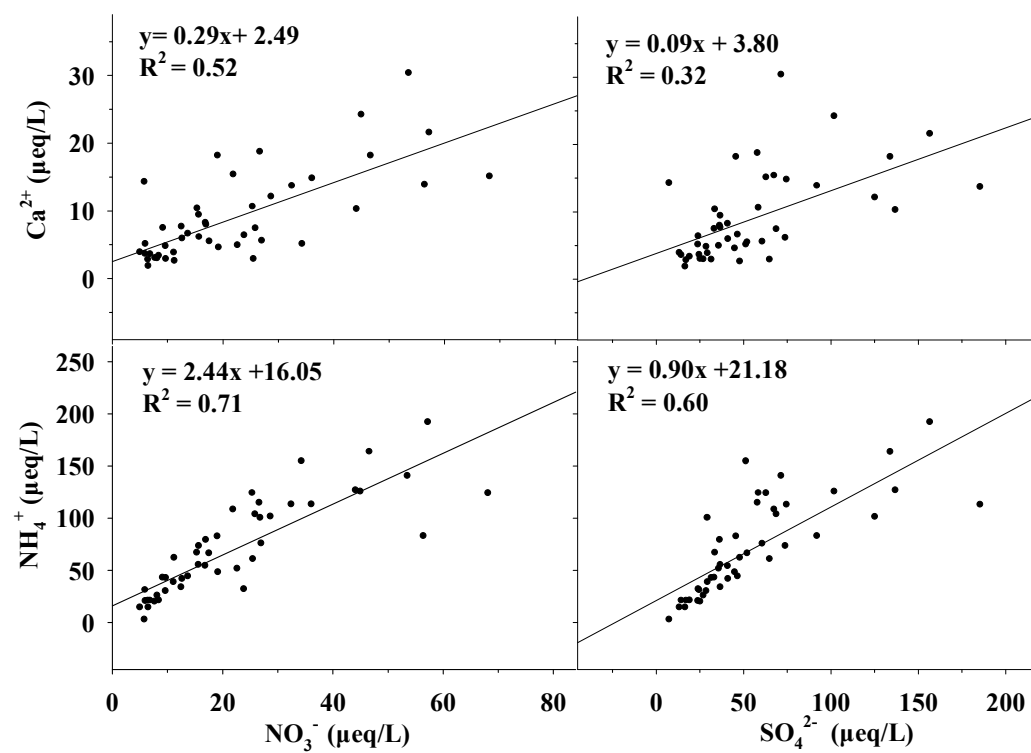


Figure 1. 6 Correlations between major cations NH_4^+ , Ca^{2+} and major anions NO_3^- and SO_4^{2-} .

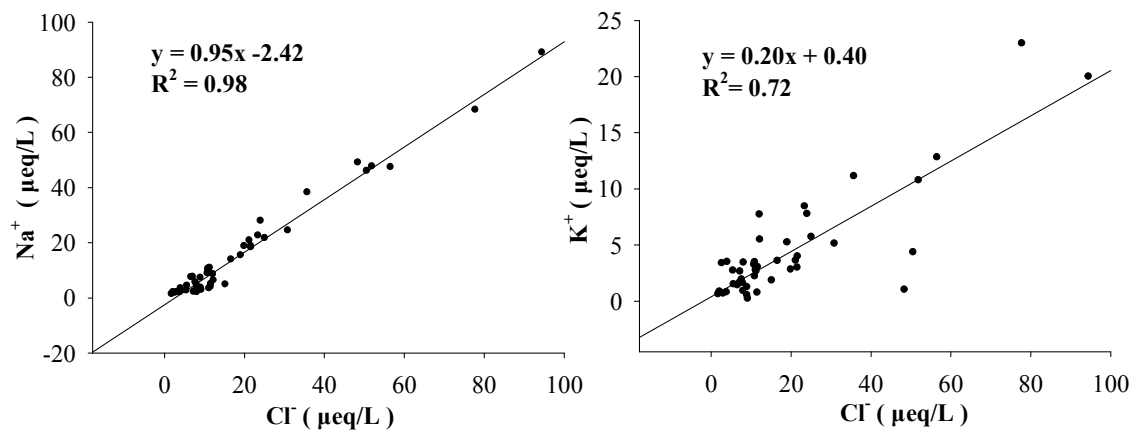


Figure 1. 7 Correlations between Cl⁻ and Na⁺, K⁺ in precipitation.

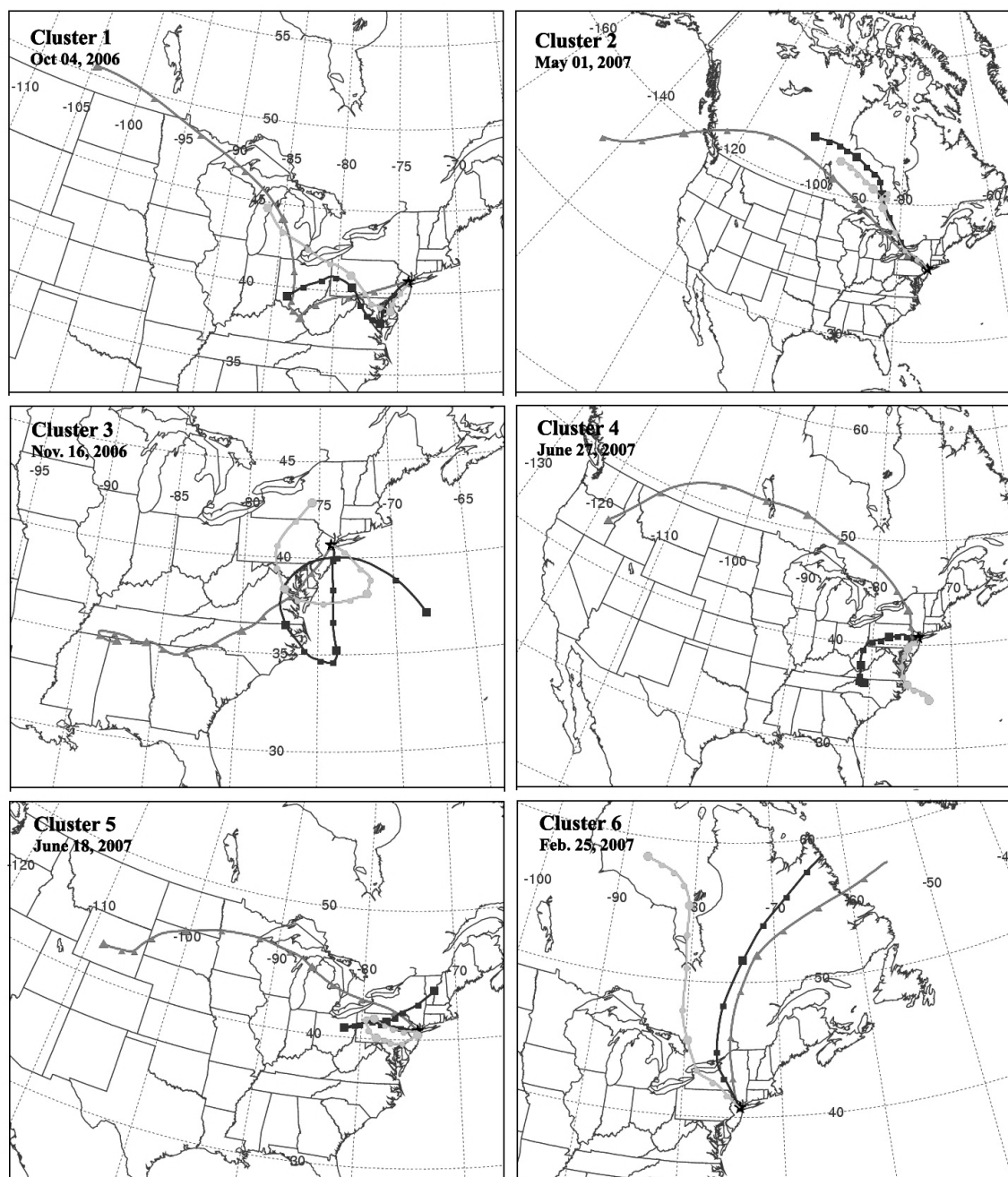


Figure 1. 8 Examples of the air mass back-trajectories for each cluster of the precipitation with height of 20m, 500m and 2000m.

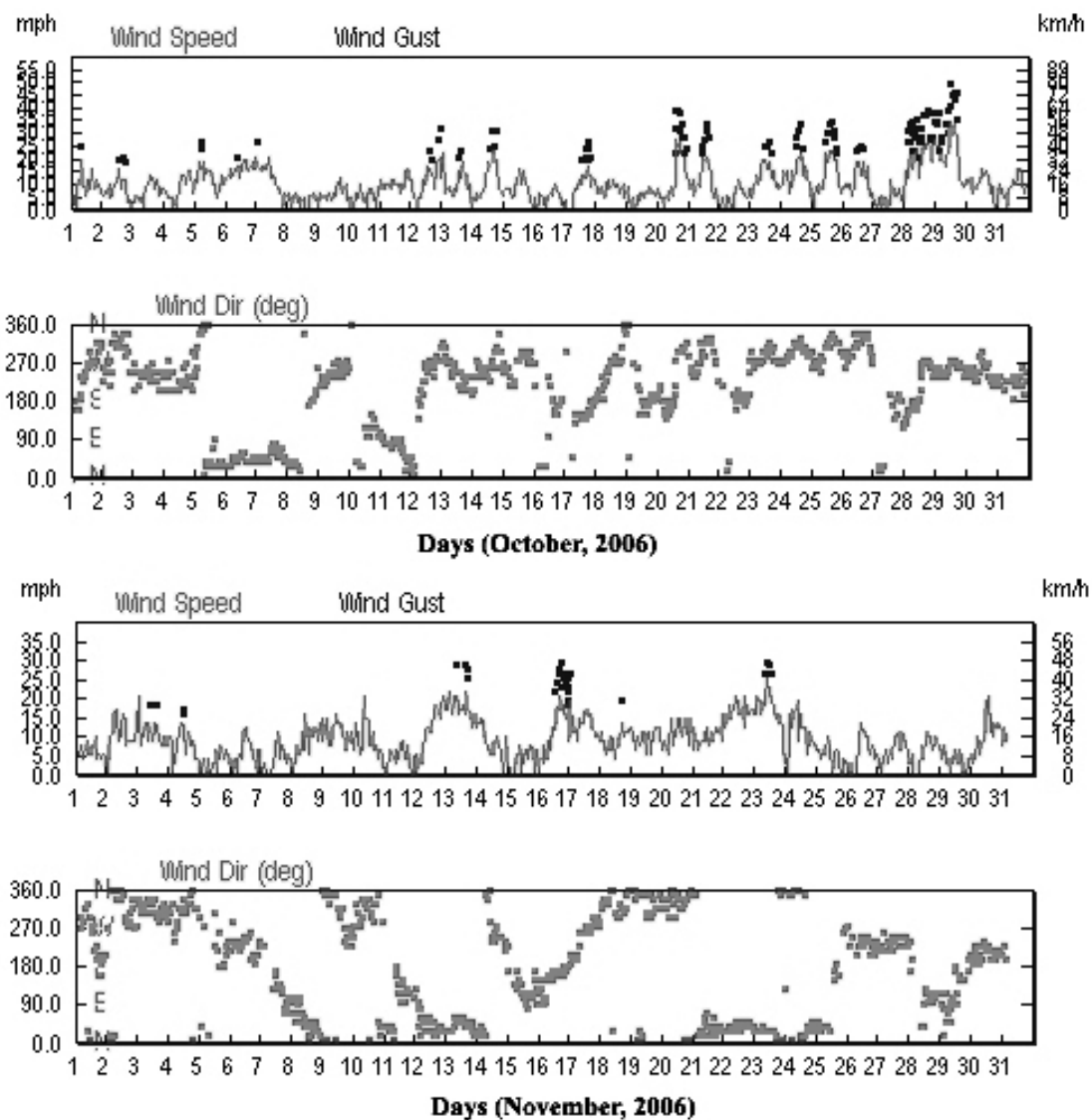


Figure 1. 9 Examples of the wind speed and wind directions in precipitation periods.

**Chapter 2 . Size Distributions of Trace Elements Associated with
Ambient Particular Matter in the Affinity of Highways
in the New Jersey-New York Metropolitan Area on the
US East Coast***

** This work has been submitted to Atmospheric Environment and it is under review as of April, 16th 2011.*

Abstract

To characterize the size distributions of trace elements associated with particulate matter in the areas heavily impacted by traffics, 11 sets of size segregated aerosol samples were taken using a MOUDI sampler in winter and summer of 2007-2008 along the side of a highway in the northeast New Jersey near New York City. Selected trace metals (Al, Cd, Co, Cr, Cu, Fe, Mn, Ni, Pb, Sb, Sc, V and Zn) in aerosol samples were determined by ICPMS. Results showed that the concentrations of these elements varied seasonally. A typical mass-size bimodal distribution with peaks at the size range of 0.32-0.56 μm and 3.2-5.6 μm was identified, and the general size distributions of the mass concentrations did not change significantly with seasons. Trace metals of potential anthropogenic origin, including Cd, Fe, Ni, Pb, Zn, Sb and Co, had higher concentrations and enrichment levels in winter, especially for fine particles. For trace metals of crustal origin, such as Fe and Sc, their size distributions of enrichment factors showed significant seasonal variations while no such variations found for anthropogenic trace metals such as Cd, Cr, Ni, Pb, Sb, V, Zn and Co. The size distributions of trace metal enrichment factors showed primarily monotonic decline patterns with overwhelmingly high peaks in the size range of 0.18-0.32 μm for most of the trace metals from pollution sources. Crustal elements, including Fe, Cu (summer), Mn (summer) and Sc (winter), however, showed tilted normal distributions pattern with peaks at 1.0-1.8 μm . Two groups of size distributions in trace metal concentrations were identified using cluster analysis: (1) coarse particles (>1.0 μm) with accumulation of mainly crustal trace metals such as Al, Fe, Sc, and Mn; (2) fine particles (<1.0 μm) with accumulations of trace metals of anthropogenic origins such as Cd, Pb, Ni, V and Co. Three major types of sources for

these metals were identified at this location: (1) brake wear, fuel combustion, (2) primary fuel combustion, and (3) tire abrasion and fuel combustion. The particulate trace metals in the study area are primarily characterized by either the mixed sources or the exhaust emissions source. Weather factors, in particular temperature, wind speed and precipitation, were found to significantly ($\alpha = 0.05$) influence the concentrations of trace metals and their size distributions.

Key Words: Size distributions, trace metals, urban air pollution, traffic emission.

2.1. Introduction

Atmospheric trace metals and their size distributions in particulate matters can influence both human health and ecology environment (Berggren et al., 1990; Hinds, 1999; Ghio et al., 1999; Allen et al., 2001; Gao et al., 2002). By inhalation and respiration, airborne particles enriched with potentially toxic trace metals could deposit in human body and cause chronic and acute health problems (Chapman et al., 1997; Wichmann and Peters, 2000; Stieb et al., 2002, Pope et al., 2002). The particle size is an important factor controlling the deposition efficiency of trace metals (Hinds, 1999), and thus can influence greatly on the trace metals' toxicity effects (Allen et al., 2001). Previous studies found that the finer the particle, the deeper it could be deposited in the human body, and thus the more serious damages it could cause (Oberdorster et al., 2005; Karakoti et al., 2006; Ntziachristos et al., 2007). However, the knowledge for different trace metals accumulations in human bodies remains limited due to the lack of information on their size distributions and processes affecting their size characteristics such as aerosol aging, sources, and the ambient atmospheric conditions (Ondov and Wexler, 1998; Birmill et al., 2006). On the other hand, the air born trace metals in aerosols could also affect the terrestrial and coastal ecosystems via air-to-land and air-to-sea deposition (Church et al., 1984; Yang et al., 1996; De Vries and Bakker, 1996; Allen et al., 2001), and the size of atmospheric particles is an important factor affecting the rate of atmospheric dry deposition and their life time in the atmosphere (Jaenicke, 1998; Allen et al., 2001; Ntziachristos et al., 2007). Moreover, the extent of direct and indirect aerosol radioactive forcing in the earth climate system is largely dependent on the size distributions of aerosol particles, and some elements in aerosols, such iron oxides minerals, may affect

significantly on light absorption (Lafon et al., 2006). Therefore characterizing the size distributions of trace elements in aerosol particles is relevant to climate studies (IPCC, 2001).

The size distributions of trace metals in aerosols are mainly controlled by their sources, life time in the atmosphere, and the meteorological conditions (Kuhn et al., 2005; Seinfeld and Pandis, 2006; Ntziachristos et al., 2007). Trace metals from anthropogenic sources tend to accumulate in fine mode ($<1.0\mu\text{m}$) (Allen et al., 2001), while the crustal sources contribute to trace elements mainly in coarse mode ($>1.0\mu\text{m}$) (Handler et al., 2008). After particulate matter being emitted into the atmosphere, the sizes of particles may increase by coagulation or decrease due to evaporation of the water content in particles (Zhang and Wexler, 2004), resulting the changes in the size distributions. Besides, meteorological parameters, such as wind speed, temperature and relative humidity, could also influence the size distributions of trace metals in aerosols (Zhang et al., 2004; Kuhn et al., 2005). Therefore, the size distributions of trace metals in aerosols are the reflection of multiple chemical and physical processes occurring in the atmosphere.

In urban regions, vehicle related emissions including fuel combustion, tire abrasion and brake wear, and the re-suspension of road dust, are among the important sources of trace metals in the ambient air (Handler et al., 2008). Particularly, the vehicle exhausts from fuel combustion could contribute greatly to the enrichment of Cu, Fe, and Sb in aerosol particles (Pakkanen et al., 2003; Ntziachristos et al., 2007). The brake wear are also among the important sources of Pb and Mn. (Garg et al., 2000; Young et al., 2002). Besides, the additives such as Ca and Mg in motor oils could be the potential

sources for these elements in the air (Cadle et al., 1997). In general, the fine mode particles were found mainly derived from combustion processes, while the coarse particles are mainly come from the road dust re-suspensions and abrasions processes (Handler et al., 2008). However, the smallest size of road dust particles may extent to about $0.1\mu\text{m}$ that could also contribute to the mass of fine particles (Kleeman and Cass, 1998).

Although the mass size distributions of aerosols and associated trace metals in the ambient air have been studied in some regions (Berggren et al., 1990; De Vries and Bakker, 1996; Allen et al., 2001; Pakkanen et al., 2003; Ntziachristos et al., 2007; Handler et al., 2008), such studies, in particular in the affinity of heavy traffics, are limited in the US east coast region. The size distributions of trace metals enrichment factors and their potential sources categories still need further investigations. To fill the data gap in trace metal size-distributions in this region and to provide insights into the metal-health relationships, we carried out an ambient aerosol measurement focusing on the characteristics of trace metals in different size fractions. A total of 11 sets of size segregated aerosol samples were collected at the road side of the New Jersey Turnpike, one of the busiest highways in New Jersey-New York City metropolitan area. The objectives of this study are: (1) to characterize the mass size distribution of particulate mass and associated trace metals, (2) to investigate the enrichment levels of trace metals in size segregated aerosol particles and their size distributions, (3) to identify the major categories of sources contributing to the enrichments of trace metals, and (4) to explore the influences of weather conditions on the concentrations of selected trace metals and their size distributions.

2.2. Methods

2.2.1. Sampling

Intensive aerosol sampling was carried out in winter (Dec. 2007-Feb. 2008) and summer (July 2008) at Carlstadt, NJ (N40.81, W74.06) (Fig. 2.1). The sampling site was ~5m away from the roadside of the NJ Turnpike, a busy expressway connecting New Jersey and New York. The 8-stages MOUDI (Micro-Orifice Uniform Deposit Impactor, MSP) was deployed on a platform ~ 5m above the ground. The 50% cutoffs of the MOUDI sampler are 0.18, 0.32, 0.56, 1.0, 1.8, 3.2, 5.6, 10 and 18 μm , with the sampling flow rate being maintained at ~ 30.0L/min. In this study, aerosol particles with diameters below 1 μm were defined as fine particles, while the particles with the diameters between 1 μm and 18 μm were considered as coarse particles. Sampling duration for each MOUDI sample set ranged from 72 - 96 hours. As shown in Table 2.1, 6 sets of samples were collected in the winter and 5 sets in the summer. Teflon filters (Pall Corp., 47mm diameter, 1 μm pore size) were used as sampling media to collect the size-segregated particulate samples. Both loading and unloading of the filters were conducted in a 100-class laminar flow clear-room hood. After each sampling, filters were stored immediately in a refrigerator until chemical analysis. To obtain aerosol mass, filters were weighted before and after samplings in a temperature and humidity controlled room using a microbalance (Model MT-5, Mettler Toledo) at Environmental and Occupational Health Sciences Institute at Rutgers University.

2.2.2. Chemical Determination

To determine the trace metal concentrations in aerosol samples, sample filters were first put into teflon digestion vessels, and then pure nitric acid (Optima A460-500,

Fisher Scientific) and hydrofluoric acid (Optima A463-250, Fisher Scientific) were added for the digestion of trace metals from samples. The digestion process was conducted in Microwave Accelerated Reaction System (MARS, CEM). There were three steps in the digestion process: (1) heating to 170 ± 5 °C in 5.5 min, (2) remaining at 170 ± 5 °C for 30 min for the completion of digestion, and (3) cooling down for 20 min. Then, digested solutions were diluted with Milli-Q water to reach a solution acidity of ~4% before injection into the ICP-MS system. To quantify the digestion recovery, standard reference materials (No.SRM2783, National Institute of Standard and Technology) were digested in the same way as the samples. The results showed that the recoveries of Al, Cu, Fe, Pb, V, Zn, Co, and Cr ranged from 91% to 103%. After digestion, trace metals solutions were quantitatively transferred into vials and diluted for the ICPMS determination. Selected trace metals in sample solutions, including Aluminum (Al), Cadmium (Cd), Cobalt (Co), Chromium (Cr), Copper (Cu), Iron (Fe), Manganese (Mn), Nickel (Ni), Lead (Pb), Antimony (Sb), Scandium (Sc), Vanadium (V), Zinc (Zn), were analyzed using High Resolution Inductively Coupled Plasma Mass Spectrometry (HR-ICP-MS) (Finnigan™ ELEMENT2, Thermo Scientific) at the Institute of Marine and Coastal Science of Rutgers University. The detection limits for all tested trace metals are less than 1ppq and the precision of the method is ~2%. The overall average blank levels were ~2% for Teflon filters relative to samples. All numbers for samples were obtained after subtraction of their appropriate blank values.

2.2.3. Data Processing

Statistical method of cluster analysis (Centroid Linkage Method) was carried out for quantitative identification of major mass size distributions patterns of trace metals in

aerosols. In this procedure, the concentrations of trace metals in atmosphere were first normalized to relative concentrations by setting the peak concentration in one sample set as 1 and the concentrations of other size ranges were converted to the ratios to its peak concentration, using the following equation:

$$\text{Normalized } C_i = C_i / \max_{1 \leq i \leq 8} C_i \quad (2-1)$$

where i is integer from 1 to 8 representing the 8 different size fractions in one sample set.

The major size distributions of the trace metal enrichment levels were also distinguished by cluster analysis, using the normalized enrichment factor values which were calculated similarly to the above method. At last, Factor Analysis (Principal Component Analysis, Varimax Rotation) was employed to identify the potential major sources of those trace metals associated with particulate matter in the study area. The cluster analysis and factor analysis were accomplished in MinTab 14 Statistical Software (Minitab Inc.) and SAS 9.1 (SAS).

2.3. Results

2.3.1. Concentrations and Seasonal Variations

The concentrations of trace metals in all size ranges showed seasonal variability, especially for those associated with fine mode particles as indicated by the Relative Standard Variations (RSV) in Table 2.2. This pattern may be due to the seasonal variation of local source emissions and regional weather conditions. The concentrations of the typical crustal elements, such as Al, in both fine and coarse mode particles, were mainly higher in summer, while for other trace metals, possibly dominated from anthropogenic sources, such as Cd, Cr, Cu, Fe, Ni, Pb, Zn, Sb, Co and Mn, their relatively high concentrations happened in winter, even though the total mass

concentrations were higher in summer (Table 2.2).

The seasonal RSV of trace metals in coarse particles ranged from 3% to 51%, varying among different metals. The concentrations of Co and Sc did not show significant seasonal variations, while Cd, Ni and Zn were found with RSV ~ 50%, indicating the significant seasonal variation of their sources. In the fine mode particles, the seasonal RSV of the concentrations of most trace metals (Al, Cd, Cr, Pb, V, Zn, Sc, Co) were found higher compared with those in coarse mode particles, ranging from 2% to more than 100%. Besides the seasonal variations, the inter-seasonal variations of the concentrations in each season were also observed (Table 2.2). Compared with coarse particles in summer, the variations of trace metal concentrations on the event-basis were higher in fine particles and in winter. Such variations could be caused by the instability of source emissions and the ambient atmospheric conditions (Ondov and Wexler, 1998; Seinfeld and Pandis, 2006). During the winter time, the Al, Cd, Pb and Cu showed more inter-seasonal variations in both fine and coarse mode particles, while in summer only Cu showed significant inter-seasonal variations.

2.3.2. Trace Metal Enrichment Factors

To estimate the strength of the crustal source influences, the crustal enrichment factors of trace elements were calculated based on Equation (2-2).

$$EF_{Al}(X_i) = \frac{(X_i/Al)_{PM10}}{(X_i/Al)_{Crust}} \quad (2-2)$$

where $(X_i/Al)_{Crust}$ is the average ratios of the element of interests (X) and crustal representative element (Al) (Turekian and Wedepohl, 1961; Ronov and Yaroshevsky, 1969; Weaver and Tamey, 1984; and Taylor, 1985). The EFs calculations indicate that common crustal elements (Fe, Sc and Mn) and Co were relatively lowly enriched, while all the

other trace metals were enriched from medium to high levels, primarily from anthropogenic sources. According to their crustal Enrichment Factors (EFs) in both fine and coarse particles (Table 2.3), the extents of the enrichment of trace metals with respect to the crustal source were grouped into three levels: (1) Low Enrichment (EFs<10), (2) Medium Enrichment (10< EFs<100), and (3) High Enrichment (EFs>100).

The enrichment factors of trace metals showed significant seasonal variations with much higher enrichment levels happened in winter for trace metals in both fine and coarse modes (Table 2.3), indicating possibly more contributions from anthropogenic pollution sources in that season. In addition, the magnitude of such seasonal variations was different between fine particles and coarse particles. Compared with coarse particles mainly from re-suspension of road dust and soil particles (Handler et al., 2008), trace metals in the fine mode showed more increased enrichments in winter. This suggests that the enhanced vehicle fuel combustion and domestic heating in winter could contribute more to the enrichments of trace metals in fine mode particles.

2.4. Discussions

2.4.1. Mass Size Distributions of Particulate Matter

A bimodal size distribution of the aerosol mass concentrations was observed in both winter and summer at this location (Fig. 2.2). The pattern of mass size distributions was consistent between winter and summer at a similarity level of 98.2% (Table 2.4). The two peaks were centered at $\sim 0.32\text{-}0.56\mu\text{m}$ in fine mode particles and $\sim 3.2\text{-}5.6\mu\text{m}$ in coarse mode particles. The aerosol mass was slightly more accumulated in fine particles than in coarse particles, accounting for about 56% and 54% of the total mass in winter and summer, respectively, different to the fine-particles dominating pattern in urban

Newark, NJ (Zhao and Gao, 2008) that the fine particles accounted for 64–82% of the total mass. In addition, different to the results of Zhao and Gao (2008) that mass concentrations of aerosol particles in all size ranges in winter were lower than those in summer, the mass concentrations at each size range observed in this study showed no significant seasonal variations, suggesting that the constant vehicle emissions at this site could dominate the aerosol mass in its affinity area and thus obscure the possible seasonal variations of mass concentrations caused by other factors. This comparison provides different aerosol size-distribution characteristics between an urban center and intensive vehicle emission location. On the other hand, results from this study is consistent to the conclusion of Zhao and Gao (2008) that local ambient conditions and in situ production mechanisms could be more important to the evolution of the observed mass size distributions.

Significant differences in the size distributions during different sampling events were found, especially in summer. The similarity levels of the distributions for different sampling events were 82% and 75% in winter and summer, respectively (Table 2.4), suggesting the variability in mass size distributions of particulate matter on a short-term basis. As shown in Fig. 2.2, the mass size distributions of samples #1 (in winter) and #7 (in summer) were shifted from the averaged distributions of other samples, which suggest the fluctuations of the ambient conditions on daily and weekly basis that impact the size distributions of particulate matter at this location. Many factors including the mixing layer height changes, emission intensity variations and seasonality of air mass origins may jointly contribute to the observed differences (Gerasopoulos et al., 2007; Venzac et al., 2009).

2.4.2. Mass Size Distributions of Trace Metals

The mass size distributions of trace metals did not vary significantly between winter and summer at this location, probably due to the fact that the sampling site is close to the highway thus the dominating traffic related emissions could cover the seasonality; however the variability of the mass size distributions of these metals in each season were high, especially in winter (Table 2.4). The mass size distributions of Co and Cd showed more seasonal variations while the seasonal variations of Ni and V were small. This may indicate that the source types in both seasons for Ni and V were similar and that the in situ situations such as weather conditions could not significantly change the mass size distributions of Ni and V. Most trace metals, especially Cd, Cr, Cu and Zn, showed more variations in their mass size distributions in winter, indicating their major contributing sources varied more in winter than in summer. Besides, the meteorological parameters (Temperature, Wind Speed and Humidity) changed substantially (Table 2.1) due to the longer span of sampling period (Dec-Feb) in winter than that in summer (July), which could attributed to the observed variations. In summer, Pb and Zn also showed high variations in their mass size distributions.

The mass size distributions of trace metals could be characterized into 2 groups based on the results of cluster analysis: Group I- coarse particles accumulations dominated in particles larger than $1\mu\text{m}$ and Group II- fine particle accumulations dominated in particles of smaller than $1\mu\text{m}$. Then three clusters were derived from each group (Table 2.5 and Fig. 2.3). All potential crustal trace metals including Al, Fe, Sc and Mn were included in Group I, and most of the potentially anthropogenic trace metals such as Cd, Pb, Ni, V and Co were categorized in Group II. This is consistent with the

size distribution characteristics of both crustal and anthropogenic trace metals found in other locations (Allen et al., 2001; Singh et al., 2002; Pakkanen et al., 2003).

In general, the mass size distributions in Group I showed bimodal patterns with primary peak at the size range of 3.2-5.6 μm , and secondary peak at the size range of 1.0-1.8 μm (Fig. 2.3), and this was divided further into three clusters (1, 2, 3)(Table 2.5; Fig. 2.4). Cluster 1, consisted with crustal trace metals (Al, Fe, Sc and Mn) and Cr in both winter and summer, was characterized by relatively higher primary peak while the secondary peak was much lower. For the trace metals in Cluster 2 (Cu and Sb), the secondary peak was almost as high as the primary peak, showing a typical bimodal pattern. The size distribution of Co in summer was similar to that of Cluster 1 except for the peak at size range of 0.18-0.32 μm , and thus it was distinguished from other elements and stood alone as Cluster 3. The mass size distributions of trace metals in Group II that was also further divided into three clusters (4, 5, 6) were mainly characterized by a decreasing trend in size from fine to coarse modes, with a major peak at 0.18-0.56 μm (Fig. 2.4). The mass size distribution of Cd in winter, the only element in Cluster 4, was unique and characterized by a bimodal distribution with the primary peak at the size range of 0.56-1.0 μm and secondary peak at 3.2-5.6 μm . The Pb and Zn in both seasons and Cd in summer were grouped into Cluster 5, which was characterized by three decreasing peaks at the size ranges of 0.32-0.56 μm , 1.0-1.8 μm and 3.2-5.6 μm , respectively. The trace metals in Cluster 6 also showed a decreasing pattern in mass size distributions with a high peak at 0.18-0.32 μm , although a smaller peak existed at the size range of 3.2-5.6 μm in the distributions. The Ni, V in both seasons and Co in winter were included in Cluster 6.

Compared with previous studies, different mass size distributions for Zn, Co, Cu, Pb, Sb, Ni, and V were found at this location (Fig. 2.4). The accumulation levels of these metals in fine particles were relatively high compared with the results from other regions, such as the United Kingdom (Allen et al., 2001), Los Angeles Basin (CA) in the US (Singh et al., 2002) and Finland (Pakkanen et al., 2003). Besides, the Pb, Zn, Co, Ni and V showed the highest accumulation levels at the size range of 0.18-0.32 μ m in the fine particles, while for Cu and Sb the accumulation levels at each size range of fine particles were similar. These results indicated the characteristics of the traffic related trace metal pollutions and the important contributions of combustion exhaust emissions, which will be discussed further Section 4.4 of this paper.

2.4.3. Enrichment Factor Size Distributions of Trace Metals

In-season and seasonal variations of the EF size distributions of trace metals were different for both crustal elements (Cu, Fe and Sc) and trace metals of potential anthropogenic origins (Cd, Cr, Ni, Sb, V, Zn and Co), as shown in Table 2.3. In general, the EF size distributions of trace metals for potential crustal trace metals showed much higher seasonal and in-season variations. Compared with summer, the intra-season variations of the EF size distributions were greater in winter. While for anthropogenic trace metals, both the seasonal and intra-season variations of EF size distributions were much less, indicating that the anthropogenic sources of trace metals did not change much during different seasons or sampling events since the vehicle related emissions were the major sources. Comparatively, the intra-season variations of the EF size distributions were higher in summer.

For most trace metals, the EF size distributions were found approximately a

monotonic decline pattern with highest enrichment level in very fine particulate, except some common crust originated metals such as Fe, Mn, Sc (winter) and Cu (summer). This is consistent to the previous findings that most trace metals are more enriched in fine particulate matter in urban regions dominated by anthropogenic emissions (Bayens and Dedeurwaerder, 1991; Chan et al., 1997; Wang et al., 2006). As shown in Fig. 2.5, 3 clusters were identified representing the major EF size distributions of trace metals using normalized EFs data. Both Clusters 1 and 2 showed tilted normal distributions with peak at the size range of 1.0-1.8 μm . However, for Cluster 1, the trace metals in fine particles were more enriched than in coarse mode, while the reverse situations were observed for Cluster 2. The common potential crustal elements Fe, Sc (winter), Mn and Cu (summer) were the major trace metals that showed EF size distributions of cluster 1 and 2, indicating the possibly less influence caused by fine particle related vehicle direct emissions via fuel combustion, and this was consistent with their low enrichment levels (Table 2.3). The EF size distributions for the other trace metals fell into the Cluster 3, which showed overwhelmingly high peak at the size of 0.18-0.32 μm and decreasing enrichment levels from small to big particles size. Besides, a tiny peak may also occur in the size range of 0.56-1.8 μm for the EF size distributions of Cluster 3. The differences in the enrichment levels of these trace elements across a wide range of particle sizes indicate the different sources, transportation and production processes for these elements (Birmili et al., 2006; Moreno et al., 2006; Chen et al., 2008).

2.4.4. Trace Metal Sources Identification

Using the concentrations data of trace metals in both fine and coarse particles, Factors Analysis (with Principal Component Factor Analysis and Varimax Rotation

methods) was employed to find the latent underlying factors which account for the correlations among observed trace metals, thus to better explain the potential sources for these trace metals. As shown in Table 2.6, three factors were extracted that represent different types of sources relating to traffic emissions, with the key elements highlighted in bold: Factor 1, brake wear, fuel combustion, and urban pollutions; Factor 2, primary fuel combustion; and Factor 3, tire abrasion and fuel combustion. The factor analysis divided the traffic pollution into two main emission types successfully: exhaust and non-exhaust pollution that will be discussed in more details below. In addition, it also divided the non-exhaust emissions into two major types: brake wear emissions and tires abrasion emissions (Thorpe and Harrison, 2008). A total of 86.9% variations could be explained by the extracted 3 major source categories.

Fuel combustion (known as “exhaust emissions”), which was found contributing to all 3 major sources, was exclusively dominate in Factor 2, while brake wear and tire abrasions were the major non-exhaust emission sources represented in Factors 1 and 3. Factor 1 was characterized by Fe, Sb, Pb and Cd. Fe and Sb are the two most common trace metals found in brake related emissions caused by frictional contacts between brake systems components (Thorpe and Harrison, 2008; Gietl et al., 2010). In addition, Pb could also be originated from brake wares related emissions (Garg et al., 2000; Young et al., 2002; Pakkanen et al., 2003). However, the direct vehicle emissions could also generate Fe, Sb, Pb and Cd pollution (Pacyna, 1986; Garg et al., 2000; Young et al., 2002; Pakkanen et al., 2003; Ntziachristos et al., 2007). Sb and Cd were commonly found in the urban industry processes such as high temperature combustion and waste incineration (Pacyna, 1998; Gao et al., 2002). The trace metals charactering Factor 1 explained ~35%

variations of trace metals. The Factor 2 included Cr, Ni, V and Cu, which were primarily emitted from vehicle fuel combustion processes (Pacyna, 1998; Ntziachristos et al., 2007). A total of ~28.3% variations of trace metals concentrations observed at this location could be explained by the Factor 2. Zn and Co, both are additives of tires and road marking paint (Sorme et al., 2001), were coupled together, serving as Factor 3, which explained ~23.7% variations. The tire abrasion emission has been recognized as an important source of Zn, and a significant amount of this element was found in re-suspended tire abrasions (Adachi and Tainosho, 2004, Councell et al., 2004, Schauer et al., 2006). In addition, Zn and Co could also come from fuel combustion of different kinds (Pacyna, 1998; Weckwerth, 2001; Al-Momani, 2003). In summary, the three factors identified in this study could explain ~86.9% variations of trace metals observed at this location.

To further characterize the sources of each sampling event, cluster analysis was carried out using the Ward's method. We used the results from factor analysis instead of the original concentration data to reduce noise caused by errors in the original data (Song and Gao, 2009). Four clusters were extracted (Table 2.7), with their dominant influencing factors being interpreted: Cluster 1 with no specific source factors dominating in summer; Cluster 2 with exhaust emissions as the dominant source in winter; Clusters 3 and Cluster 4, with each including only one sample set and having brake wear and tire abrasion as a dominant source. This indicates that the dominant source for most air-borne trace metals at this location is traffic emissions, although other sources also exist. As shown in Fig. 2.6, the air mass back trajectories calculated by the NOAA HYSPLIT model indicate that the air mass for Cluster 1 was mainly from marine/coast or rural regions, which could reduce

the impact of local traffic emissions on the concentrations of trace metals in the ambient air. For Cluster 2, its air mass came mainly from the long-distance east/northeast urban areas, and thus could change the atmospheric characteristics of trace metals from local traffic pollution, as the combustion related fine particles could be transported from other urban regions into this area and thus increase the dominance of such source observed at this site. For Clusters 3 and 4, the air mass mainly originated from neighbor states in relatively short-distance, New York and Pennsylvania, and the short-distance transport may increase the chance of the transport of large aerosol particles, adding to the accumulation of trace metals associated with coarse particles mainly from local brake wear and tire abrasion. Therefore, the concentrations and size characteristics of trace metals observed at this location were affected by many sources.

2.4.5. Weather Influence on Trace Metal Concentrations and Size Distributions

The differences of trace metals concentrations and size distributions in different events and seasons indicated significant ($\alpha = 0.05$) influences from weather conditions such as temperature, wind speed and precipitation. As shown in Table 2.8, the temperature could influence significantly trace metals concentrations in both coarse and fine particulate, especially in fine particulate mode. In particular, common anthropogenic trace metals (Pb, Zn, Co, Ni) showed negative concentration-temperature correlations, which could be explained by the influence of ambient temperature on vehicle exhaust emissions (Mulawa and Cadle, 1997). Wind speed was found of effective effects to reduce the air mass and trace metals concentrations in roadside region because of the potential disperse effects. As shown in Table 2.8, the high wind speed tends to accumulate trace metals (such as Al, Pb and Sc) in fine particulate mode, and the high

precipitation volume tends to accumulate trace metals (such as Al, V and Sc) in coarse particulate mode. However, local wind direction was not found of obvious influences on trace metal concentrations and size distribution. On the other hand, the precipitation could also reduce the air mass and trace metals concentrations effectively because of the flushing effects, especially for fine particles as shown in Table 2.8. The weather influences on the concentrations of trace metal differed at different size ranges, thus leading to the change of its size distributions.

2.5. Conclusions

Results from this study on size distribution characteristics of trace metals and their enrichment factors carried out during 2007-2008 in Carlstadt, NJ lead to the following conclusions:

The mass size distributions in both seasons showed typical bimodal patterns, with peaks in the size ranges of 0.32-0.56 μm and 3.2-5.6 μm . The vehicle related emissions could be influential to the mass concentrations of particulate matter in the ambient air.

The patterns of mass size distributions of trace metals did not show significant seasonal variations; however, the concentrations of trace metals in all size ranges showed seasonal variations, especially for trace metals in fine particles. In both fine and coarse particles, the concentrations of crustal elements such as Al and Sc were higher in summer while the typical anthropological elements Cd, Fe, Ni, Pb, Zn, Sb and Co showed higher concentrations in winter. The elements, Zn, Co, Cu, Pb, Sb, Ni, and V, were found of more accumulated in fine mode.

The enrichment factors of trace metals showed different seasonal variations in different size ranges, with higher enrichment levels in winter than in summer, especially

for fine particles. For crustal trace metals such as Cu, Fe, Sc, their EF size distributions showed large seasonal variations, while no such obvious variations were found with anthropogenic trace metals including Cd, Cr, Ni, Pb, Sb, V, Zn and Co. The EF size distributions of most trace metals showed a monotonic decline pattern. Specifically, 3 clusters of the major EF size distributions patterns were identified: (1) declined normal distribution with fine particles accumulations and peak in 1.0-1.8 μm for Cu (summer) and Fe (winter); (2) inclined normal distribution with coarse particles accumulations and peak in 1.0-1.8 μm for Fe (summer), Sc (winter) and Mn (summer); (3) monotonic decline patterns with overwhelming peak in 0.18-0.32 μm for rest of trace metals.

Using cluster analysis method, the mass size distributions of the 13 trace metals were characterized into 2 groups: (1) coarse particle accumulation with crustal trace metals such as Al, Fe, Sc and Mn, showing bimodal pattern with primary peak at the size range of 3.2-5.6 μm , and secondary peak at 1.0-1.8 μm range; (2) fine particle accumulation for most of the typical anthropogenic trace metals such as Cd, Pb, Ni, V and Co, showing decreasing concentrations from small to large particles with major peaks at 0.18-0.32 μm range.

Three primary sources explaining a total of ~86.9% variations in trace metal mass-size distributions were: (1) brake wear, fuel combustion and urban pollutions, (2) primary fuel combustion, and (3) tire abrasion and fuel combustion. Weather parameters, in particular temperature, wind speed and precipitation, were found to be effective on the concentrations and size distributions of trace elements observed at this location.

Acknowledgment

This work was sponsored by The US EPA with the Award #XA97268501. Additional support was provided by Rutgers University through a New Faculty Start-up Fund to YG. We thank Jin Young Shin, Christopher Thuman, and Irene Jung for assistance with sampling and M. Paul Field and Christine Theodore for assistance with ICPMS analysis. We are grateful to Francisco Artigas and Christine Hobbie for the operation of the sampling sites during this study.

2.6. References

- Adachi, K., Tainosho, Y., 2004. Characterization of heavy metal particles embedded in tire dust. *Environment International* 30, 1009-1017.
- Allen, A.G., Nemitz, E., Shi, J.P., Harrison, R.M., Greenwood, J.C., 2001. Size distribution of trace metals in atmospheric aerosols in the United Kingdom. *Atmospheric Environment* 35, 4581-4591.
- Al-Momani, I. F., 2003. Trace metals in atmospheric precipitation at Northern Jordan measured by ICP-MS: acidity and possible sources. *Atmospheric Environment* 37, 4507–4515.
- Bayens, W., Dedeurwaerder, H., 1991. Particulate trace metals above the southern bight of the north sea - II. Origin and behaviour of the trace metals. *Atmospheric Environment* 25, 1077–1092.
- Berggren, D., Bergkvist, B., Falkengrengrerup, U., Folkesson, L., Tyler, G., 1990. Metal solubility and pathways in acidified forest ecosystems of south Sweden. *Science of the Total Environment* 96, 103–114.
- Birmili, W., Allen, A.G., Bary, F., Harrison, R.M., 2006. Trace Metal Concentrations and Water Solubility in Size-Fractionated Atmospheric Particles and Influence of Road Traffic. *Environ. Sci. Technol.* 40 (4), 1144–1153.
- Cadle, S.H., Mulawa, P.A., Hunsanger, E.C., Nelson, K., Ragazzi, R.A., Barrett, R., Gallagher, G.L., Lawson, D.R., Knapp, K.T., Snow, R., 1999. Composition of light-duty motor vehicle exhaust particulate matter in the Denver, Colorado area. *Environmental Science and Technology* 33, 2328–2339.
- Chan, Y.C., Simpson, R.W., McTainsh, G.H., Vowles, P.D., Cohen, D.D., Bailey, G.M.,

1997. Characterisation of chemical species in PM_{2.5} and PM₁₀ aerosols in Brisbane, Australia. *Atmospheric Environment* 31, 3773–3785.
- Chapman, R.S., Watkinson, W.P., Dreher, K.L., Costa, D.L., 1997. Ambient particulate matter and respiratory and cardiovascular illness in adults: particle-borne transition metals and the heart–lung axis. *Environmental Toxicology and Pharmacology* 4 (3–4), 331–338.
- Chen, Y., Paytan, A., Chase, Z., Measures, C., Beck, A. J., Sañudo-Wilhelmy, S. A. and Post A. F., 2008, Sources and fluxes of atmospheric trace elements to the Gulf of Aqaba, Red Sea, *J. Geophys. Res.*, 113, D05306, doi:10.1029/2007JD009110.
- Church, T.M., Tramontano, J.M., Scudlark, J.R., Jickells, T.D., Tokos, J.J., Knap, A.H., 1984. The wet deposition of trace metals to the Western Atlantic Ocean at the Mid-Atlantic coast and on Bermuda. *Atmospheric Environment* 18, 2657–2664.
- Council, T.B., Duckenfield, K.U., Landa, E.R., Callender, E., 2004. Tire-wear particles as a source of zinc to the environment. *Environmental Science & Technology* 38, 4206–4214.
- De Vries, W., Bakker, D.J., 1996. Manual for calculating critical loads of heavy metals for soils and surface waters. Report 114, DLO, Winland Staring Centre, Wageningen, The Netherlands.
- Duce, R.A., Hoffman, G.L., Zoller, W.H., 1975. Atmospheric trace metals at remote northern and southern hemisphere sites: pollution or natural? *Science* 187, 339–342.
- Gao, Y., Nelson, E.D., Field, M.P., Ding, Q., Li, H., Sherrell, R.M., Gigliotti, C.L., Van Ry, D.A., Glenn, T.R., Eisenreich, S.J., 2002. Characterization of atmospheric trace metals on PM_{2.5} particulate matter over the New York–New Jersey harbor estuary.

- Atmospheric Environment 36, 1077–1086.
- Garg, B.D., Cadle, S.H., Mulawa, P.A., Groblicki, P.J., Laroo, C., Parr, G.A., 2000. Brake wear particulate matter emissions. *Environmental Science and Technology* 34, 4463–4469.
- Gerasopoulos, E., Koulouri, E., Kalivitis, N., Kouvarakis, G., Saarikoski, S., Makela, T., Hillamo, R., Mihalopoulos, N., 2007. Size-segregated mass distributions of aerosols over Eastern Mediterranean: seasonal variability and comparison with AERONET columnar size-distributions. *Atmospheric Chemistry and Physics* 7, 2551–2561.
- Ghio, A.J., Stonehuerner, J., Dailey, L.A., Carter, J.D., 1999. Metals associated with both the water-soluble and insoluble fractions of an ambient air pollution particle catalyze an oxidative stress. *Inhalation Toxicology* 11 (1), 37- 49.
- Gietl, J.K., Lawrence, R., Thorpe, A.J., Harrison, R.M., 2010. Identification of brake wear particles and derivation of a quantitative tracer for brake dust at a major road. *Atmospheric Environment* 44, 141-146.
- Handler, M., Puls, C., Zbiral, J., Marr, I., Puxbaum, H., Limbeck, A., 2008. Size and composition of particulate emissions from motor vehicles in the Kaisermuhlen-Tunnel, Vienna. *Atmospheric Environment* 42, 2173–2186.
- Hinds, W.C., 1999. *Aerosol Technology*, 2nd edition, Wiley, New York.
- International Panel of Climate Change (IPCC), 2001. Aerosols, their direct and indirect effects. *Climate Change 2001: The Scientific Basis (Chapter 5)*: 289-348
- Jaenicke, R., 1998. Atmospheric aerosol size distribution. In: Harrison, R.M., Van Grieken, R.E. (Eds.), *Atmospheric Particles*. Wiley, New York, pp. 1–28.
- Karakoti, A.S., Hench, L.L., Seal, S., 2006. The potential toxicity of nanomaterials—the

- role of surfaces. JOM— Journal of the Minerals Metals and Materials Society 58 (7), 77–82.
- Kleeman, M.J., Cass, G.R., 1998. Source contributions to the size and composition distribution of urban particulate air pollution. *Atmospheric Environment* 32, 2803–2816.
- Kuhn, T., Biswas, S., Sioutas, C., 2005. Diurnal and seasonal characteristics of particle volatility and chemical composition in the vicinity of a light-duty vehicle freeway. *Atmospheric Environment* 39, 7154–7166.
- Lafon, S., I. N. Sokolik, J. L. Rajot, S. Caquineau, and A. Gaudichet, 2006. Characterization of iron oxides in mineral dust aerosols: Implications for light absorption, *J Geophys. Res.*, 111, D21207, doi:10.1029/2005JD007016.
- Moreno, T., Querol, X., Alastuey, A., Viana, M., Salvador, P., Sánchez de la Campa, A., Artiñano, B., de la Rosa, J. and Gibbons, W. ,2006. Variations in atmospheric PM trace metal content in Spanish towns: illustrating the chemical complexity of the inorganic urban aerosol cocktail. *Atmospheric Environment* (2006) 40, 6791-6803.
- Mulawa, P.A., Cadle, S.H., 1997. Effect of ambient temperature and E-10 fuel on primary exhaust particulate matter emissions from light-duty vehicles. *Environmental Science and Technology* 31, 1302-1307.
- Ntziachristos, L., Ning, Z., Geller, M. D., Sheesley, R.J., Schauer, J.J., Sioutas, C., 2007. Fine, ultrafine and nanoparticle trace element compositions near a major freeway with a high heavy-duty diesel fraction. *Atmospheric Environment* 41, 5684–5696.
- Oberdorster, G., Oberdorster, E., Oberdorster, J., 2005. Nanotoxicology: an emerging discipline evolving from studies of ultrafine particles. *Environmental Health*

- Perspectives 113 (7), 823–839.
- Ondov, J. M., Wexler, A. S. 1998. Where do particulate toxins reside? An improved paradigm for the structure and dynamics of the urban mid-Atlantic aerosol. *Environ. Sci. Technol.*, 32, 2547–2555.
- Pacyna, J.M., 1986. In: Nriagu, J.O., Davidson, C.I. (Eds.), *Toxic Metals in the Atmosphere*. Wiley, New York.
- Pacyna, J.M., 1998. Source inventories for atmospheric trace metals. In: Harrison, R.M., van Grieken, R.E. (Eds.), *Atmospheric Particles, IUPAC Series on Analytical and Physical Chemistry of Environmental Systems, Vol. 5*. Wiley, Chichester, UK, pp. 385–423.
- Pakkanen, T. A., Kerminen, V., Loukkola, K., Hillamo, R. E., Aarnio, P., Koskentalo, T., Maenhaut, W., 2003. Size distributions of mass and chemical components in street-level and rooftop PM1 particles in Helsinki. *Atmospheric Environment* 37, 1673-1690.
- Pope, C.A. III, Burnett, R.T., Thun M.J., Calle E.E., Krewski D., Ito K., 2002. Lung cancer, cardiopulmonary mortality, and long-term exposure to fine particulate air pollution. *JAMA, J. Am. Med. Assoc.*, 287, 1132-1141.
- Ronov, A. B. and A. A. Yaroshevsky. 1969. Chemical composition of the Earth's crust. In P. J. Hart (ed.), *The Earth's Crust and Upper Mantle*, pp. 37-57.
- Schauer, J.J., Lough, G.C., Shafer, M.M., Christensen, W., Arndt, M.F., DeMinter, J.T. Park, J.S., 2006. Characterization of metals emitted from motor vehicles. *Health Effects Institute*, 88.
- Seinfeld, J. H., Pandis, S. N., 2006. *Atmospheric Chemistry and Physics: From Air*

- Pollution to Climate Change. Wiley-Interscience, 2 edition.
- Singh, M., Jaques, P.A., Sioutas, C., 2002. Size distribution and diurnal characteristics of particle-bound metals in source and receptor sites of the Los Angeles Basin. *Atmospheric Environment* 36, 1675-1689.
- Song, F., Gao, Y., 2009. Chemical characteristic of precipitation at metropolitan Newark in the US East Coast. *Atmospheric Environment* 43, 4903-4913.
- Sorme, L., Bergback, B., Lohm, U., 2001. Goods in the anthroposphere as a metal emissions source-a case study of Stockholm, Sweden. *Water, Air, and Soil Pollution: Focus* 1, 213- 227.
- Stieb, D.M., Judek, S., Burnett, R.T., 2002. Meta-analysis of time-series studies of air pollution and mortality: effects of gases and particles and the influence of cause of death, age, and season. *Journal of Air and Waste Management Association* 52, 470-484.
- Taylor, S.R., McLennan, S.M., 1985. *The continental crust: Its composition and evolution*, Blackwell Sci. Publ., Oxford, 330.
- Thorpe, A., Harrison, R.M., 2008. Sources and properties of non-exhaust particulate matter from road traffic: A review. *Science of the Total Environment* 400, 270-282.
- Turekian, K.K., Wedepohl, K.H., 1961. Distribution of the element in some major units of the earth's crust. *Geological Society America Bulletin* 72, 175-192.
- Venzac, H., Sellegri, K., Villani, D., Picard, D., Laj, P., 2009. Seasonal variation of aerosol size distributions in the free troposphere and residual layer at the puy de Dome station, France. *Atmospheric Chemistry and Physics* 9, 1465–1478.
- Wang, X., Sato, T., Xing B., 2006. Size distribution and anthropogenic sources

- apportionment of airborne trace metals in Kanazawa, Japan. *Chemosphere* 65, 2440–2448
- Weaver, B.L., Tamey, J., 1984. Major and trace element composition of the continental lithosphere. *Physics and Chemistry of the Earth*, 39-68.
- Weckwerth, G., 2001. Verification of traffic emitted aerosol components in the ambient air of Cologne (Germany). *Atmospheric Environment* 35, 5525–5536.
- Wichmann, H.-E., Peters, A., 2000. Epidemiological evidence of the effects of ultrafine particle exposure. *Philosophical Transactions of the Royal Society London A* 358, 2751–2769.
- Yang, X., Miller, D.R., Xu, X., Yang, L.H., Chen, H.-M., Nikolaidis, N.P., 1996. Spatial and temporal variations of atmospheric deposition in interior and coastal Connecticut. *Atmospheric Environment* 30, 3801–3810.
- Young, T.M., Heeraman, D.A., Sirin, G., Ashbaugh, L.L., 2002. Resuspension of soil as a source of airborne lead near industrial facilities and highways. *Environmental Science and Technology* 36, 2484–2490.
- Zhang., K. M. and Wexler, A. S., 2004. Evolution of particle number distribution near roadways—Part I: analysis of aerosol dynamics and its implications for engine emission measurement. *Atmospheric Environment* 38, 6643-6653.
- Zhao, Y., Gao, Y., 2008. Mass size distributions of water-soluble inorganic and organic ions in size-segregated aerosols over metropolitan Newark in the US east coast. *Atmospheric Environment* 42, 4063-4087.

Table 2. 1 Summary of meteorological parameters during the sampling period*.

Sampling #	Period (2007-2008)	T (°C)	Humidity (%)	Precipitation (inch)	Wind Speed (mph)
1	12/11-12/14	3.1	73.3	0.24	4
2	12/14-12/18	-0.3	59.8	0.18	9
3	12/18-12/21	1.7	66.5	0.22	3.5
4	1/29-2/1	1.9	56.3	0.22	5.5
5	2/21-2/24	-1.7	63	0.17	6
6	2/24-2/27	0.8	64.5	0.08	4
7	07/03-07/07	24.3	73.6	0.02	4
8	07/07-07/11	25.9	61.2	0.05	3.8
9	07/11-07/15	24.7	60.2	0.004	3.4
10	07/15-07/19	27.0	50.8	0.00	2.2
11	07/19-07/23	27.8	63.2	0.22	5

* Weather data were obtained from www.wunderground.com.

Table 2. 2 Summary of trace metal concentrations and the relative standard variations.

	Coarse Particle					Fine Particle				
	Winter		Summer		Seasonal	Winter		Summer		Seasonal
	C ¹	RSV ²	C	RSV		C	RSV	C	RSV	
Mass	8.15	27%	9.47	26%	11%	10.3	49%	11.0	32%	5%
Al	124	55%	180	31%	26%	4.81	77%	31.1	67%	104%
Cd	0.08	72%	0.04	27%	51%	0.12	108%	0.05	38%	62%
Co	0.12	30%	0.10	33%	9%	0.15	66%	0.05	37%	73%
Cr	1.26	40%	0.96	35%	19%	0.47	41%	0.21	61%	55%
Cu	20.2	50%	15.6	79%	18%	6.07	61%	5.88	90%	2%
Fe	332	50%	262	30%	17%	27.3	37%	21.5	28%	17%
Mn	-	-	3.89	31%	-	-	-	0.78	25%	-
Ni	1.59	19%	0.83	30%	45%	2.28	39%	1.21	27%	43%
Pb	2.04	70%	1.41	28%	26%	2.82	44%	1.27	28%	54%
Sb	1.92	50%	1.19	33%	33%	0.70	43%	0.49	34%	26%
Sc	0.03	40%	0.04	42%	3%	0.01	41%	0.00	51%	44%
V	0.94	49%	0.82	21%	10%	1.91	56%	2.58	41%	21%
Zn	14.8	29%	7.53	30%	46%	15.7	34%	5.59	20%	67%
Mean	-	45%	-	34%	24%	-	54%	-	41%	44%

¹ C: Concentrations of mass ($\mu\text{g}/\text{m}^3$) and trace metals (ng/m^3) in atmosphere.

² RSV: Relative Standard Variance, calculated as $\text{Standard Variance}/|\text{mean}| * 100\%$.

Table 2. 3 Crustal enrichment factors of trace metals in fine, coarse and all particles.

<i>Enrichment Level</i>	<i>Trace Metals</i>	<i>Fine Particle</i>		<i>Coarse particle</i>		<i>All particle</i>	
		Winter	Summer	Winter	Summer	Winter	Summer
Low	Fe	5.74	0.996	4.66	3.70	4.73	2.12
	Sc	0.0427	1.22	0.71	1.55	0.67	1.04
	Co	68.1	4.29	3.54	3.14	7.77	2.44
	Mn	-	1.77	-	3.15	-	1.98
Medium	Cr	85.5	17.4	18.4	19.0	22.7	13.2
	Ni	305.2	39.5	9.78	5.01	29.1	9.99
	V	156.3	47.0	4.80	4.51	14.7	11.1
High	Cu	1020	246	254	239	304	170.6
	Cd	10600	778	443	187	1110	243
	Sb	38700	526	7370	4570	9430	3360
Medium/ High	Pb	2090	190	90.5	65.6	222	69.7
	Zn	2340	226	147	90.6	290	89.5

Table 2. 4 Similarity levels of size distributions in/between different seasons (Centroid Linkage Method).

	Concentrations			Enrichment Factors		
	Winter ¹	Summer ¹	Seasonal ²	Winter ¹	Summer ¹	Seasonal ²
Mass	81.8%	74.5%	98.2%	-	-	-
Al	88.2%	86.8%	98.6%	-	-	-
Cd	46.2%	83.1%	82.3%	84.5%	87.1%	93.7%
Cr	68.8%	72.7%	91.8%	67.4%	38.3%	91.0%
Cu	63.1%	86.9%	97.7%	67.4%	76.1%	81.3%
Co	75.7%	84.3%	70.8%	96.6%	92.7%	99.3%
Fe	91.6%	92.9%	97.6%	66.2%	77.6%	57.5%
Mn	-	93.3%	-	-	53.9%	-
Ni	83.1%	87.7%	99.9%	98.7%	96.7%	99.5%
Pb	90.9%	60.3%	89.8%	91.1%	85.8%	97.0%
Sb	89.6%	86.3%	97.3%	93.3%	76.0%	89.8%
Sc	91.2%	86.3%	95.6%	44.6%	43.1%	15.5%
V	92.2%	98.8%	99.8%	98.7%	96.8%	99.3%
Zn	62.5%	64.1%	91.0%	93.1%	88.6%	94.4%

¹ Variations in each season.

² Seasonal variations of averaged patterns.

Table 2. 5 Size distributions of trace metals by cluster analysis.

Group	Cluster	Similarity	Component	
			Winter	Summer
Group I	C1	93.9%	Al, Cr, Fe, Sc	Al, Cr, Fe, Sc, Mn
	C2	89.5%	Cu, Sb	Cu, Sb
	C3	100%	-	Co
Group II	C4	100%	Cd	-
	C5	92.4%	Pb, Zn	Cd, Pb, Zn
	C6	93.1%	Ni, V	Ni, V, Co

Table 2. 6 Factor Analysis Result of trace metals concentrations.

	Factor1	Factor2	Factor3	Communality
Cd	0.875	-0.093	0.306	0.867
Cr	0.605	0.739	-0.071	0.917
Cu	0.007	0.89	0.208	0.835
Co	0.04	0.106	0.969	0.951
Fe	0.823	0.426	0.039	0.861
Ni	0.285	0.645	0.549	0.798
Pb	0.936	0.235	0.119	0.945
Sb	0.723	0.516	0.307	0.884
V	0.257	0.735	-0.336	0.719
Zn	0.377	-0.094	0.875	0.917
Variance	3.50	2.83	2.37	8.69
Var%	0.350	0.283	0.237	0.869

Table 2. 7 Identified Clusters of MOUDI sampling events and their dominant factors.

CLUSTER	Dominant Factors	MOUDI Sampling #	
		Winter	Summer
C1	None	2	8, 9, 10, 11
C2	F2	1, 3, 4	7
C3	F3	5	-
C4	F1	6	-

Table 2. 8 Correlations between weather parameters and trace metal concentrations.

Coarse Particles					Fine Particles				
Item	Mid Dp	Temp.	Wind Speed	Precip.	Item	Mid Dp	Temp.	Wind Speed	Precip.
Mass	4.4	0.684* (0.02)**	-0.772 (0.005)	-0.69 (0.019)		0.78	0.61 (0.046)	-	-
Al	7.8	-	-0.626 (0.039)	-	Al	0.44	0.729 (0.011)	-	-0.765 (0.006)
Cr	7.8	-	-0.617 (0.043)	-		0.25	0.694 (0.018)	-	-0.685 (0.02)
Ni	14	-	0.62 (0.042)	-	Pb	0.44	-0.617 (0.043)	-	-
	7.8	-0.632 (0.037)	-	-		0.25	-0.608 (0.047)	-	-
Pb	14	-	-0.69 (0.019)	-	V	0.44	-	-0.751 (0.008)	-0.661 (0.027)
	7.8	-	-0.759 (0.007)	-		0.25	-	-0.724 (0.012)	-0.63 (0.038)
Sc	14	-	-0.798 (0.003)	-	Zn	0.44	-0.699 (0.017)	-	-
	7.8	0.649 (0.031)	-0.714 (0.014)	-		0.25	-0.713 (0.014)	-	0.665 (0.025)
	4.4	0.713 (0.014)	-	-	Sc	0.78	0.865 (0.001)	-	-0.681 (0.021)
	2.5	0.669 (0.024)	-	-		0.44	0.919 (<0.001)	-	-0.731 (0.011)
	1.4	0.812 (0.002)	-	-		0.25	0.945 (<0.001)	-	-0.645 (0.032)
Co	2.5	-	-	0.633 (0.037)	Co	0.44	-0.644 (0.033)	-	0.618 (0.043)

* Correlation factors.

** Significant levels.

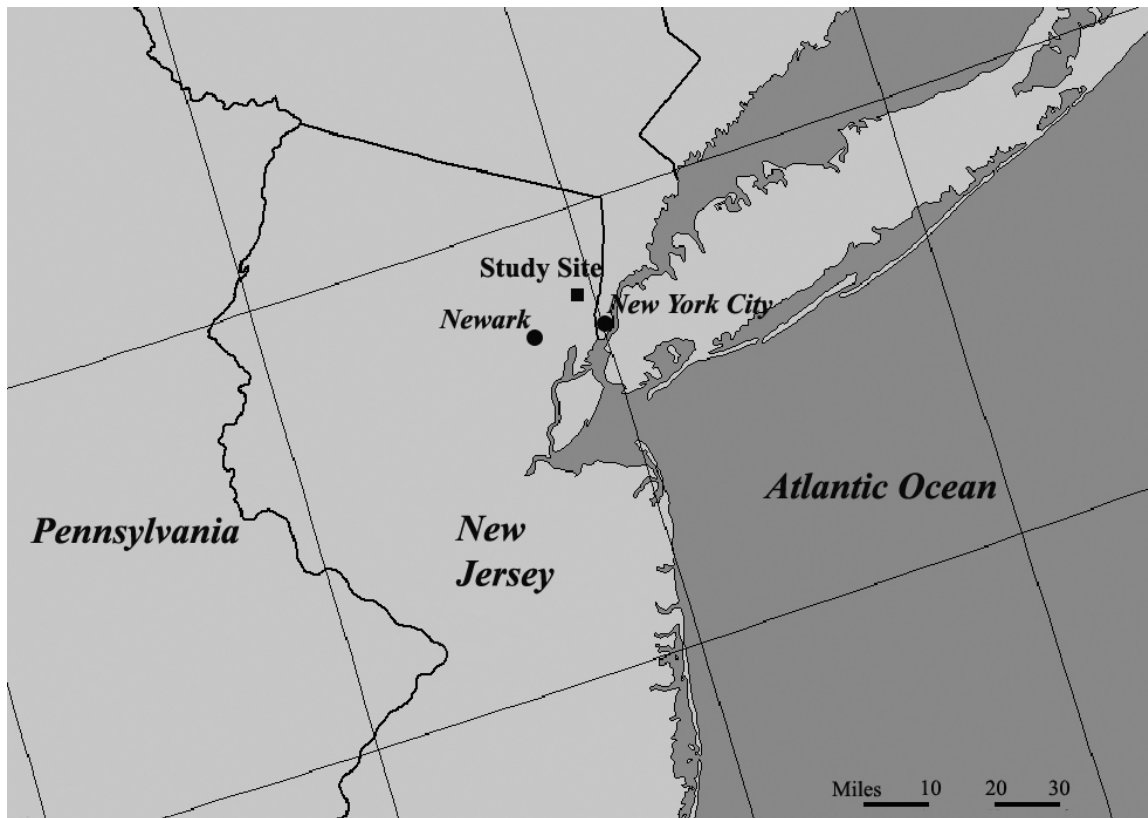


Figure 2. 1 Map of sampling location.

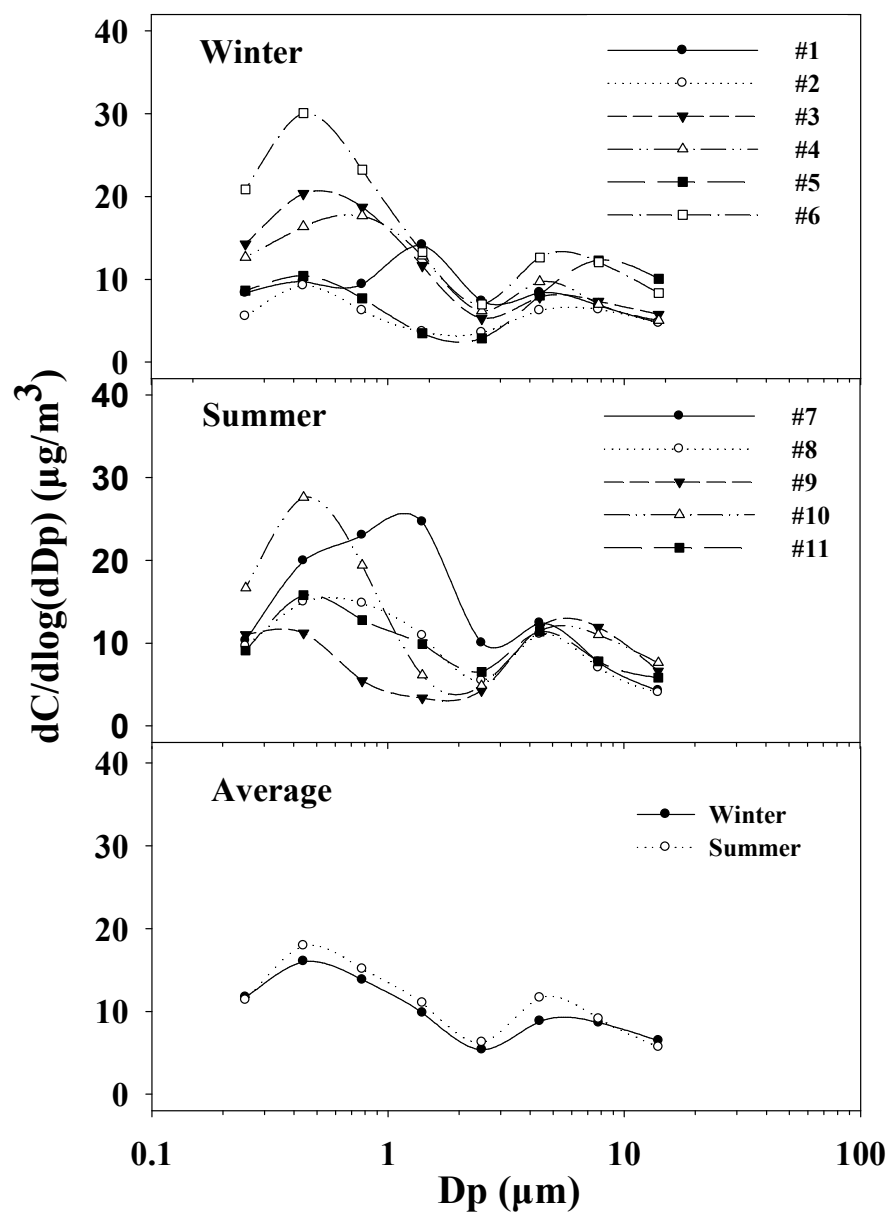


Figure 2. 2 The mass size distribution of particles in winter and summer.

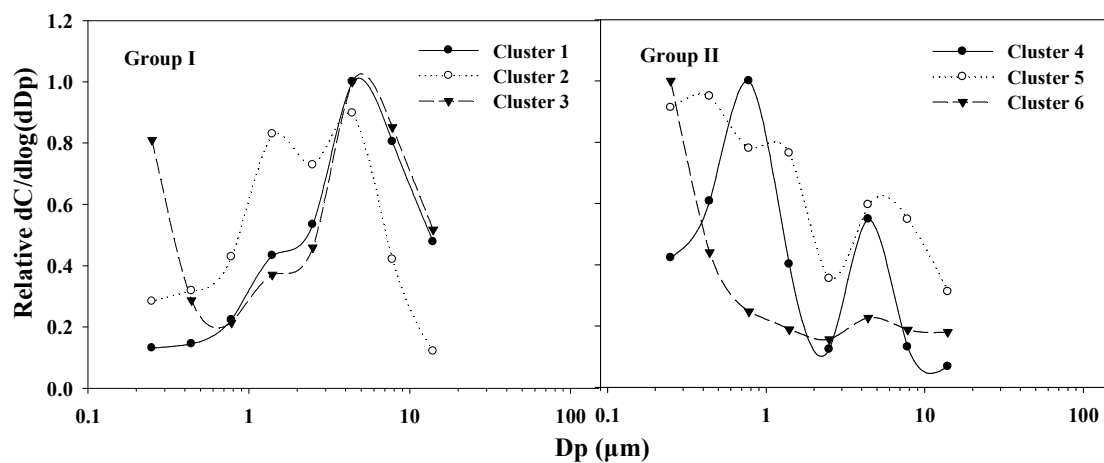


Figure 2. 3 The mass size distribution trace metals in two groups: (I) Coarse Particle Accumulation and (II) Fine Particle Accumulation.

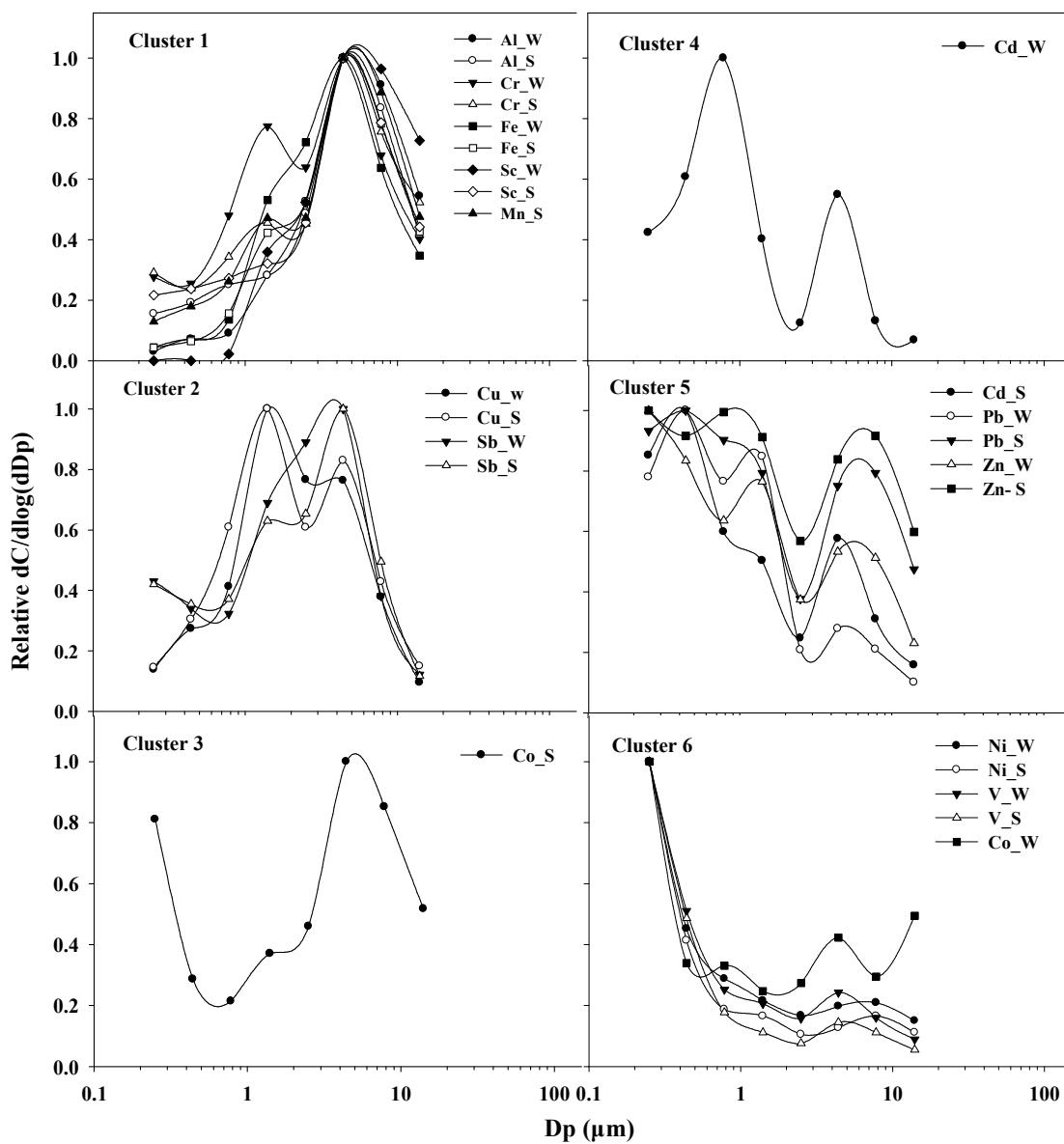


Figure 2. 4 The mass size distributions of the 6 identified clusters of trace metals in atmosphere (In the figure labels, *W* means winter while *S* means summer).

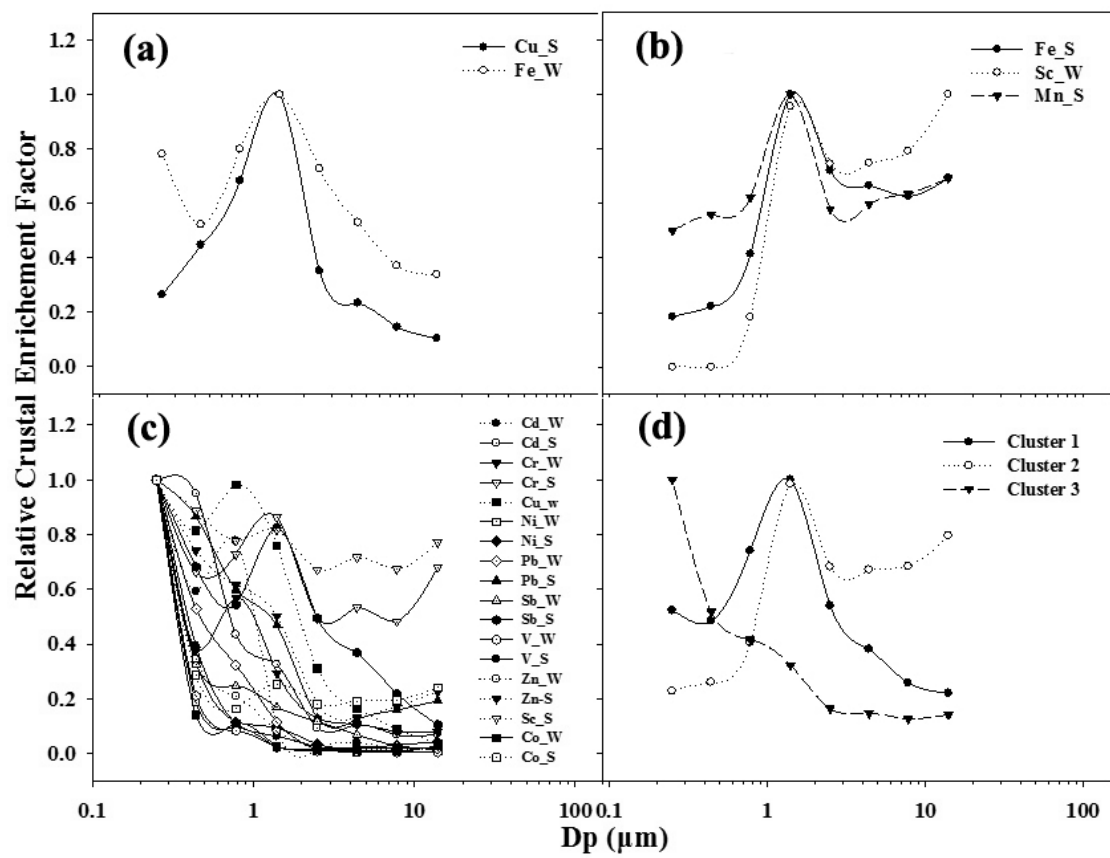


Figure 2. 5 The EF size distributions of the trace metal in three different clusters: (a) Cluster 1, (b) Cluster 2, (c) Cluster 3 and (d) Comparison of the average patterns of the three clusters.

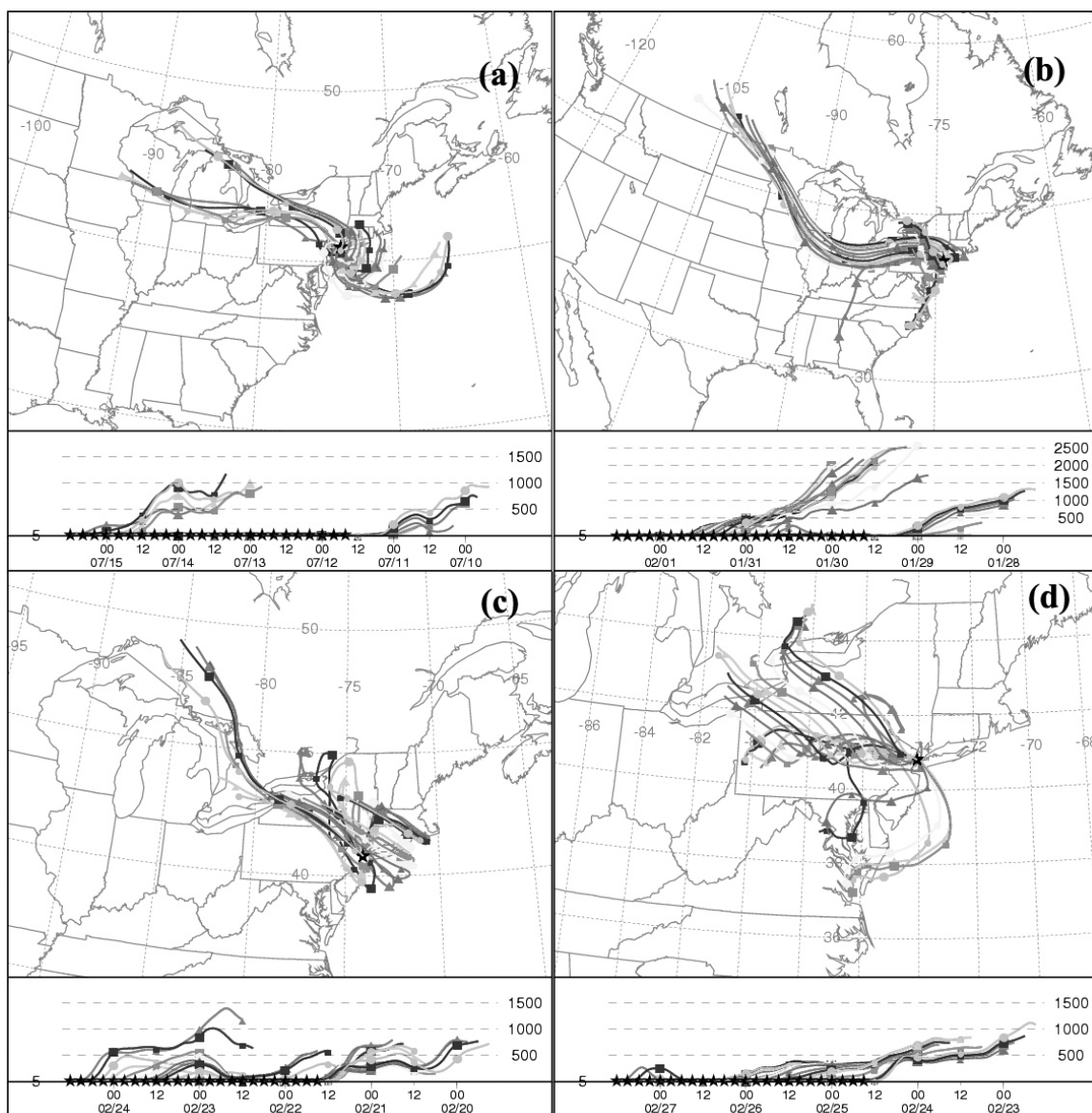


Figure 2. 6 Back-Trajectories of air mass using NOAA HYSPLIT Model with arriving height 5 m and duration 48 hours: (a). Cluster 1 (Sampling set #9 as example), (b). Cluster 2 (Sampling set #4 as example), (c). Cluster 3 (Sampling set #5 as example), (d). Cluster 4 (Sampling set #6 as example). For each sampling period (3- 4days), a total of 24 Back-Trajectories were calculated with same interval (3-4 hours).

**Chapter 3 . Relationships among the Springtime Ground-level
NO_x, O₃ and NO₃ in the Vicinity of Highways in the
US East Coast***

** This work is in press by Atmospheric Pollution Research (APR) and is scheduled to be published in the third issue in 2011.*

Abstract

To characterize the relationships among the springtime NO_x ($\text{NO} + \text{NO}_2$), O_3 and NO_3^- (defined as the combination of gaseous nitric acid, HNO_3 , and aerosol nitrate, NO_3^-) concentrations in the ambient air of the vicinity of highways, an intensive sampling was carried out in spring 2007 at Lyndhurst, NJ in the US East Coast. Ambient concentrations of O_3 and NO_x were measured by O_3 and NO_x analyzers, while NO_3^- was collected using a ChemComb cartridge and determined by ion chromatography. Significant variations in O_3 concentrations were observed diurnally as well as between weekdays and weekends, with higher concentrations occurring during the daytime and on weekends. The 24-h diurnal variations of O_3 and NO_x could be divided into four periods: (1) morning NO_x peak, (2) mid-day O_3 formation, (3) afternoon NO_x accumulation and (4) nighttime balancing. Daily averaged relative humidity and wind speed were the two important weather parameters affecting O_3 levels and the corresponding photochemical reactions, and daily maximum temperature was positively correlated to maximum O_3 . Via photochemical reactions and emission-diffusion balance, NO_x showed primarily negative influences on the daily O_3 variations with decayed exponential correlations, in particular during nighttime and weekdays, indicating a possible VOC-sensitive characteristic of the study area. A negative correlation between NO_3^- and O_3 concentrations was found while no obvious influences of HNO_3 on O_3 was observed. Results by a multi-regression model involving three parameters (NO_2/OX ratio, NO_2 and HNO_3) reveal that the NO_2/OX ratio is an important parameter controlling the ground O_3 level in the study area.

Key words: O_3 , NO_x , NO_3^- , influences, variations.

3.1. Introduction

Ozone (O₃) and nitrogen oxides (NO_x = NO + NO₂) are two of the six principle pollutants in the National Ambient Air Quality Standards (NAAQS) in the US since 1990, as at high concentrations they could induce serious adverse effects on human health and the environment (Lee et al., 1996; WHO, 2000; Kampa and Castanas, 2007). Besides, the photochemical reactions between NO_x and O₃ play key roles in altering the atmospheric oxidation/reduction capacity and in transferring nitrogen from the atmosphere to the aquatic ecosystems that affect many biogeochemical processes.

In the near-ground atmosphere, NO_x and O₃ are connected via photochemical inter-conversions as shown below (Seinfeld and Pandis, 2006):

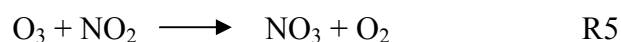


These reactions may change the ratios of NO/NO₂, NO₂/NO_x, and NO₂/O₃, but they cannot change the NO_x or OX (= NO₂ + O₃) level, an indicator of oxidizing level of the ambient atmosphere (Clapp and Jenkin, 2001). However, certain volatile organic compounds (VOC) could influence NO_x-O₃ photochemical reactions (Seinfeld and Pandis, 2006; Wei et al., 2007). With the existence of OH radicals, VOC can oxidize NO to NO₂ and thus promote O₃ production during daytime (Atkinson, 2000; Seinfeld and Pandis, 2006).

Ground level O₃ comes from two major sources: regional background O₃ primarily from the influx of O₃ from the stratosphere and in situ local O₃ production mainly via photochemical reactions (shown in R1-R3) involving many precursors, such

as NO_x and VOC, emitted from a variety of anthropogenic and nature sources (Clapp and Jenkin, 2001; Vingarzan, 2004; Cofala et al., 2007; The Royal Society, 2008; and Rappenglück et al., 2008). Combustion processes are the major sources of NO_x in the air, especially vehicle emissions in high traffic areas. In the eastern United States, the vehicle emission source contributed more than half of the total NO_x emissions (Butler et al., 2005) that could significantly affect the ambient O₃ levels, and this emission source has showed an increasing trend since the 1990s (Parrish, 2006). In such high NO_x emission regions, O₃ is often depleted locally/regionally by titration. OX is therefore a more stable entity to study, as it is an indication of the potential for renewed ozone production downwind of the sources. However, the cycling between NO and NO₂ is rapid and NO₂ could be lost via dry deposition and chemistry, these processes may complicate the observed NO_x and O₃ in the ambient air, affecting the ratio of NO₂/NO_x.

On the other hand, the production of Nitrate (NO₃), defined in this study as the combination of gaseous nitric acid (HNO₃) and aerosol nitrate (NO₃⁻), is also related to the ground-level O₃. In daytime, HNO₃ could be directly produced via R4 when the VOC/NO₂ ratio is small (on average < 5.5 in urban areas). In nighttime, different HNO₃ production mechanisms exist as shown in R5-R7 (Seinfeld and Pandis, 2006), and NO₃⁻ could be produced via acid-alkali reactions of HNO₃.



Although many studies have been carried out on the photochemical characteristics

of NO_x and O_3 , in particular in the US west coast (CARB, 2003; Qin et al., 2004a and 2004b; Yarwood et al., 2008; Alvarez et al., 2008), few such studies have been conducted recently in the US east coast, especially in high-traffic areas. Besides, while NO_x was known as an O_3 precursor, the role of NO_3 on the variations of O_3 levels was seldom studied. In order to characterize NO_x and O_3 in a typical high-traffic area in the US east coast and to explore the influences of both NO_x and NO_3 on O_3 variations, we carried out an intensive sampling campaign at Lyndhurst in northeast New Jersey (NJ), which is surrounded by many highways. The field measurements took place in spring 2007, because the spring is a transitional season from cold to warm weather when the O_3 concentrations are relatively higher (Monks, 2000; Lehman et al., 2004; Kaiser et al., 2007) and the exceedances of the NAQQS standard for O_3 have happened often in NJ (<http://www.state.nj.us/dep/>). The results from this study will fill the data gap for urban ground level O_3 , NO_x , and NO_3 in the region, help better understand the mechanisms controlling O_3 concentrations and variations, and provide useful information for modeling and prediction of O_3 concentrations.

3.2. Method

3.2.1. Sampling

In spring 2007 from Feb. 22nd to May 21st, real-time monitoring of NO_x and O_3 was conducted at the Meadowlands site housed at Meadowlands Environmental Research Institute in Lyndhurst, NJ (41°N, 74°W), ~ 1 km away from major high-ways (Fig. 3.1). Measurements of NO and NO_2 were made continuously with a 42i NO_x Analyzer (Thermo Electron Corporation, Franklin, MA). A model 49i UV photometric ozone analyzer (Thermo Electron Corporation, Franklin, MA) was used for the continuous

measurement of O_3 . The air detected was pumped through two monitoring instruments via two lengths of separated plastic tubing with inlets installed on the roof of a building, ~8 m above the ground. The instruments have 1-minute resolution, with detectable limits of 0.40ppb for NO_x and 0.50ppb for O_3 . During the measurement period, the two analyzers were calibrated biweekly which resulted in certain gaps in data collection.

Sampling of the gaseous HNO_3 and aerosol NO_3^- was conducted daily using a ChemComb Cartridge (Model 3500, Thermo Scientific), with a flow rate maintained at 15L/Min. Nylon filters (Pall Corporation, 1.0 μ m pore size) were used for HNO_3 collection while NO_3^- was collected on Teflon filters (Pall Corporation, 1.0 μ m pore size). The sampling inlet was set at the same place where the inlets for NO_x and O_3 were installed. All samples were kept in refrigerator until analysis.

To assist data interpretation, certain meteorological parameters including air Temperature (T), Solar Radiation (SR), Rainfall, Relative Humidity (RH) and Wind Speed (WS) were also collected in the study area. The time interval for weather data retrievals was 15 minutes.

3.2.2. Chemical determinations

Determinations of NO_x were made online by detecting the chemiluminescence in the range of 600nm to 3000nm generated by NO_2 radicals produced from reactions between O_3 and NO , based on the principle that NO and O_3 react to create luminescence with an intensity linearly proportional to the NO concentration. Determination of O_3 was carried out by the UV photometric method, since O_3 molecules absorb UV radiation at a wavelength of 254nm and the relationship between the absorbance of the UV light and the ozone concentration follows the Lambert-Beer law.

Gaseous HNO_3 and aerosol NO_3^- were measured using IC (ICS-2000, Dionex) in the Atmosphere Chemistry Lab of Rutgers University at Newark based on the procedures of Lee et al (1994) and Zhao and Gao (2008). Sample filters were ultrasonically extracted in DI water for 30 minutes, and then the solutions were filtered with a PTFE syringe filter (Fisher brand, $0.45 \mu\text{m}$). Sample solutions were injected into the IC via automated sampler (AS40, Dionex) using 0.5ml vials. An AS11 analytical column (2_250mm2, Dionex), KOH eluent generator cartridge (EGC II KOH, Dionex) and $25\mu\text{l}$ sample loop were employed for the determinations. The detection limit of the method is below 0.01ppm, and the precision of the analysis is $\sim 1\%$.

3.2.3. Data processing

The 1-minute interval data was integrated to obtain hourly averaged data by averaging all qualified data in one hour using homogeneity testing. The hourly averaged data in each day were then divided into two parts: daytime (7:00 to 19:00) and nighttime (19:01 to 6:59), considering the average solar radiation changes of a day in the spring in NJ. To better interpret the data, Pearson Correlation, Factor Analysis, Cluster Analysis, and Multi-regression Simulation Modeling were used in this study, and all the statistical analyses in the study were carried out using MiniTab 14 (Minitab Statistical Software).

3.3. Results and Discussions

3.3.1. Overall Concentrations and 24-hour Variations Characteristics

3.3.1.1. Concentrations

The average concentrations of ground level NO , NO_2 and O_3 in the study area were 13.8ppb, 21.3ppb and 24.0ppb, respectively, satisfying NAAQS's primary and secondary standards requirement (Table 3.1). Different from other locations (Qin et al.,

2004b; Mazzeo et al., 2005), the NO_2 concentrations at the Meadowland site in this study were high and even greatly exceeded the NO concentrations, indicating a higher oxidizing level of the environment in this region. High concentrations of NO_2 were also observed in another two sites in NJ at Chester and Elizabeth listed in Table 3.1, although compared with these two sites, the NO_x concentrations at the Meadowlands site were moderate. The concentrations of HNO_3 and NO_3^- were close to each other, averaging $1.24\mu\text{g}/\text{m}^3$ and $1.80\mu\text{g}/\text{m}^3$, respectively. Compared with other sites (Danalatos and Glavas, 1999; Bari et al., 2003; Lin et al., 2006), the HNO_3 concentration was low while the level of NO_3^- was found comparable.

During the study period, the daily averaged concentrations of O_3 and HNO_3 showed less variation, compared with those of NO_x and NO_3^- (Fig. 3.3). The concentrations of O_3 were limited to a range from $\sim 7\text{ppb}$ to $\sim 40\text{ppb}$ with a roughly normal distribution, while the concentrations of NO_x , especially NO , fluctuated over a larger range and were biased away from normal distributions at high concentrations. Similar situations happened for aerosol NO_3^- . Both NO_x and NO_3^- showed more extreme high values, and this may reflect the existence of irregular high emissions of NO_x in the study region.

As shown in Fig. 3.4, the weekly averaged concentrations of O_3 slightly increased during the study period, while those of NO_x and NO_3^- decreased. Besides the influences of weather changes, such as temperature, solar radiation *etc*, the emission-diffusion balance of NO_x and regional O_3 could also be a reason for the variations in the time series, considering the fact that NO_x showed maximum values in late autumn and winter (Tu et al., 2007), while O_3 regional background could reach its maximum in spring and summer

(Monks, 2000; Lehman et al., 2004; Kaiser et al., 2007).

3.3.1.2. 24-hour Variations

Diurnal variations of NO, NO₂ and O₃ were observed in this study, especially for O₃. The concentrations of NO and O₃ were higher in daytime while opposite trends exist for NO₂ and NO_x (Table 3.2), attributed to the photochemical reactions of NO_x and O₃ and the balance between emissions (natural and anthropogenic) and mixing processes of both horizontal dispersions and vertical convections. During daytime, NO₂ is oxidized by hydroxyl radical (OH) and produced gaseous HNO₃; while in the nighttime, O₃ could oxidize NO to NO₂ without solar radiation. The further oxidation of NO₂ by O₃ formed nitrate radical NO₃. In addition, the relatively low air temperature near the ground at night could prevent the vertical dispersion of NO_x, contributing to its accumulation and resulting in higher night-time concentrations.

The 24-h temporal variations of NO_x and O₃ can be divided into four periods (Fig. 3.5). The variations in each period can be explained by photochemical processes and the emissions-dilution balance of NO_x and O₃. In the first period (3:00-7:00), the NO_x concentrations at the study site increased suddenly, reflecting increased emissions of motor vehicles during the morning rush hours and from industrial activities. The newly emitted NO could react with O₃ without solar radiation, producing more NO₂ and reducing O₃ concentrations. During the second period (7:00-15:00), the solar radiation increased greatly and the photochemical processes that produce O₃ dominated, especially at the beginning of this period. Oxygen atoms produced in the photolysis of NO₂ could react with O₂ to produce O₃ as described by R1 and R2. Around 15:00, O₃ showed peak values when NO_x had the lowest concentrations. In this period, the NO_x accumulations

were not significant because of the high NO_x photochemical consumption and increased air mass dilution as the height of the boundary layer increases. The boundary layer height should reach a maximum sometimes in the afternoon, plus additional venting of the boundary layer by convection.

Then, in the 3rd period (15:00-20:00), the photochemical production of O_3 decreased while the NO_2 level increased. The reduced O_3 level could be explained mainly by the decrease of SR, which then would lower the level of photochemical production. NO_x could accumulate again because of afternoon-hour high-traffic emissions in the period. However, due to the high dilution level similar to the 2nd period, the 3rd period NO_x could not accumulate as high as in the 1st period. In the 4th period (20:00-3:00), the NO_x and O_3 balance arrived quickly and was maintained; as there was no solar radiation and both source emissions and dilution effects decreased significantly.

3.3.2. Weekday/Weekend and Diurnal Variation

Both NO_x and O_3 concentrations showed a difference between weekdays and weekends. Compared with weekends, the concentrations of NO , NO_2 and NO_x on weekdays were higher while the O_3 concentration was lower (Table 3.2), consistent with the results from studies in other locations (Cleveland et al., 1974; Marr and Harley, 2002; Qin et al., 2004a). In addition, similar to the results of Pudasainee et al. (2006), the concentrations of O_3 for weekends were ~13.4% higher than weekdays in this area. However, the mechanisms for the weekday/weekend variations of NO_x and O_3 are not clear. The California Air Resource Board (CARB) (2004) proposed a hypothesis that VOCs become sensitive to O_3 formation when NO_x emission decreases on weekends (Altshuler et al., 1995; Blanchard and Fairley, 2001; a et al., 2004). The weekly pattern of

traffic flows was also thought to affect the weekday/weekend variations of NO_x and O_3 (Shutters and Balling, Jr., 2006). It is possible that the study site is under a VOC-sensitive environment, based on the fact that the concentrations of NO_x and O_3 are negatively correlated (which will be discussed later) and the fact that NO_x concentrations decreased on weekends.

Diurnal variations of NO_x and O_3 were also observed in this study, especially for O_3 . The concentrations of NO and O_3 were higher in daytime while opposite trends exist for NO_x (Table 3.2), attributed to the photochemical reactions of NO_x and O_3 . During daytime, NO_2 is oxidized by hydroxyl radical (OH) and produced gaseous HNO_3 ; while in the nighttime, O_3 could oxidize NO to NO_2 without solar radiation. The further oxidation of NO_2 by O_3 formed nitrate radical NO_3 . In addition, the relatively low air temperature near the ground at night could prevent the vertical dispersion of NO_x , contributing to its accumulation and resulting in higher night-time concentrations.

Fig. 3.6 shows that the 24-h diurnal variation patterns of NO_x and O_3 were also different between weekdays and weekends. The weekday morning peaks of NO_x and O_3 concentrations were higher than those over the weekends, indicating higher traffic emissions during rush hours. On weekends, in the 1st period, NO_x showed less accumulation due to less traffic and industries emissions, while O_3 concentrations were higher. During the second period, the O_3 accumulation continued and NO_x started to decrease. The 3rd period lasted much longer in weekends as the O_3 concentrations were higher while NO_x inputs were lower. The 4th period was shorter with less variation in the concentrations compared with those for weekdays; as a result of rapid chemistry and advection out of the area, the lower values observed at daytime in weekends does not

affect night time NO_x levels that much. However, on weekends, NO_x showed an increase after 24:00 to 3:00 of the following day, probably due to increased traffic volumes at late night on weekends compared with weekdays.

3.3.3. Weather Influences on Concentrations

3.3.3.1. Daily Concentrations

The daily averaged meteorological parameters (Temperature (T), Solar radiation (SR), relative Humidity (RH) and Wind speed (WS) were found to influence the concentrations of NO_x , O_3 and NO_3^- (Table 3.3), consistent with previous studies (Mazzeo et al., 2005; Nevers, 2000; Tu et al., 2007). However, in contrast to the conclusion of previous studies (O'Connor et al., 2005; Pudasainee et al., 2006; Castell et al., 2007), the daily averaged T did not show much influences on O_3 concentrations at this location. This suggests that the correlation between pollution levels and meteorology is weaker during spring, compared with summer (O'Connor, 2005). In addition, the averaged daily data used in the calculations could further reduce the correlation, as the recalculated correlation between daily maximum T and O_3 showed significant positive correlation ($p < 0.01$). On the other hand, the proximity to anthropogenic emissions may also mask correlation between ozone and temperature, according to a recent study by Castell (2007) who found in Castellon (Spain) on the Western Mediterranean area, the correlations between ozone and meteorological variables at inland stations (away from anthropogenic emissions) are better than those at coastal stations (close to human emissions). T and SR were found to influence NO_3^- only, and the higher T and SR would more probably induce a higher HNO_3 level and lower NO_3^- level, respectively.

RH and WS were found to be of more importance in this study compared with

other weather parameters. In general, the results showed that when RH increased, NO_x and NO_3^- increased but O_3 decreased, indicating that high RH may retard the O_3 production to some extent, while the underlying mechanism is not clear due to limited data collection during this study. Possible mechanisms driving this phenomenon should be explored through future investigations. High WS could lower NO_x and NO_3^- concentrations due to the dilution effect. However, the positive correlations between WS and O_3 were found, and this could be caused by the transport of high O_3 air into this area from upwind pollution sources. The results relating the effects of weather conditions certainly reveal the complexity of the observed NO_x and O_3 levels affected by many processes happening both instantaneously and over time.

3.3.3.2. Diurnal Variations

Primarily, the 24-h diurnal variation patterns of NO_x and O_3 in different weather conditions were similar, as shown in Fig. 3.7. To characterize the potential weather influences on the 24-h temporal variations of these species, the study period was categorized into three groups using cluster analysis with respect to the values of SR, RH and precipitation,: clear days, cloudy days and rainy days, with each counting about 1/3 of the entire study period (Table 3.4). In all weather conditions, the O_3 peaks appeared in the period of 14:00 to 16:00, and the maximum O_3 concentration (>40 ppb) during that period was associated with clear days (Fig. 3.7a), reflecting the strong influence of SR on the *in situ* photochemical accumulation of O_3 and enhanced mixing from aloft. Coinciding with high traffic hours, the NO_x concentration peaks appeared in early morning and evening, indicating the influence of high vehicle emissions on NO_x levels during those periods of time. The NO_x peaks were more obvious in the morning than

those in the afternoon, strengthened by the atmospheric inversion developed over the night hours. Compared with cloudy and rainy days, the NO_x level was lower and O_3 accumulated to a higher level during clear days, possibly due to photochemical reactions that were more intensive in clear days.

3.3.4. Correlations between NO_x and O_3

Fig. 3.8 shows that the concentrations of NO_x and O_3 were negatively correlated exponentially throughout the study period, suggesting possible VOC-sensitive characteristics of the study site, as described in Seinfeld and Pandis (2006). While the instantaneous photochemical reaction dynamics during the day affect the production rate of O_3 , the correlations between averaged NO_x and O_3 concentrations over certain period of time reflect the mixed effects of chemical reactions, transport patterns, atmospheric dispersion and etc. The nature of the negative correlations between NO_x and O_3 indicates that the study site is not NO_x sensitive but possibly VOC sensitive, assuming that the higher O_3 levels appear when the VOC concentrations increase. A high level of NO_x would consume more OH radicals through HNO_3 -forming reactions and thus lower the oxidizing ability of VOC and NO_2 , which are the two precursors of O_3 (Sillman and He, 2002; Seinfeld and Pandis, 2006; Cofala et al., 2007). The fact that the NO_2/NO_x ratio decreased greatly as NO_x increased that could be newly emitted could also support the VOC-sensitive nature of the region (Fig. 3.2). Nevertheless, VOC may also be emitted by traffic, and more detailed relationships among NO_x , VOC and O_3 in this area need to be explored through future studies.

Compared with those for nighttime and weekdays, the daytime and weekend NO_x levels showed less negative influence on O_3 concentrations (Fig. 3.8). While O_3

consumption through reactions with NO_x dominated during nighttime, NO_x could either produce O_3 or consume O_3 production during the daytime: on one hand, when VOC was sufficient, NO_2 could react with O_2 to produce O_3 . On the other hand, the newly produced O_3 would oxidize NO to NO_2 and thus lower the O_3 level when VOC was limited. Therefore the negative influences of NO_x on O_3 were more significant during the nighttime. The lower negative effects of NO_x on O_3 during weekends could be attributed to two reasons: (1) NO_x may not accumulate much, and (2) the effect of VOC may be more active during weekends (CARB, 2004); both lead to increased O_3 production.

3.3.5. Correlations between NO_x and OX

The level of OX, an oxidizing level indicator of the NO_x - O_3 regime, could be increased in two ways: (1) the net increase of NO_2 through NO_x emissions and then oxidization of NO to NO_2 by radical species such as RO_2 (where R is a hydrogen atom or carbon containing fragment), OH etc. (Atkinson, 2000; Seinfeld and Pandis, 2006), and (2) the net increase of O_3 via regional background input. The direct input of NO_2 is mainly controlled by net NO_x emission and the original NO_2/NO_x ratio, which could be approximated by the lower end ratios while NO_x increases (Carslaw, 2005; Seinfeld and Pandis, 2006). As shown in Fig. 3.8, the NO_2/NO_x ratios in the study area varied and finally reached balance at $\sim 20\%$ when NO_x increased. This is consistent with the conclusion of an increasing NO_2/NO_x ratio obtained at a roadside in London, reaching to $\sim 17\%$ (Carslaw, 2005), and the increase in the NO_2/NO_x emissions ratio from road traffic in recent years is believed to have a significant effect on recent trends in roadside NO_2 concentrations in the area. The feature in NO_2/NO_x ratio in European emissions is primarily driven by light duty diesel vehicles after treatment technologies (Alvarez et al.,

2008). Thus the contribution of NO_x to OX via NO_2 input found in this study could be treated as 20% which might indirectly represent the current emission situations in these regions, although the detailed explanations still need to be explored further. The other OX could be explained by regional O_3 input and the radical reactions producing net OX.

The net effect of photochemical reactions between NO_x and O_3 was the consumption of O_3 , especially in daytime and weekends as shown in Fig. 3.8. As stated earlier, the ground level O_3 is mainly composed of background O_3 and local production of O_3 . Because NO_x plays a critical role in the local O_3 production as shown in equation R1-R3, the background O_3 can be approximated from the total O_3 concentrations in the scenario that NO_x does not exist. The regional O_3 background level thus could be interpreted as the intercepts of the OX- NO_x linear relation in Fig. 3.9 (Clapp and Jenkin, 2001). The derived background O_3 concentration was higher than the daily averaged total O_3 (Table 3.1) in the study area. It suggests that the net effect of NO_x related local processes is the consumption of O_3 . Thus in the study area, the O_3 consumption, which mainly happened at night, exceeded the O_3 production via photochemical reactions involving VOC and NO_x during the day.

The OX level of the study area was controlled mainly by the net NO_x emissions, while photochemical reactions of NO_x and O_3 contributed much less to OX. As shown in Fig. 3.9, the slopes of the OX- NO_x linear relations were ~ 0.20 , close to the original NO_2/NO_x ratio in the study area shown in Fig. 3.2. Considering the fact that the quick cycling between NO and NO_2 would not change the ratio of OX/ NO_x as shown in R1-R3, this result indicates the dominant influence of NO_x accumulations on OX. For weekdays, the slopes were smaller than 0.20, indicating the NO_2 consumption exceeded NO_2

formation, especially in daytime. However, with the higher NO_x levels, the NO_3 concentrations for weekdays were lower (Table 3.2), suggesting that other NO_2 consumption mechanisms may also exist in addition to the mechanisms shown in R5-R7. For weekends, the slopes were higher than 0.20 (Fig. 3.9), indicating that NO_2 oxidizations were significant and O_3 net production may exist. This is consistent with the higher O_3 level during weekends and daytime shown in Table 3.2.

3.3.6. Relationships between NO_3 and O_3

Preliminary results from this study show that NO_3^- was involved in the O_3 variations, and a higher NO_3^- level was primarily associated with a lower O_3 level. As shown in Table 3.3, the daily averaged concentrations of NO_3^- showed significantly negative correlation with those of O_3 , attributed to R5-R7, while no correlations between HNO_3 and O_3 were found. Strong positive correlations between NO_3^- and NO_x were also observed, which was consistent with the negative relationships between NO_3^- and O_3 . In addition, in high NO_x environments, O_3 is depleted locally by titration, while NO_3^- could be buildup, which also supports the negative NO_3^- - O_3 correlation. Through factor analysis (PCA method with Varimax Rotation), the concentrations of NO_x and O_3 , NO_3^- and O_3 , were grouped to factor 1 and factor 2, respectively, with HNO_3 alone serving as factor 3 (Table 3.5). These results suggest the significant correlations between NO_3^- and O_3 and no correlations for HNO_3 . However, the underlying mechanisms for their relationships are not clear and should be explored through future studies.

3.3.7. Multi-Regression analysis of the NO_x - O_3 - NO_3 system

Multi-regression methods were used to explore the ground-level O_3 concentration variations with respect to the influences of daily averaged level of NO_2/OX ratio, NO_2

and HNO_3 observed in this study. The results show that the NO_2/OX ratio was the most influential factor on the O_3 level, suggested by its large coefficients and the average NO_2/OX (Table 3.6). The NO_2 concentration, which was found to have negative influence on the O_3 level as discussed in previous sections, functioned as the compensatory correction to the influences of the NO_2/OX ratio on O_3 . HNO_3 , which was less important, is considered as a conditional explaining factor. These three factors selected could account for a total of 85.7% of the variations of O_3 for the entire study period.

The NO_2/OX ratio became a more powerful factor when the NO_x level increased. For better simulation, the whole investigation period was divided into 4 clusters, using cluster analysis (Ward's method) with the concentrations of NO_x , NO_3 and O_3 (Table 3.6). From cluster 1 to 4, the NO_x , NO_3^- , NO_2/OX increased while O_3 , NO_2/NO_x , HNO_3/NO_3 decreased. The results from these multi-regression functions (Table 3.6) of each cluster can explain the O_3 variations, and the most important factor was NO_2/OX . However, the weight of each factor changed greatly. When the NO_x level was low, the NO_2 concentrations played a more important role, and such influence was reduced greatly when NO_x levels increased. HNO_3 was only used to explain the O_3 variations when NO_x levels were either low or high.

3.4. Conclusions

Results from this study on the influences of NO_x and NO_3 on O_3 levels carried out during the springtime of 2007 lead to the following conclusions:

The study area was a relatively highly oxidizing level environment, with the NO_2/NO_x ratio higher than many other regions. Ground level O_3 concentrations showed both weekday/weekend and diurnal variations, with high concentrations on weekends

possibly due to the increased VOC sensitivity and decreased NO_x emissions, and in daytime due to the photochemical production of O_3 accompanied by lower O_3 consumption. In the time series, the O_3 concentrations generally increased from the beginning to the end of the study period.

Due to the variations of photochemical processes and emissions-diffusion balancing, the 24-h temporal variations patterns of NO_x and O_3 could be divided into four periods: (1) morning NO_x peak, (2) O_3 formation, (3) afternoon NO_x accumulation, and (4) night balancing. Certain meteorological parameters, in particular relative humidity and wind speed, played more important roles in O_3 concentration variations and the photochemical reactions of NO_x and O_3 . Different 24-h temporal variations of NO_x and O_3 were observed during different weather conditions. The daily maximum temperature showed positive correlation to the daily maximum O_3 level.

The net effect of NO_x on O_3 concentrations was negative with a decayed exponential correlation, especially in nighttime and weekdays, indicating a possible VOC-sensitive characteristic of the study area as observed by previous studies. The OX levels were mostly controlled by NO_x emissions and were less influenced by photochemical reactions. The photochemical reactions of NO_x and O_3 led to a net O_3 consumption.

Significant negative correlations between NO_3^- and O_3 were found during this study, indicating either a high connection between NO_x and NO_3^- or an O_3 retarding characteristic for NO_3^- . HNO_3 was not found to be related to the NO_x - O_3 system, with no influence on the O_3 level.

NO_2/OX ratio, NO_2 and HNO_3 could be used to explain the O_3 concentration

variations for about 85.7% of the O₃ variations as shown in the whole study period. The NO₂/OX ratio was the most important factor in controlling O₃ levels, and this influence increased when NO_x concentrations increased.

Acknowledgement

This work was primarily supported by Meadowlands Environmental Research Institute of the New Jersey Commission. Additional support was provided by a New Faculty Start-up Fund to YG at Rutgers University. We thank Yunliang Zhao, Kyung Hwa Jung, and Christopher Thuman for sampling assistances and data collation.

3.5. References

- Altshuler, S.L., Arcado, T.D., Lawson, D.R., 1995. Weekday vs. weekend ambient ozone concentrations: discussion and hypotheses with focus on northern California. *Journal of the Air and Waste Management Association* 45, 967–972.
- Alvarez, R., Weilenmann, M., Favez J., 2008. Evidence of increased mass fraction of NO₂ within real-world NO_x emissions of modern light vehicles — derived from a reliable online measuring method. *Atmospheric Environment* 42, 4699-4707.
- Arnold, J.R., Luke, W. T., 2007. Nitric acid and the origin and size segregation of aerosol nitrate aloft during BRACE 2002. *Atmospheric Environment* 41, 4227–4241.
- Atkinson, R., 2000. Atmospheric chemistry of VOCs and NO_x. *Atmospheric Environment* 34, 2063–2101.
- Bari, A., Ferraro, V., Wilson, L.R., Luttinger, D., Husain, L., 2003. Measurements of gaseous HONO, HNO₃, SO₂, HCl, NH₃, particulate sulfate and PM_{2.5} in New York. *Atmospheric Environment* 37, 2825 – 2835.
- Blanchard, C.L., Fairley, D., 2001. Spatial mapping of VOC and NO_x limitation of ozone formation in central California. *Atmospheric Environment* 35, 3861–3873.
- Butler, J. T., Likens, E. G., Vermeylen, M. F., Stunder, J.B. B., 2005. The impact of changing nitrogen oxide emissions on wet and dry nitrogen deposition in the northeastern USA. *Atmospheric Environment* 39, 4851-4862.
- CARB, 2003. The ozone weekend effect in California. Staff Report, The Planning and Technical Support Division, The Research Division, California Air Resources Board, Sacramento, CA, 30 May. 37, 4205–4215.
- Carslaw, D. C., 2005. Evidence of an increasing NO₂/NO_x emissions ratio from road

- traffic emissions. *Atmospheric Environment* 39, 4793–4802.
- Castell, N., Mantilla, E., Millan, M.M., 2008. Analysis of tropospheric ozone concentration on a western mediterranean site: Castellon (Spain), *Environmental Monitoring and Assessment* 136 (1), 3-11.
- Clapp, L.J., and Jenkin, M.E., 2001. Analysis of relationship between ambient levels of O₃, NO₂ and NO as a function of NO_x in the UK. *Atmospheric Environment* 35, 6391-6405.
- Cleveland, W.S., Graedel, T.E., Kleiner, B., Warner, K.L., 1974. Sunday and workday variations in photochemical air pollutants in New Jersey and New York. *Science* 186, 1037–1038.
- Cofala, J., Amann M., Klimont, Z., Kupiainen, K., Hoglund- Isaksson L., 2007. Scenarios of global anthropogenic emissions of air pollutants and methane until 2030. *Atmospheric Environment* 41, 8486 – 8499.
- Danalatos, D., Glavas, P., 1999. Gas phase nitric acid, ammonias and related particulate matter at a Mediterranean coastal site, Patra, Greece. *Atmospheric Environment* 33, 3417–3425.
- Gaffney, J. S., Marley, N. A., Drayton, P. J., Doskey, P. V., Kotamarthi, V. R., Cunningham, M. M., Baird, J. C., Dintaman, J., and Hart, H. L., 2002. Field observations of regional and urban impacts of NO₂, ozone, UV-B and nitrate radical production rates in the Phoenix air basin, *Atmospheric Environment* 36, 825–833, 2002.
- Kaiser, A., Scheifinger, H., Spangl, W., Weiss, A., Gilge, S., Fricke, W., Ries, L., Cemas, D., Jesenovec, B., 2007. Transport of nitrogen oxides, carbon monoxide and ozone

- to the Alpine Global Atmosphere Watch stations Jungfrauoch (Switzerland), Zugspitze and Hohenpeissenberg (Germany), Sonnblick (Austria) and Mt. Kravavec (Slovenia). *Atmospheric Environment* 41, 9273 - 9287.
- Kampa, M., Castanas, E., 2007. Human health effects of air pollution. *Environmental Pollution* 151, 362-367.
- Lee, D.S., Holland, M.K., Falla, N., 1996. The potential impact of ozone on materials in the UK. *Atmospheric Environment* 30, 1053–1065.
- Lee, G.W., J.T. Merrill, and B.J. Huebert, Variation of free tropospheric total nitrate at Mauna Loa Observatory, *Journal of Geophysical Research* 99, 12,821-12,831, 1994.
- Lee, H.S., Wadden, R.A., Sche!, P.A., 1993. Measurement and evaluation of acid air pollutants in Chicago using an annular denuder system. *Atmospheric Environment* 27A, 543-553.
- Lehman, J., Swinton, K., Bortnick, S., Hamilton, C., Baldrige, E., Eder B., Cox, B., 2004. Spatio-temporal characterization of tropospheric ozone across the eastern United States, *Atmospheric Environment* 38, 4357–4369.
- Lin, Y., Cheng, M., Ting, W., Yeh, W., 2006. Characteristics of gaseous HNO₂, HNO₃, NH₃ and particulate ammonium nitrate in an urban city of Central Taiwan. *Atmospheric Environment* 40, 4725–4733.
- Marr, L.C. and Harley, R.A., 2002. Spectral analysis of weekday–weekend differences in ambient ozone, nitrogen oxide, and non-methane hydrocarbon time series in California, *Atmospheric Environment* 36, 2327–2335.
- Mazzeo, A.N., Venegas, E.L., Choren, H., 2005. Analysis of NO, NO₂, O₃ and NO_x concentrations measured at a green area of Buenos Aires City during wintertime.

- Atmospheric Environment 39, 3055-3068.
- Monks, P.S., 2000. A review of the observations and origins of the spring ozone maximum. *Atmospheric Environment* 34, 3545–3561.
- Nevers, N.D., 2000. *Air Pollution Control Engineering*, second ed. McGraw-Hill Companies, Inc., New York, 571–573.
- O'Connor, J.R., Roelle, P.A., Aneja, V.P., 2005. An ozone climatology: relationship between meteorology and ozone in the southeast United States. *International Journal of Environment and Pollution* 23 (2), 123-139.
- Parrish, D.D., 2006. Critical evaluation of US on-road vehicle emission inventories, *Atmospheric Environment* 40, 2288–2300.
- Pudasainee, D., Sapkota, B., Shretha, L. M., Kaga A., Konda A., Inoue Y., 2006. Ground level ozone concentrations and its association with NO_x and meteorological parameters in Kathmandu Valley, Nepal. *Atmospheric Environment* 40, 8081-8087.
- Qin, Y., Tonnesen, G. S., Wang, Z., 2004a. Weekend/weekday differences of ozone, NO_x, CO, VOCs, PM10 and the light scatter during ozone season in southern California. *Atmospheric Environment* 38, 3069-3087.
- Qin, Y., Tonnesen, G.S., Wang, Z., 2004b. One hour and eight hour average ozone in California south coast Air Basin: trends in peak values and sensitivity to precursors. *Atmospheric Environment* 38, 2197–2207.
- Rappenglück B., Perna R., Zhong S., Morris G.A., 2008. An Analysis of the Vertical Structure of the Atmosphere and the Upper-Level Meteorology and their Impact on Surface Ozone Levels in Houston/TX, *Journal of Geophysical Research* ,113, D17315, doi:10.1029/2007JD009745.

- Seinfeld, J. H., Pandis, S. N., 2006. *Atmospheric Chemistry and Physics: From Air Pollution to Climate Change*, John Wiley & Sons, Inc., Hoboken, New Jersey.
- Shutters, T. S. and Balling, Jr. C. R., 2006. Weekly periodicity of environmental variables in Phoenix, Arizona. *Atmospheric Environment* 40, 304–310.
- Sillman, S., and He, D., 2002. Some theoretical results concerning O₃-NO_x-VOC chemistry and NO_x-VOC indicators. *J. Geophys. Res.*, 107, 4659-4673.
- The Royal Society, 2008. *Ground-level ozone in the 21st century: future trends, impacts and policy implications*. The Royal Society, RS Policy document 15/08.
- Tu, J., Xia, Z., Wang, H., Li, W., 2007. Temporal variations in surface ozone and its precursors and meteorological effects at an urban site in China. *Atmospheric Research*, 85 (3-4), 310-337.
- Vardoulakis, S., Kassomenos, P., 2008. Sources and factors affecting PM10 levels in two European cities: Implications for local air quality management. *Atmospheric Environment* 42, 3949-3963.
- Vingarzan, R., 2004. A review of surface ozone background levels and trends. *Atmospheric Environment* 38 (21), 3431-3442.
- Walker, J.T., Whitall, D.R., Robarge, W., Paerl, H.W., 2004. Ambient ammonia and ammonium aerosol across a region of variable ammonia emission density. *Atmospheric Environment* 38, 1235–1246.
- Wei, X.L., Lib, Y.S., Lam, K.S., Wang, A.Y., Wang, T.J., 2007. Impact of biogenic VOC emissions on a tropical cyclone-related ozone episode in the Pearl River Delta region, China. *Atmospheric Environment* 41, 7851–7864.
- WHO, 2000. *Guidelines for Air Quality*. World Health Organization, Geneva, 190.

- Yarwood, G., Grant, J., Koo, B., Dunker, A. M., 2008. Modeling weekday to weekend changes in emissions and ozone in the Los Angeles basin for 1997 and 2010. *Atmospheric Environment* 42, 3765-3779.
- Zhao, Y., Gao, Y., Mass size distributions of water-soluble inorganic and organic ions in size-segregated aerosols over metropolitan Newark in the US east coast. *Atmospheric Environment* 42, 4063-4078.

Table 3. 1 Ground level concentrations of NO, NO₂, O₃, HNO₃ and NO₃⁻.

Sites	NO (ppb)	NO ₂ (ppb)	O ₃ (ppb)	HNO ₃ (µg/m ³)	NO ₃ ⁻ (µg/m ³)
^a MERI daily average	13.8	21.3	24.0	1.24	1.80
^b Rural (Busy street), UK	-	9.4 (59)	-	-	-
^c Buenos Aires, Argentina	240	65	30	-	-
^d Southern California	2-76	23-38	9-81	-	-
^e Phoenix, Arizona	-	1-10	15-35	-	-
^f Central Taiwan, China	-	-	-	1.5	8.5
^g Patras, Greece	-	-	-	2.6	1.1
^h Manhattan, NY, USA	-	-	-	1.7	-
ⁱ Clinton, NC, USA	-	-	-	0.5	1.7
^j Tampa, Florida, USA	-	-	-	~6	1.4
^h Chester NJ (2005 yearly average)	4	11	-	-	-
^h Elizabeth NJ (2005 yearly average)	42	32	-	-	-
ⁱ EPA Standard (8 hours)	-	53	84	-	-

^aThis work; ^b Clapp and Jenkin, 2001; ^cMazzeo et al., 2005; ^dQin et al., 2004; ^eGaffney et al., 2002; ^fLin et al., 2006; ^gDanalatos and Glavas, 1999; ^hBari et al., 2003; ⁱWalker et al., 2004; ^jArnold and Luke, 2007; ^hNJDEP website (<http://www.state.nj.us/dep/>); ⁱEPA website (<http://www.epa.gov/>).

Table 3. 2 Weekday/weekend and diurnal differences of NO_x, O₃ and NO₃.

		NO (ppb)	NO ₂ (ppb)	NO _x (ppb)	O ₃ (ppb)	HNO ₃ (µg/m ³)	NO ₃ ⁻ (µg/m ³)	NO ₃ (µg/m ³)
Daytime	Weekdays	16.7	21.4	38.1	26.6	-	-	-
	Weekends	9.49	13.5	23.0	32.6	-	-	-
	All	14.7	19.2	33.9	28.3	-	-	-
Nighttime	Weekdays	12.9	23.9	36.8	19.7	-	-	-
	Weekends	12.5	22.2	34.8	19.9	-	-	-
	All	12.8	23.4	36.3	19.7	-	-	-
Whole day	Weekdays	14.8	22.6	37.4	23.1	1.22	1.76	2.98
	Weekends	11.0	17.9	28.9	26.3	1.29	1.89	3.18
	All	13.8	21.3	35.1	24.0	1.24	1.80	3.04

Table 3. 3 Pearson correlations efficient among NO_x, O₃, NO₃ and selected weather parameters.

	Weather Parameters (daily average)				NO ₃ (daily average)	
	T	SR	RH	WS	HNO ₃	NO ₃ ⁻
NO	-	-	0.247*	-0.454***	0.111	0.321**
NO ₂	-	-	0.385**	-0.544***	0.114	0.448***
O ₃	-	-	-0.597***	0.56***	0.106	0.588***
HNO ₃	0.422***	-	-	-	1	-0.513***
NO ₃ ⁻	-	-0.274**	0.451***	-0.407***	-	1

* $p < 0.05$, ** $p < 0.01$, *** $p < 0.001$. (In addition, the correlation efficient between daily maximum T and maximum daily O₃ is 0.482 with $p < 0.01$.)

Table 3. 4 Descriptive data of NO_x, O₃, NO₃ under different weather conditions.

		Groups		
		Clear	Cloudy	Rainy
NO _x , O ₃ and NO ₃	NO (ppb)	7.13	17.13	18.03
	NO ₂ (ppb)	16.02	21.40	26.32
	NO _x (ppb)	23.15	38.53	44.35
	O ₃ (ppb)	29.34	22.99	19.78
	HNO ₃ (ug/m3)	1.15	1.18	1.36
	NO ₃ ⁻ (ug/m3)	1.07	1.89	2.57
Weather Data	T (F)	52.82	42.00	47.86
	RH (%)	45.41	56.14	69.59
	Rainfall (cm)	0.00	0.00	2.60
	SR (W/m ²)	269.5	155.7	108.6
	WS (mph)	9.43	9.16	8.05

Table 3. 5 Rotated Factor Loadings for the factor analysis of NO_x, NO₃ and O₃.

Variable	Factor1	Factor2	Factor3	Communality
HNO ₃	0.036	0.255	0.928	0.927
NO ₃ ⁻	0.273	0.91	0.221	0.951
NO ₃	0.238	0.838	0.481	0.99
NO	0.964	0.106	0.097	0.95
NO ₂	0.867	0.414	0.017	0.923
NO _x	0.966	0.237	0.068	0.995
O ₃	-0.616	-0.578	0.348	0.834
Variance	3.1259	2.1674	1.2762	6.5695
% Var	0.447	0.31	0.182	0.938

Table 3. 6 Cluster analysis results with respect to NO_x, NO₃ and O₃.

		Cluster 1 (25 days)	Cluster 2 (26 days)	Cluster 3 (18 days)	Cluster 4 (7 days)	All (76 days)
Description Parameters	NO (ppb)	1.31	5.34	17.4	70.9	12.9
	NO ₂ (ppb)	8.84	17.9	30.6	49.8	20.9
	O ₃ (ppb)	34.0	24.4	16.5	9.14	24.3
	HNO ₃ (ppb)	1.21	1.17	1.36	1.31	1.24
	NO ₃ ⁻ (ppb)	0.70	1.79	2.44	4.20	1.81
	NO ₂ /OX	0.21	0.42	0.65	0.84	0.44
	NO ₂ /NO _x	0.87	0.77	0.66	0.42	0.74
	HNO ₃ /NO ₃	0.63	0.45	0.39	0.30	0.48
	RH (%)	48.7	57.0	62.9	68.8	56.7
	SR (W/m ²)	200	188	184	120	185
	WS (mph)	11.8	8.00	7.43	4.95	8.83
O ₃ Multi- Regression Model Parameters	Constants	38.8	42.9	45.7	64.4	41.6
	NO ₂ /OX	-191	-103	-66	-68.1	-67.3
	NO ₂	3.67	1.39	0.455	0.088	0.472
	HNO ₃	2.16	-	-	-1.61	2.28
	R ²	92.8%	98.8%	98.1%	99.7%	85.7%

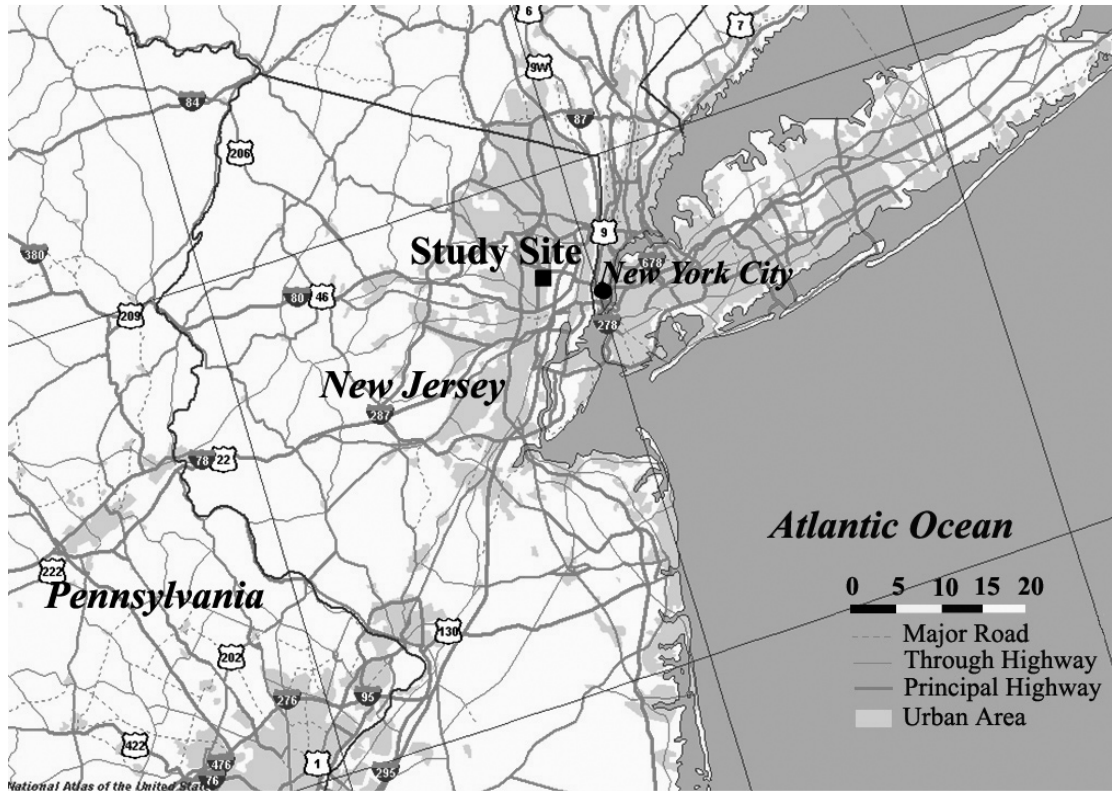


Figure 3. 1 Study sampling site map.

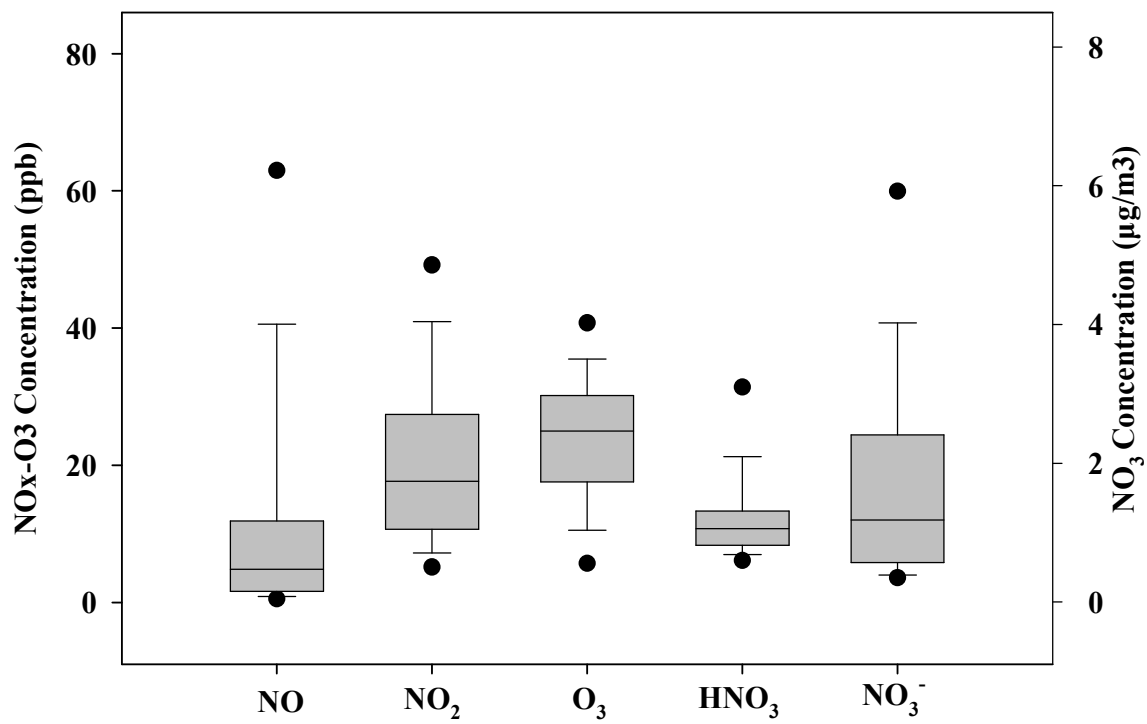


Figure 3. 2 Box-whisker plot of daily averaged NO, NO₂, NO_x and O₃ concentrations in whole spring monitoring period.

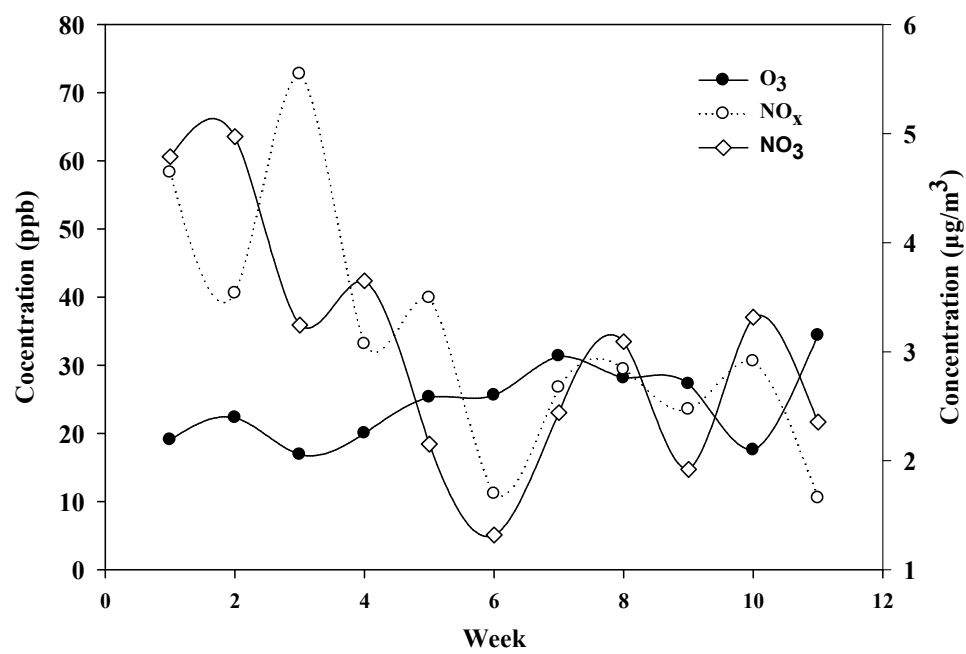


Figure 3. 3 Time series of weekly averaged NO_x, O₃ and NO₃ concentrations in spring (Feb. 26th -May 20th 2007).

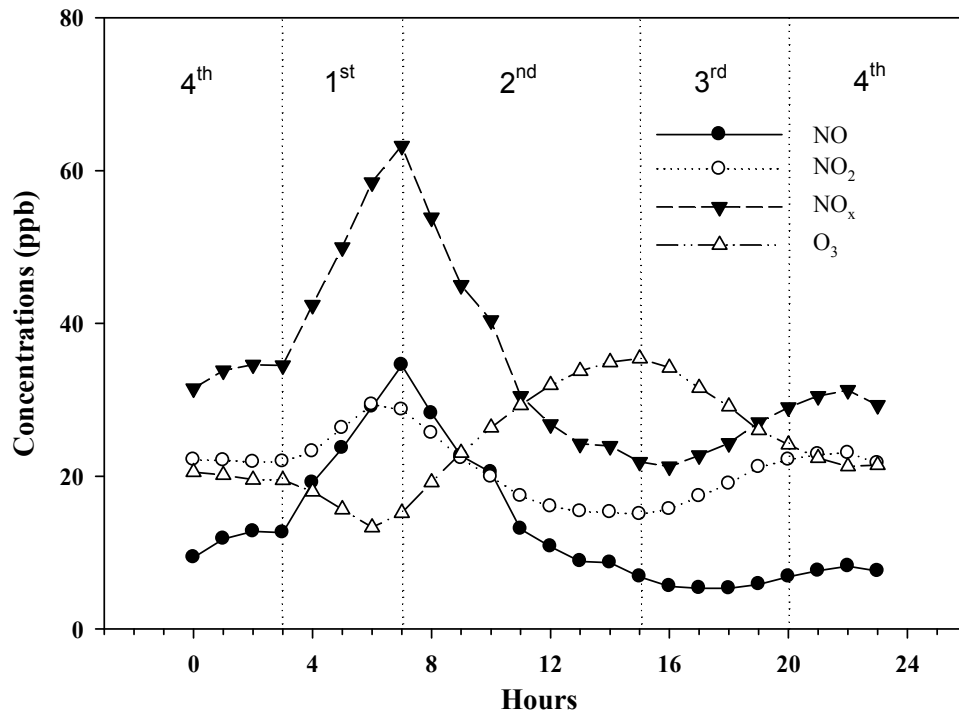


Figure 3. 4 The 24-h temporal variations of hourly averaged NO_x and O₃.

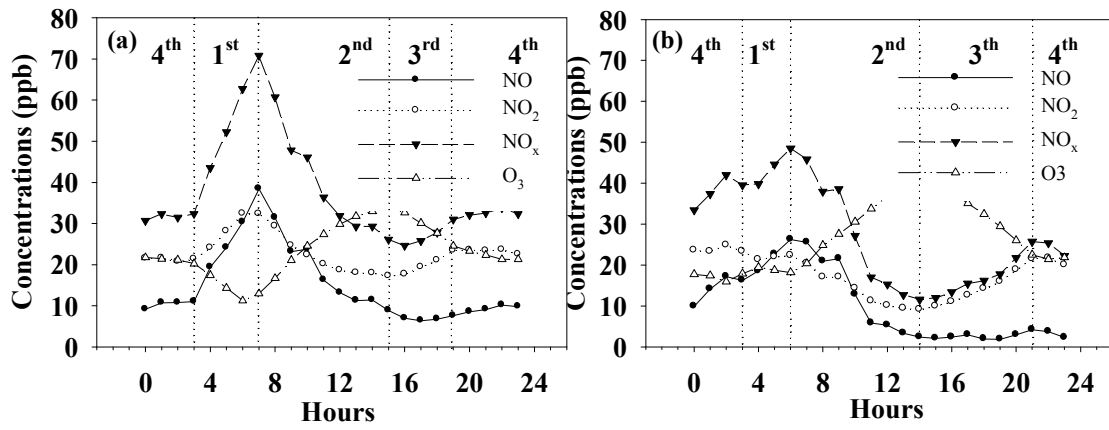


Figure 3. 5 The 24-h temporal variations of hourly averaged NO_x and O₃ concentrations in weekdays (a) and weekends (b).

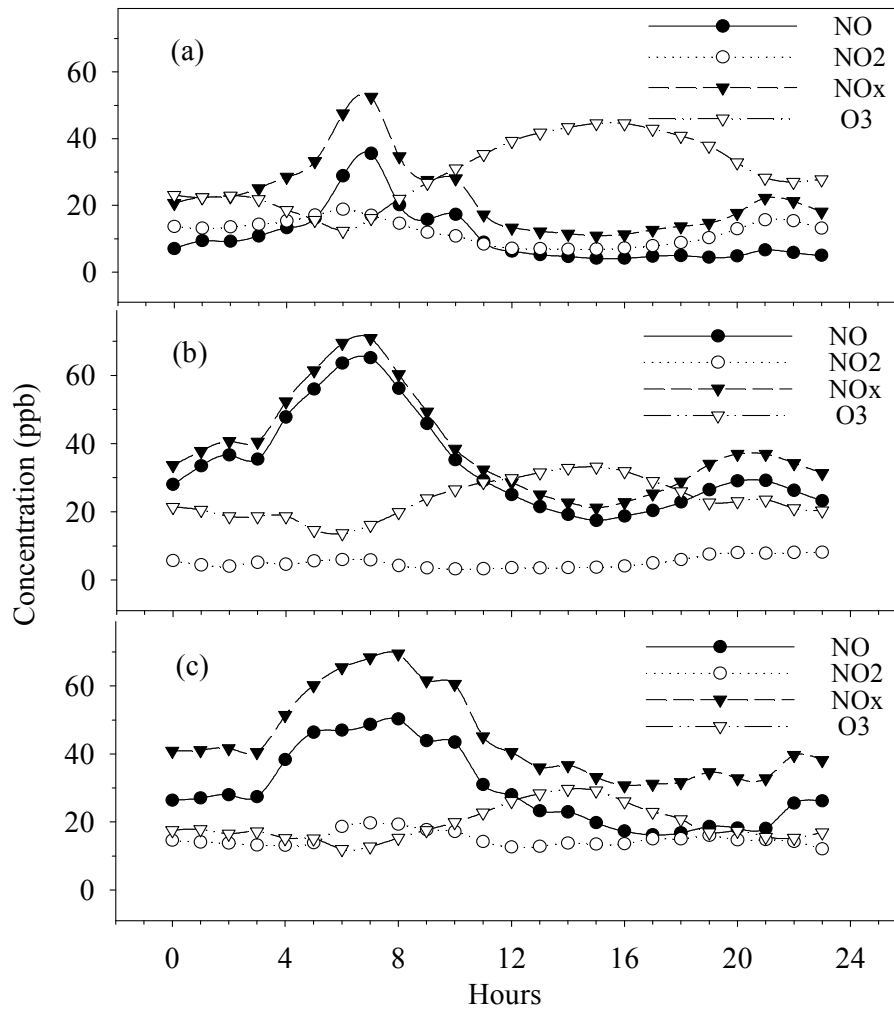


Figure 3. 6 The 24-h temporal variations of NO_x and O₃ in Clear days (a), Cloudy days (b) and Rainy days (c).

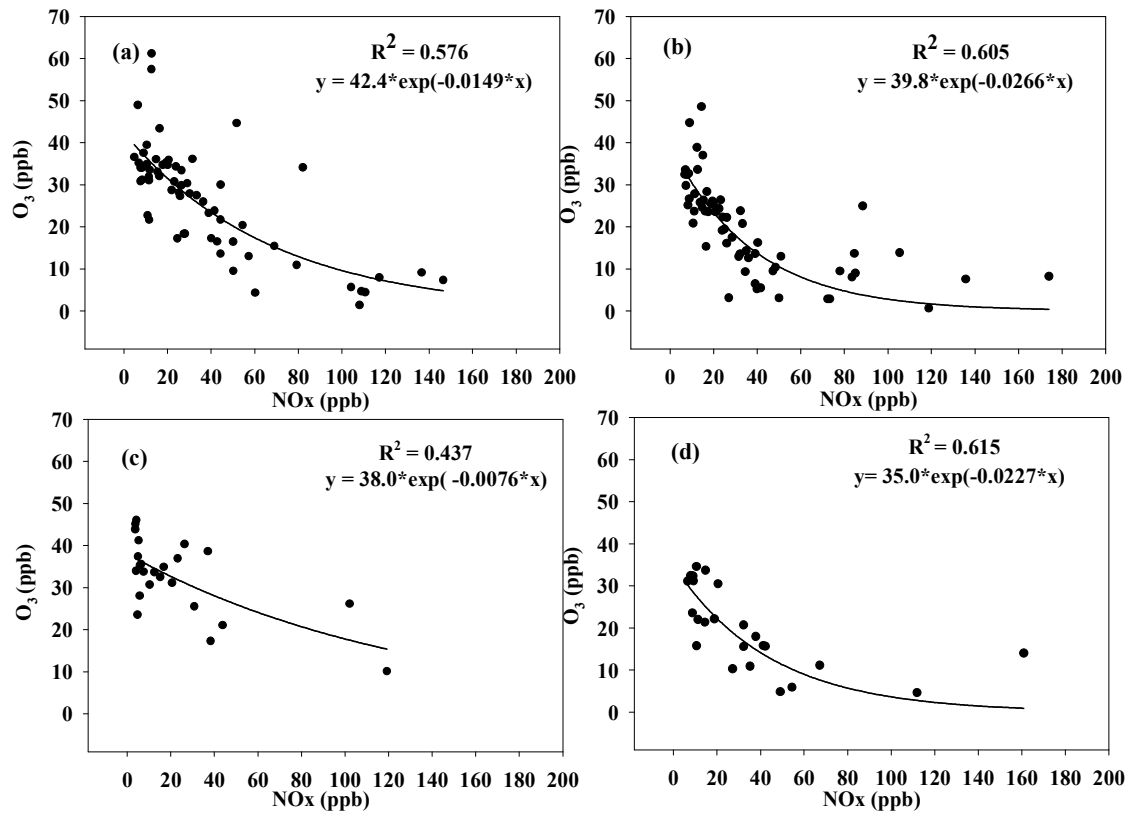


Figure 3. 7 Correlations between daytime averaged NO_x and O₃ in weekdays (a), weekends (c), and between nighttime averaged NO_x and O₃ in weekdays (b) and weekends (d).

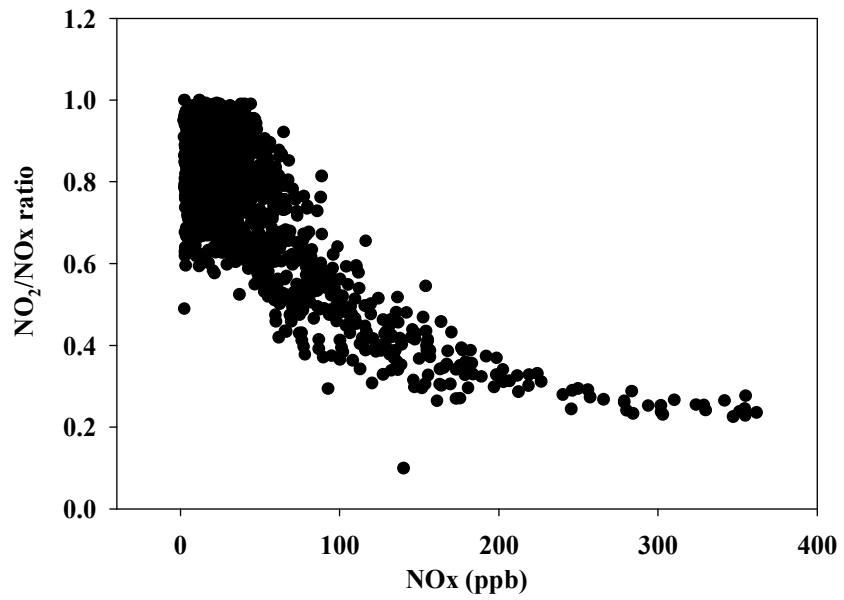


Figure 3. 8 Correlations between NO_x and NO₂/NO_x ratio.

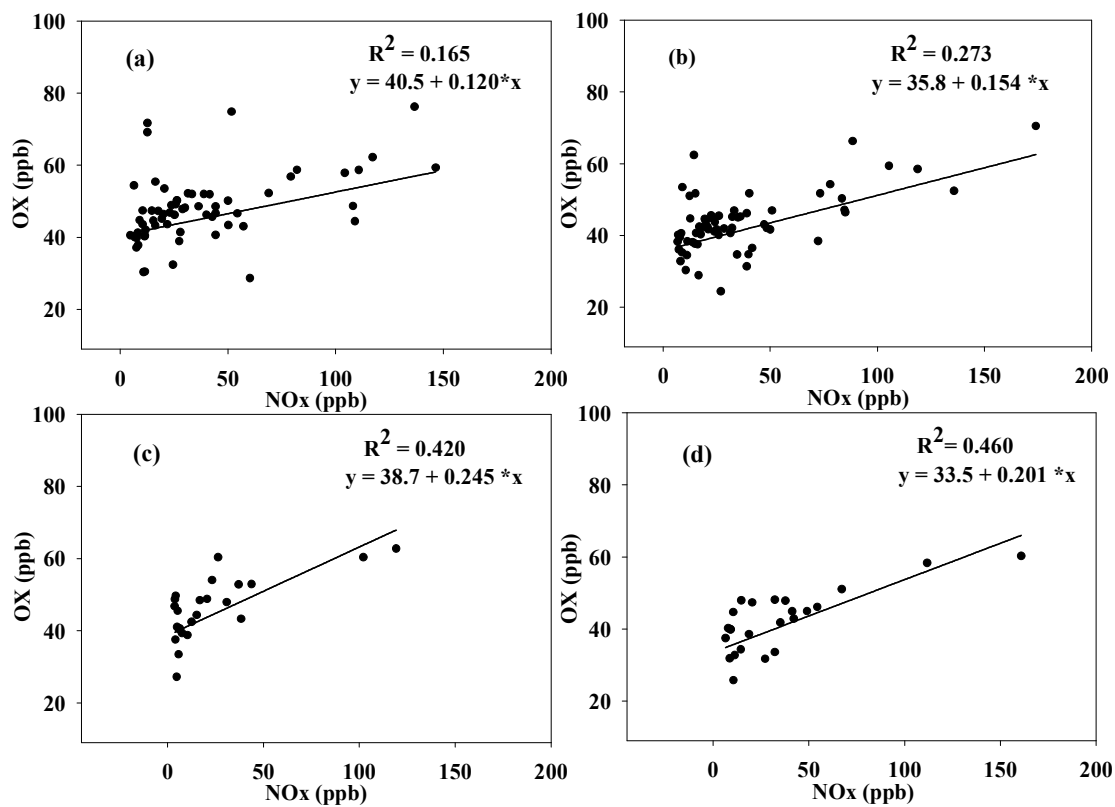


Figure 3. 9 Correlations between daytime averaged NO_x and OX in weekdays (a), weekends (c), and between nighttime averaged NO_x and O₃ in weekdays (b) and weekends (d).

Chapter 4 . Conclusions

4.1. Conclusions of the three studies

Based on three studies conducted during this dissertation research and discussed above, which covered the all three phases of air pollution, a primary air pollution characteristics with a typical urban area in the northeast US coastal region has been discovered. Main conclusions are listed below.

4.1.1. Pollution Sources

The precipitation characteristics in this region reflect significant influences from Marine, continental crust and anthropogenic sources. For each specific source, its influence varied with respect to different elements. For example, Na^+ , Cl^- , Mg^{2+} and K^+ are primarily of marine origin and Fe, Co and Al are mainly from crust sources, while Pb, V, Cr, Ni (moderately enriched) and Zn, Sb, Cu, Cd and F^- (highly enriched) are mainly of anthropogenic influences. Six major sources characterizing the precipitation chemistry were derived: (1) nitrogen-enriched soil, (2) secondary pollution processes, (3) marine sources, (4) incineration processes, (5) oil combustion and (6) malonate-vanadium-enriched sources.

The traffic related source, as one of the important anthropogenic sources, could be further divided to the following three types: (1) brake wear, fuel combustion and urban pollutions, (2) primary fuel combustion, and (3) tire abrasion and fuel combustion. They explained about 86.9% variations of trace metals' mass-size distributions in aerosols.

For the two major gaseous pollutants, NO_x and O_3 , besides the anthropogenic sources that affect their concentrations, certain meteorological conditions, such as local dispersion and regional transport, also play important roles. In addition, the vertical convections of the air showed influences, especially to the concentrations of O_3 .

4.1.2. Temporal Variation Patterns

Among the identified main sources for pollutions in precipitation, the nitrogen-enriched soil contributed much in spring. During summer, secondary pollution, incineration and oil combustion showed great influences, while marine sources influenced the precipitation composition significantly during autumn. In winter, however, no specific sources controlled the chemical characteristics of precipitation.

The pollution level of aerosols indicated by the enrichment factors showed different seasonal variations in different size ranges. Primarily, higher enrichment levels appeared in winter than in summer, especially for fine particles. In addition, the enrichment factor size distributions of crustal trace metals such as Cu, Fe, Sc, showed large seasonal variations, while no such obvious variations were found with anthropogenic trace metals including Cd, Cr, Ni, Pb, Sb, V, Zn and Co.

For the ground level O₃, its concentrations showed both weekday/weekend and diurnal variations, with higher concentrations being found on weekends possibly due to the increased VOC sensitivity and decreased NO_x emissions and in daytime due to the photochemical production of O₃ accompanied by lower O₃ consumption. In the time series, the O₃ concentrations generally increased from the beginning to the end of the spring time. Due to the variations of photochemical processes and emissions-diffusion balancing, the 24-h temporal variations patterns of NO_x and O₃ could be divided into four periods: (1) morning NO_x peak, (2) O₃ formation, (3) afternoon NO_x accumulation, and (4) night balancing.

4.1.3. Size Distribution Characteristics of Aerosol Mass and Associated Trace Metals

The size distributions of the total mass in both seasons showed typical bimodal

patterns, with peaks in the size ranges of 0.32-0.56 μm and 3.2-5.6 μm . The mass size distributions of the 13 trace metals were characterized into 2 groups: (1) coarse particle accumulation with crustal trace metals such as Al, Fe, Sc and Mn, showing bimodal pattern with primary peak at the size range of 3.2-5.6 μm , and secondary peak at 1.0-1.8 μm range; (2) fine particle accumulation for most of the typical anthropogenic trace metals such as Cd, Pb, Ni, V and Co, showing decreasing concentrations from small to large particles with major peaks at 0.18-0.32 μm range.

In addition, the size distribution patterns of trace metal accumulation factors could also be classified into 3 groups: (1) declined normal distribution with fine particles accumulations and peak in 1.0-1.8 μm for Cu (summer) and Fe (winter); (2) inclined normal distribution with coarse particles accumulations and peak in 1.0-1.8 μm for Fe (summer), Sc (winter) and Mn (summer); (3) monotonic decline patterns with overwhelming peak in 0.18-0.32 μm for rest of trace metals.

4.1.4. Others

Precipitation samples collected in this study area showed an obvious acidic nature, with volume weighted average pH around 4.6. SO_4^{2-} and NH_4^+ are the two most dominant components of major ions in mass, controlling the acidity of the precipitation. Besides, NO_3^- (22%), organic acids (14%), and Ca^{2+} and Mg^{2+} , are other major additional acidity and neutralization contributors, respectively.

Meteorological parameters were found of important influences on air pollution characteristics in this study. For aerosols, weather parameters, in particular temperature, wind speed and precipitation, were found to be influential on the concentrations and size distributions of trace elements observed at the study location. For the gaseous pollution,

certain meteorological parameters, in particular relative humidity and wind speed, played more important roles in the O_3 concentration variations and photochemical reactions of NO_x and O_3 . Different 24-h temporal variations of NO_x and O_3 were observed during different weather conditions. The daily maximum temperature showed positive correlation to the daily maximum O_3 level.

A potential VOC-sensitive characteristic of the study area was found, with the net negative effects of NO_x on O_3 concentrations, especially in nighttime and weekdays. The photochemical reactions of NO_x and O_3 led to a net O_3 consumption. Significant negative correlations between NO_3^- and O_3 were found, indicating either a high connection between NO_x and NO_3^- or an O_3 retarding characteristic for NO_3^- . However, HNO_3 was not found to be related to the NO_x - O_3 system, with no influence on the O_3 level.

4.2. Recommendation for future research

To further chemically characterize precipitation, more studied could be carried out in two aspects. Firstly, the study area and length could be extended to gain more information. On one hand, we could extend our monitoring sites to other locations nearby, which could represent typical environments such as rural, suburban besides urban areas, to study the potential differences, thus highlighting the influences of urban anthropogenic influences on precipitation chemistry. On the other hand, the measurement time could also be extended to a longer period to study the long-term patterns of the precipitation characteristics in one region. Secondly, instead of collecting the whole event based wet precipitation samples; sequential samples could be collected in a row during the whole precipitation event to study the precipitation dynamics, such as its flushing characteristics of the aerosol particulate pollutants.

For studying the size distributions of aerosol, the current sampling period covers about 3 to 4 days in order to get enough aerosols for chemical determinations. If technology allows, shorter period MOUDI sampling is definitely needed for much detailed information on the chemical processes of aerosol formation. Alternatively, discontinuous MOUDI sampling could be carried out, for example daytime and nighttime, to study the diurnal variations of the size distribution patterns. Similar sampling could be also carried out under different weather conditions.

While for the gaseous pollution study of NO_x and O_3 , apparently we could conduct more research in other seasons beside the spring to gain seasonal variations of these gas-phase pollutants. Also, certain photochemical laboratory experiments for the dynamics of the NO_x - O_3 regime may be conducted to better understand the potential mechanisms relating to NO_x and O_3 chemistry in the ambient air.

At last, the simultaneous sampling of all precipitation, aerosols and gaseous samples would be necessary to finally connect air pollutants in all three phases together. The results of such simultaneous research could shed lights on the potential physical and chemical inter-processes of air pollutants in different phases. Results from this PhD dissertation research serves as the first step for such integrated studies on urban air pollutions in this region.

Appendices

Appendix I. Precipitation sampling information and chemistry data.

I-1. Sampling information, precipitation amount and pH.

I- 2. Inorganic ions concentrations data (ppm).

I- 3. Organic acids concentrations data (ppm).

I- 4. Trace metals concentrations data (ppb).

I-1. Sampling information, precipitation amount and pH.

Samples #	Sampling Dates		Container #	Precipitatio n (cm)	pH
	Start	End			
1	9/24/2006	9/27/2006	1	0.03	4.2
2	9/28/2006	9/28/2006	2	0.79	4.6
3	10/4/2006	10/4/2006	3	2.36	4.4
4	10/11/2006	10/11/2006	4	4.09	4.7
5	10/17/2006	10/17/2006	5	2.77	4.8
6	10/17/2006	10/18/2006	6	2.77	4.7
7	10/20/2006	10/20/2006	7	1.04	4.2
8	10/27/2006	10/28/2006	8	5.61	4.8
9	11/1/2006	11/2/2006	9	0.84	4.4
10	11/7/2006	11/8/2006	10	11.07	4.9
11	11/8/2006	11/8/2006	11	11.07	5.0
12	11/12/2006	11/12/2006	12	0.33	4.3
13	11/16/2006	11/16/2006	13	1.24	4.8
14	11/23/2006	11/23/2006	14	3.20	5.0
15	12/31/2006	1/1/2007	15	3.53	4.7
16	1/7/2007	1/8/2007	17	3.84	4.9
17	1/10/2007	2/25/2007	18	0.53	4.2
18	2/25/2007	2/26/2007	19	0.97	5.0
19	3/1/2007	3/2/2007	20	5.08	4.6
20	3/7/2007	3/7/2007	21	0.25	5.9
21	3/15/2007	3/15/2007	22-snow	0.61	6.4
22	4/12/2007	4/12/2007	22	3.76	4.7
23	4/15/2007	4/16/2007	23	17.02	4.7
24	4/25/2007	4/25/2007	24	0.30	4.5
25	4/26/2007	4/27/2007	25	5.99	4.5
26	5/1/2007	5/1/2007	26-1	1.37	4.3
27	5/12/2007	5/12/2007	26-2	0.41	4.4
28	5/16/2007	5/16/2007	27-1	1.35	4.6
29	6/4/2007	6/4/2007	27-3	3.58	5.2
30	6/18/2007	6/18/2007	28	1.09	4.8
31	6/19/2007	6/20/2007	29	1.96	4.2
32	6/21/2007	6/21/2007	30	1.63	4.4
33	6/27/2007	6/27/2007	31	3.07	4.0
34	7/4/2007	7/6/2007	32	4.52	4.5
35	7/11/2007	7/11/2007	33	4.14	4.5
36	7/17/2007	7/18/2007	34	1.27	3.9
37	7/23/2007	7/23/2007	35	6.35	4.6
38	7/29/2007	7/30/2007	36	0.46	4.0
39	8/4/2007	8/5/2007	37	1.30	3.8
40	8/8/2007	8/8/2007	38	7.92	4.2

41	8/10/2007	8/10/2007	39	4.93	4.5
42	8/17/2007	8/20/2007	40	1.93	4.0
43	8/21/2007	8/22/2007	41	2.44	4.6
44	9/10/2007	9/11/2007	42	3.40	4.4
45	9/22/2007	9/22/2007	43	0.94	4.5
46	10/9/2007	10/10/2007	44	1.63	4.3

I-2. Inorganic ions concentrations data (ppm).

Sample #	Cl ⁻	F ⁻	NO ₃ ⁻	SO ₄ ²⁻	NH ₄ ⁺	Ca ²⁺	Mg ²⁺	K ⁺	Na ⁺
1	35.8	6.9	46.8	67.2	81.6	9.0	5.5	3.4	38.1
2	23.6	<0.01	26.8	29.2	57.1	9.3	4.2	4.6	22.4
3	1.9	<0.01	19.3	22.7	23.8	2.3	0.3	1.3	1.2
4	11.7	4.3	8.5	9.8	10.4	1.6	0.4	1.3	3.9
5	25.6	<0.01	5.3	8.3	12.8	1.8	2.1	1.3	17.6
6	36.4	<0.01	6.7	16.7	17.8	1.7	2.9	1.6	30.9
7	9.3	3.5	25.6	32.6	30.2	1.4	0.1	1.3	2.7
8	56.7	<0.01	6.1	12.1	10.1	2.5	6.4	1.5	47.2
9	2.3	<0.01	22.7	18.1	25.5	2.4	0.4	1.2	1.9
10	11.1	3.5	5.0	10.2	8.7	1.3	0.5	<0.01	5.5
11	7.3	3.6	8.3	6.6	5.2	0.5	0.0	<0.01	1.6
12	52.1	<0.01	27.2	30.5	37.6	2.7	5.4	2.1	47.5
13	94.6	<0.01	12.6	18.5	16.6	3.8	10.0	2.6	88.8
14	8.1	<0.01	6.9	7.4	10.3	1.8	0.4	<0.01	4.8
15	21.8	<0.01	7.8	12.8	9.8	1.5	2.0	1.4	18.6
16	9.1	<0.01	6.6	8.7	10.3	1.4	0.6	1.2	7.1
17	50.7	4.4	68.3	31.6	61.8	7.5	2.2	2.1	45.9
18	48.5	3.6	24.0	12.3	15.7	3.1	0.5	<0.01	48.9
19	21.7	<0.01	12.8	20.7	20.6	2.9	1.5	1.4	18.2
20	528.4	4.9	26.9	14.8	49.9	41.7	3.5	2.9	473.3
21	24.2	<0.01	5.9	3.9	1.2	7.1	3.9	2.0	27.8
22	7.2	<0.01	9.7	14.5	14.7	2.4	0.8	1.2	7.5
23	21.3	<0.01	8.2	13.7	12.6	1.4	1.8	1.4	20.7
24	12.2	3.9	53.6	35.9	70.0	15.1	3.8	2.2	8.4
25	11.0	3.7	17.1	18.3	39.3	3.9	1.1	1.4	10.4
26	5.6	3.3	36.2	37.5	56.3	7.4	1.3	1.9	2.5
27	10.9	4.1	25.5	29.5	61.8	5.3	1.6	2.1	8.7
28	4.2	3.4	19.2	23.0	41.1	9.0	1.7	1.4	3.4
29	6.8	3.0	5.1	6.8	6.9	1.9	0.7	1.5	7.4
30	11.0	3.6	15.8	18.5	27.3	4.7	1.7	2.3	9.5
31	8.1	<0.01	26.0	34.6	51.6	3.7	0.8	2.1	3.0
32	2.8	<0.01	22.0	33.9	53.9	7.6	1.7	1.9	1.7
33	7.4	<0.01	28.8	62.8	50.5	6.0	1.3	1.9	2.0
34	7.8	<0.01	11.3	24.1	30.7	1.3	0.9	1.5	5.5
35	4.0	<0.01	9.8	16.0	21.1	1.4	0.4	<0.01	1.9
36	11.3	<0.01	44.2	68.6	63.1	5.1	1.4	2.3	3.3
37	25.2	<0.01	17.0	20.7	26.8	4.1	2.8	1.6	21.5
38	11.8	<0.01	56.5	46.2	41.2	6.9	1.5	<0.01	4.9
39	8.2	<0.01	32.6	92.9	56.3	6.8	1.7	1.9	2.0
40	3.1	<0.01	15.8	37.1	36.4	3.0	0.3	<0.01	1.9

41	16.8	<0.01	11.2	14.8	19.1	1.9	1.8	1.4	13.8
42	12.3	<0.01	57.4	78.5	95.8	10.8	2.7	4.1	6.2
43	15.3	<0.01	9.3	16.8	21.2	3.7	0.9	1.4	4.7
44	11.5	<0.01	17.6	26.2	32.9	2.7	1.3	1.5	10.7
45	20.0	5.5	13.8	23.5	21.8	3.3	1.4	<0.01	18.6
46	77.9	4.6	45.1	51.1	62.6	12.1	11.5	3.2	68.0

I-3. Organic acids concentrations data (ppm).

Sample #	Acetate	Formate	Malonate	Oxalate
1	<0.01	<0.01	<0.01	1.44
2	7.98	6.50	<0.01	<0.01
3	1.96	4.37	<0.01	<0.01
4	2.06	<0.01	<0.01	<0.01
5	1.26	<0.01	0.59	<0.01
6	1.47	<0.01	0.43	<0.01
7	2.11	4.26	<0.01	<0.01
8	<0.01	<0.01	<0.01	<0.01
9	2.78	4.20	<0.01	<0.01
10	1.14	<0.01	0.20	<0.01
11	1.09	<0.01	2.64	<0.01
12	2.52	5.01	<0.01	<0.01
13	<0.01	<0.01	<0.01	<0.01
14	1.49	<0.01	<0.01	<0.01
15	2.47	<0.01	0.08	<0.01
16	2.66	<0.01	<0.01	<0.01
17	3.61	<0.01	1.28	<0.01
18	2.60	<0.01	<0.01	<0.01
19	1.82	<0.01	<0.01	<0.01
20	<0.01	<0.01	<0.01	<0.01
21	<0.01	<0.01	1.44	<0.01
22	<0.01	4.31	1.34	<0.01
23	<0.01	4.57	0.24	1.09
24	1.80	7.27	0.41	1.19
25	4.99	5.76	0.56	1.66
26	2.74	5.63	<0.01	1.24
27	4.50	10.12	1.11	1.37
28	4.93	9.10	<0.01	1.66
29	<0.01	<0.01	0.46	<0.01
30	0.11	<0.01	<0.01	<0.01
31	9.17	10.11	0.05	1.30
32	10.71	12.35	0.46	1.41
33	8.50	10.88	2.58	1.15
34	7.17	7.51	<0.01	1.15
35	7.66	6.46	0.68	1.08
36	19.17	18.13	4.14	1.46
37	1.20	4.46	0.19	<0.01
38	16.02	15.19	0.81	1.39
39	12.68	10.67	0.55	1.93
40	11.55	11.39	0.12	1.32

41	6.24	8.75	0.15	1.23
42	11.18	12.21	0.58	2.51
43	1.31	5.07	0.16	1.19
44	5.33	9.25	0.18	1.28
45	<0.01	<0.01	<0.01	<0.01
46	<0.01	<0.01	<0.01	<0.01

I-4. Trace metals concentrations data (ppb).

Sample #	Sb	Pb	Al	V	Cr	Fe	Co	Ni	Cu	Zn	Cd
1	0.57	0.75	30.66	0.69	0.07	13.66	0.07	0.99	1.71	10.06	0.03
2	0.34	0.37	9.98	0.35	0.05	4.85	0.04	1.08	2.40	9.16	0.09
3	0.27	0.16	3.99	0.09	0.01	4.17	<0.01	0.41	0.95	1.93	0.01
4	0.21	0.40	5.99	0.13	0.04	5.06	0.09	0.44	0.41	2.09	0.01
5	0.17	0.60	4.61	0.30	0.05	3.75	0.01	0.40	1.10	3.20	0.01
6	0.12	0.14	1.75	0.62	0.02	0.95	<0.01	0.65	1.23	3.34	0.03
7	0.15	0.17	3.96	0.42	0.03	4.19	<0.01	0.75	1.49	2.62	0.01
8	0.12	0.16	1.65	0.57	<0.01	1.03	<0.01	0.24	0.40	1.99	<0.01
9	0.21	0.23	5.98	0.11	0.05	4.97	<0.01	0.38	0.66	4.97	0.02
10	0.10	0.13	1.58	0.08	0.01	0.71	<0.01	0.06	0.30	1.83	<0.01
11	0.04	<0.01	0.54	<0.01	<0.01	<0.01	<0.01	0.20	0.04	0.61	<0.01
12	0.38	0.59	7.66	0.33	0.05	7.86	0.01	0.61	1.70	6.20	0.02
13	0.26	0.18	3.59	0.36	0.02	2.19	0.01	0.47	0.83	2.72	0.01
14	0.09	0.15	1.89	0.02	<0.01	0.37	<0.01	0.40	0.40	1.99	0.01
15	0.08	0.06	1.14	0.39	<0.01	<0.01	<0.01	0.46	0.05	1.68	<0.01
16	0.07	0.04	0.98	0.14	<0.01	<0.01	<0.01	0.49	0.14	3.99	<0.01
17	0.75	1.86	31.68	0.59	0.24	43.20	0.09	0.99	3.61	10.91	0.03
18	0.20	0.44	7.59	0.43	0.04	3.36	0.04	0.59	-	4.72	0.01
19	1.41	1.97	5.33	0.40	0.05	5.03	0.01	0.70	2.92	12.16	0.17
20	2.13	0.39	4.05	0.08	0.08	1.29	0.06	0.67	8.24	16.95	0.04
21	0.06	0.03	0.90	0.10	<0.01	<0.01	0.01	0.45	64.32	9.44	0.01
22	0.25	0.51	4.80	0.20	0.08	4.78	0.03	0.25	0.74	12.99	0.02
23	0.22	0.28	2.63	0.19	0.33	0.32	<0.01	0.07	0.26	1.61	0.02
24	0.68	1.38	30.04	0.31	0.15	34.32	0.11	0.44	3.32	13.51	0.04
25	0.33	0.33	7.53	0.29	0.02	2.51	<0.01	0.41	0.37	2.42	0.02
26	0.26	0.35	16.90	0.16	0.06	20.83	0.07	0.47	0.84	4.71	0.02
27	0.21	0.09	9.44	0.29	0.03	2.71	0.01	0.32	0.52	3.79	0.01
28	0.16	0.29	14.27	0.09	0.06	4.02	0.04	0.15	0.83	8.90	0.01
29	0.09	0.10	2.09	0.06	0.01	<0.01	<0.01	0.65	0.70	3.64	0.01
30	0.31	0.44	8.62	0.11	0.06	9.10	0.04	1.51	4.32	15.00	0.02
31	0.22	0.32	8.27	0.19	0.04	7.48	<0.01	0.84	0.76	3.91	0.03
32	0.32	0.27	9.18	0.05	0.04	8.53	0.01	0.19	0.50	5.08	0.02
33	0.25	1.28	25.73	0.19	0.07	17.44	0.03	1.02	0.75	7.42	0.01
34	0.35	0.19	3.74	0.07	0.02	0.44	<0.01	0.59	1.08	1.50	0.01
35	0.17	0.16	4.25	0.42	0.02	3.08	<0.01	0.52	0.61	2.69	<0.01
36	0.41	0.61	12.92	0.61	0.08	17.33	0.01	0.87	2.72	8.65	0.04
37	0.25	0.27	8.05	0.24	0.05	5.08	0.01	0.60	1.37	4.05	0.01
38	0.76	0.57	17.52	0.55	0.08	23.36	0.08	0.53	2.10	5.67	0.03
39	0.34	0.63	16.56	0.50	0.09	27.37	0.02	0.56	0.99	7.40	0.03

40	0.15	0.28	5.65	0.21	0.01	2.63	<0.01	0.55	0.34	11.86	0.02
41	0.21	0.32	3.72	0.35	0.03	2.72	<0.01	0.50	0.73	3.32	0.02
42	0.75	1.18	29.01	0.47	0.14	39.72	0.05	0.84	3.46	16.27	0.06
43	0.26	0.56	16.37	0.09	0.04	8.01	0.03	0.74	1.24	12.25	0.21
44	0.36	0.55	6.34	0.42	0.04	6.99	0.02	0.54	2.01	4.71	0.01
45	0.18	0.38	6.58	0.41	0.03	4.88	0.02	0.39	1.42	5.00	0.01
46	0.65	1.33	20.0	0.47	0.10	18.40	0.04	0.51	2.21	10.97	0.05

Appendix II: The size segregated air concentrations (ng m^{-3}) of trace metals during the winter and summer intensive sampling.

- II-1. Air concentrations (ng m^{-3}) of trace metals from the 1st set of winter intensive sampling (12/11/2007-12/14/2007).
- II-2. Air concentrations (ng m^{-3}) of trace metals from the 2nd set of winter intensive sampling (12/14/2007-12/18/2007).
- II-3. Air concentrations (ng m^{-3}) of trace metals from the 3rd set of winter intensive sampling (12/18/2007-12/21/2007).
- II-4. Air concentrations (ng m^{-3}) of trace metals from the 4th set of winter intensive sampling (1/29/2008-2/1/2008).
- II-5. Air concentrations (ng m^{-3}) of trace metals from the 5th set of winter intensive sampling (2/21/2008-2/14/2008).
- II-6. Air concentrations (ng m^{-3}) of trace metals from the 6th set of winter intensive sampling (2/24/2008-2/27/2008).
- II-7. Air concentrations (ng m^{-3}) of trace metals from the 1st set of summer intensive sampling (7/3/2008-7/7/2008).
- II-8. Air concentrations (ng m^{-3}) of trace metals from the 2nd set of summer intensive sampling (7/7/2008-7/11/2008).
- II-9. Air concentrations (ng m^{-3}) of trace metals from the 3rd set of summer intensive sampling (7/11/2008-7/15/2008).
- II-10. Air concentrations (ng m^{-3}) of trace metals from the 4th set of summer intensive sampling (7/15/2008-7/19/2008).
- II-11. Air concentrations (ng m^{-3}) of trace metals from the 5th set of summer intensive sampling (7/19/2008-7/23/2008).

II-1. Air concentrations (ng m^{-3}) of trace metals from the 1st set of winter intensive sampling (12/11/2007-12/14/2007).

Stage	1	2	3	4	5	6	7	8
Mid- Point (μm)	14	7.8	4.4	2.5	1.4	0.78	0.44	0.25
Al	13.7	37.2	14.2	9.22	7.75	1.8	2.62	- ^a
Cd	0.00267	0.008	0.0063	0.00893	0.0256	0.0234	0.0202	0.0198
Cr	0.281	0.275	0.292	0.144	0.262	0.18	0.126	0.204
Cu	0.619	5.1	3.11	1.63	1.82	0.584	0.487	0.629
Fe	35.3	67.1	65.4	40.8	42.7	12.7	7.71	6.40
Ni	0.273	0.329	0.372	0.368	0.485	0.562	0.744	1.62
Pb	0.145	0.366	0.539	0.271	0.801	0.875	1.08	1.05
Sc	0.0118	0.0119	0.00859	0.00625	0.00554	0.00318	0.0029	0.00265
V	0.0886	0.193	0.241	0.168	0.462	0.488	0.611	1.24
Zn	0.776	5.18	3.05	1.93	5.5	4.13	4.7	8.92

^a Air concentrations less than filter blank

II-2. Air concentrations (ng m^{-3}) of trace metals from the 2nd set of winter intensive sampling (12/14/2007-12/18/2007).

Stage	1	2	3	4	5	6	7	8
Mid- Point (μm)	14	7.8	4.4	2.5	1.4	0.78	0.44	0.25
Al	12.4	13.2	19.2	10.1	4.8	- ^a	-	-
Cd	0.00133	0.00469	0.00514	0.00249	0.00671	0.00756	0.0179	0.00997
Cr	0.0626	0.11	0.229	0.158	0.134	0.032	0.0868	0.143
Cu	0.373	0.808	2.77	3.05	5.34	0.911	0.859	0.427
Fe	21	26.3	59.9	41.2	34.1	5.68	5.07	3
Ni	0.481	0.221	0.236	0.209	0.185	0.13	0.308	0.594
Pb	0.0655	0.101	0.195	0.125	0.367	0.234	0.613	0.428
Sc	0.00322	0.0034	0.00621	0.00462	0.00274	0.00093	0.00116	0.000934
V	0.0411	0.0563	0.104	0.0661	0.0487	0.0319	0.109	0.127
Zn	1.3	1.51	2.43	1.17	1.86	1.05	3.54	4.08

^a Air concentrations less than filter blank

II-3. Air concentrations (ng m^{-3}) of trace metals from the 3rd set of winter intensive sampling (12/18/2007-12/21/2007).

Stage	1	2	3	4	5	6	7	8
Mid- Point								
(μm)	14	7.8	4.4	2.5	1.4	0.78	0.44	0.25
Al	49.6	51.4	13.3	15	15.7	4.94	0.158	- ^a
Cd	0.00538	0.00986	0.00349	0.00731	0.0284	0.0358	0.0291	0.0218
Cr	0.331	0.41	0.235	0.325	0.371	0.203	0.0984	0.105
Cu	1.81	3.4	3.6	6.75	8.89	3.29	1.6	1.60
Fe	75.2	115	60.8	102	90.3	20	6.89	4.97
Ni	0.331	0.298	0.247	0.319	0.388	0.636	0.547	1.22
Pb	0.286	0.38	0.202	0.369	1.27	1.32	1.12	1.24
Sc	0.00939	0.0111	0.00504	0.00444	0.00486	0.00165	0.00114	0.00141
V	0.211	0.289	0.205	0.252	0.279	0.331	0.693	1.79
Zn	2.63	3.08	1.54	3.14	7.49	6.16	4.64	7.67

^a Air concentrations less than filter blank

II-4. Air concentrations (ng m^{-3}) of trace metals from the 4th set of winter intensive sampling (1/29/2008-2/1/2008).

Stage	1	2	3	4	5	6	7	8
Mid- Point								
(μm)	14	7.8	4.4	2.5	1.4	0.78	0.44	0.25
Al	22.7	52.3	75.7	56.4	16.6	4.17	4.23	2.97
Cd	0.0025	0.00602	0.00957	0.00914	0.0217	0.0347	0.0475	0.0317
Cr	0.142	0.336	0.372	0.252	0.226	0.477	0.17	0.173
Cu	0.935	3.02	5.09	13.1	16.8	7.56	2.97	1.25
Fe	42.3	95.1	139	129	62.3	19.7	12.2	8.09
Ni	0.245	0.471	0.386	0.423	0.399	0.596	0.938	1.99
Pb	0.179	0.313	0.319	0.296	0.559	0.93	1.26	1.08
Sc	0.00553	0.0111	0.012	0.0076	0.00435	0.00234	0.00188	0.00221
V	0.134	0.264	0.339	0.246	0.198	0.316	0.776	1.54
Zn	0.92	2.42	2.44	2.93	4.08	4.41	5.95	7.03

II-5. Air concentrations (ng m^{-3}) of trace metals from the 5th set of winter intensive sampling (2/21/2008-2/14/2008).

Stage	1	2	3	4	5	6	7	8
Mid- Point								
(μm)	14	7.8	4.4	2.5	1.4	0.78	0.44	0.25
Al	9.32	23.7	13.3	5.36	5.23	2.76	1.27	- ^a
Cd	0.00277	0.0132	0.145	0.00242	0.00621	0.0101	0.0103	0.0113
Cr	0.126	0.136	0.185	0.0761	0.172	0.14	0.0905	0.134
Cu	0.828	2.13	3.73	3.13	6.04	4.28	1.57	0.904
Fe	20.2	27.7	37.2	21.5	22.5	8.81	4.14	4.32
Ni	0.0893	0.467	0.202	0.147	0.225	0.251	0.49	1.16
Pb	0.144	0.0933	0.102	0.0529	0.172	0.31	0.547	0.517
Sc	0.00295	0.00282	0.00441	0.00283	0.00351	0.00124	0.00108	0.00149
V	0.0384	0.0594	0.129	0.0752	0.0813	0.105	0.264	0.515
Zn	0.878	3.22	6.83	0.539	1.46	2.5	2.59	4.76

^a Air concentrations less than filter blank

II-6. Air concentrations (ng m^{-3}) of trace metals from the 6th set of winter intensive sampling (2/24/2008-2/27/2008).

Stage	1	2	3	4	5	6	7	8
Mid- Point								
(μm)	14	7.8	4.4	2.5	1.4	0.78	0.44	0.25
Al	22.1	40.9	70.3	26.3	15	1.83	2.12	- ^a
Cd	0.0112	0.00636	0.0192	0.0145	0.0544	0.233	0.0782	0.0526
Cr	0.119	0.23	0.626	0.458	0.491	0.145	0.224	0.089
Cu	0.635	1.91	7.4	4	3.62	1.3	4.26	1.93
Fe	30.4	77.2	201	118	90.1	20.5	9.77	3.72
Ni	0.252	0.278	0.484	0.3	0.443	0.425	0.589	0.851
Pb	0.133	0.379	0.654	0.493	2.87	1.53	1.81	0.952
Sc	0.00997	0.0124	0.0163	0.00773	0.00579	0.00268	0.0028	0.00205
V	0.096	0.203	0.523	0.231	0.308	0.393	0.788	1.32
Zn	1.38	2.72	5.71	3.28	7.32	11	7.4	3.72

^a Air concentrations less than filter blank

II-7. Air concentrations (ng m^{-3}) of trace metals from the 1st set of summer intensive sampling (7/3/2008-7/7/2008).

Stage	1	2	3	4	5	6	7	8
Mid- Point								
(μm)	14	7.8	4.4	2.5	1.4	0.78	0.44	0.25
Al	18.6	29.6	47.3	17.3	28.4	35	12.7	15.6
Cd	0.00549	0.00709	0.00877	0.00507	0.0129	0.0143	0.0119	0.0121
Cr	0.195	0.285	0.485	0.151	0.216	0.257	0.0581	0.0873
Cu	1.24	4.67	8.29	7.41	14.4	9.63	3.07	1.34
Fe	26.4	50.4	79.1	32.2	34	19.6	2.64	2.8
Ni	0.126	0.211	0.305	0.0976	0.146	0.328	0.318	1.05
Pb	0.104	0.2	0.211	0.149	0.766	0.681	0.348	0.438
Sc	0.00377	0.00715	0.0106	0.00232	0.00542	0.00409	0.000708	0.000804
V	0.0796	0.154	0.239	0.12	0.259	0.67	0.797	1.86
Zn	0.848	1.93	1.32	0.861	1.25	2.53	1.4	3.17

II-8. Air concentrations (ng m^{-3}) of trace metals from the 2nd set of summer intensive sampling (7/7/2008-7/11/2008).

Stage	1	2	3	4	5	6	7	8
Mid- Point								
(μm)	14	7.8	4.4	2.5	1.4	0.78	0.44	0.25
Al	20	46.6	83.1	37.4	17	18.8	11	8.46
Cd	0.00413	0.00675	0.0141	0.00422	0.0127	0.00922	0.0146	0.0156
Cr	0.0933	0.172	0.37	0.152	0.15	0.049	0.045	0.113
Cu	0.606	1.09	3.43	1.42	1.47	0.504	0.329	0.51
Fe	41.4	67.9	116	59.1	48.7	9.37	5.12	4.96
Ni	0.134	0.148	0.496	0.0771	0.211	0.166	0.28	0.73
Pb	0.234	0.309	0.515	0.144	0.328	0.347	0.383	0.426
Sc	0.00259	0.0108	0.0162	0.00809	0.00263	0.000865	0.000581	0.00068
V	0.0939	0.194	0.376	0.166	0.243	0.235	0.708	1.64
Zn	1.57	1.8	3.1	0.79	3.22	2.05	1.65	1.84

II-9. Air concentrations (ng m^{-3}) of trace metals from the 3rd set of summer intensive sampling (7/11/2008-7/15/2008).

Stage	1	2	3	4	5	6	7	8
Mid- Point								
(μm)	14	7.8	4.4	2.5	1.4	0.78	0.44	0.25
Al	24.1	32.7	24.3	14	5.68	3.28	12.3	3.38
Cd	0.00417	0.00432	0.00327	0.00112	0.00649	0.00686	0.018	0.02
Cr	0.189	0.14	0.0742	0.0409	0.052	0.0324	0.0458	0.0413
Cu	0.909	1.58	1.35	1.05	3.48	2.64	1.41	0.47
Fe	41	45.2	31.4	14.4	22.8	10.2	4.68	2.86
Ni	0.0937	0.117	0.0516	0.0669	0.13	0.139	0.35	0.774
Pb	0.259	0.259	0.122	0.0771	0.139	0.255	0.419	0.397
Sc	0.00378	0.00447	0.0032	0.00101	0.000911	0.000745	0.000656	0.000816
V	0.11	0.171	0.112	0.059	0.169	0.277	1.01	2.32
Zn	1.21	1.34	0.648	0.611	1.25	1.43	1.6	1.32

II-10. Air concentrations (ng m^{-3}) of trace metals from the 4th set of summer intensive sampling (7/15/2008-7/19/2008).

Stage	1	2	3	4	5	6	7	8
Mid- Point								
(μm)	14	7.8	4.4	2.5	1.4	0.78	0.44	0.25
Al	47.1	89	67.5	16.3	11.5	8.14	6.3	10.4
Cd	0.00261	0.00675	0.00938	0.00433	0.0104	0.0188	0.0315	0.0245
Cr	0.185	0.414	0.4	0.124	0.126	0.0709	0.0484	0.102
Cu	0.938	2.69	4.69	4.29	5.91	4.59	2.04	1.23
Fe	52.3	107	97.7	50.7	39.2	17.6	7.75	4.7
Ni	0.107	0.21	0.169	0.122	0.0936	0.103	0.324	0.742
Pb	0.348	0.599	0.458	0.238	0.288	0.476	0.7	0.606
Sc	0.00989	0.0208	0.0131	0.00234	0.00145	0.000636	0.000561	0.000859
V	0.125	0.254	0.231	0.119	0.124	0.197	0.724	1.54
Zn	1.49	2.72	2	1.19	1.89	1.97	2.12	2.14

II-11. Air concentrations (ng m^{-3}) of trace metals from the 5th set of summer intensive sampling (7/19/2008-7/23/2008).

Stage	1	2	3	4	5	6	7	8
Mid- Point (μm)	14	7.8	4.4	2.5	1.4	0.78	0.44	0.25
Al	12.9	62.8	67.7	58.8	18.4	6.72	2.52	0.908
Cd	0.000848	0.00582	0.0202	0.00971	0.00552	0.00775	0.0149	0.00729
Cr	0.0744	0.181	0.28	0.177	0.0901	0.0271	0.0198	0.0323
Cu	0.321	1.22	1.83	1.95	1.97	0.879	0.507	0.252
Fe	21.2	66.1	69.4	61.6	35.8	9.19	3.88	2.12
Ni	0.0643	0.17	0.445	0.156	0.185	0.0916	0.207	0.472
Pb	0.122	0.347	0.357	0.221	0.245	0.301	0.347	0.218
Sc	0.00273	0.0136	0.0197	0.0113	0.00301	0.00104	0.000734	0.000914
V	0.0637	0.169	0.175	0.155	0.127	0.122	0.332	0.461
Zn	0.296	1.54	1.72	1.44	1.64	2.15	1.36	1.2

Appendix III. NO_x-O₃ study information and concentration data.

III-1. NO_x-O₃ sampling weather data.

III-2. Ground level NO_x-O₃ concentration data (ppm).

III-1. NO_x-O₃ sampling weather data.

Day	Date	T (F)	RH (%)	Precip. (cm)	SR (w/m²)	WS (mph)
Thursday	2/22/2007	35.7	76.0	0.005	56.8	5.1
Friday	2/23/2007	31.0	46.8	*	140.5	16.7
Saturday	2/24/2007	30.0	45.4	-	168.4	11.6
Sunday	2/25/2007	29.3	59.4	-	83.2	5.2
Monday	2/26/2007	31.5	93.8	0.003	35.3	4.8
Tuesday	2/27/2007	37.6	79.8	0.006	72.6	1.7
Wednesday	2/28/2007	38.9	51.9	-	169.7	6.0
Thursday	3/1/2007	35.7	60.0	0.003	127.9	5.1
Friday	3/2/2007	47.4	70.9	0.054	71.4	10.8
Saturday	3/3/2007	42.9	54.3	-	156.1	6.4
Sunday	3/4/2007	35.6	50.3	-	100.4	12.3
Monday	3/5/2007	32.0	47.4	-	106.0	15.8
Tuesday	3/6/2007	15.7	31.9	-	206.8	16.6
Wednesday	3/7/2007	17.2	63.8	0.001	90.9	4.7
Thursday	3/8/2007	24.0	43.6	-	195.4	11.2
Friday	3/9/2007	23.3	47.4	-	187.5	6.8
Saturday	3/10/2007	39.3	75.6	0.002	109.1	3.2
Monday	3/12/2007	43.3	53.1	-	170.9	5.2
Tuesday	3/13/2007	46.8	63.5	-	115.5	5.8
Wednesday	3/14/2007	55.9	68.1	-	147.3	4.8
Thursday	3/15/2007	49.6	76.5	0.007	44.6	8.9
Friday	3/16/2007	28.6	90.9	0.113	23.0	13.5
Sunday	3/18/2007	32.7	45.4	-	196.2	12.0
Monday	3/19/2007	36.2	52.9	-	148.2	8.7
Tuesday	3/20/2007	41.9	46.5	-	213.2	10.4
Wednesday	3/21/2007	33.2	51.6	-	217.8	9.0
Thursday	3/22/2007	51.0	74.3	0.000	139.5	11.4
Friday	3/23/2007	53.9	73.8	0.002	45.9	4.4
Saturday	3/24/2007	46.7	59.2	0.000	170.4	6.3
Sunday	3/25/2007	43.5	74.2	-	185.4	7.7
Monday	3/26/2007	45.2	77.3	-	128.7	8.6
Tuesday	3/27/2007	62.0	62.4	-	193.0	7.6
Wednesday	3/28/2007	55.0	47.4	-	211.1	7.7
Thursday	3/29/2007	46.5	20.8	-	246.6	11.9

Friday	3/30/2007	52.1	24.2	-	227.6	6.2
Saturday	3/31/2007	45.5	47.0	-	190.8	6.2
Sunday	4/1/2007	45.0	67.5	0.002	44.7	5.8
Monday	4/2/2007	41.8	92.3	0.012	1.4	5.4
Thursday	4/5/2007	38.4	51.4	-	233.3	15.1
Friday	4/6/2007	36.0	47.9	-	120.5	9.1
Saturday	4/7/2007	35.0	44.9	-	168.6	8.7
Sunday	4/8/2007	35.6	50.7	-	159.7	13.1
Monday	4/9/2007	38.6	46.4	-	236.7	8.5
Tuesday	4/10/2007	40.9	43.2	-	261.6	7.9
Wednesday	4/11/2007	41.5	53.7	-	215.8	7.2
Thursday	4/12/2007	41.7	75.1	0.032	33.4	10.4
Friday	4/13/2007	45.7	52.9	-	124.4	15.4
Saturday	4/14/2007	47.3	45.5	-	245.3	8.3
Sunday	4/15/2007	44.4	85.9	0.131	6.0	9.7
Monday	4/16/2007	42.1	86.4	0.152	19.7	20.3
Monday	4/23/2007	76.7	30.2	-	265.4	16.8
Tuesday	4/24/2007	69.0	40.5	-	256.3	11.0
Wednesday	4/25/2007	55.1	52.3	0.003	177.4	7.2
Thursday	4/26/2007	50.5	72.1	-	211.9	8.5
Friday	4/27/2007	52.1	88.8	0.056	39.8	4.1
Saturday	4/28/2007	61.8	64.7	-	189.8	7.9
Sunday	4/29/2007	59.3	60.0	-	137.0	8.2
Monday	4/30/2007	63.6	45.7	-	255.4	12.8
Tuesday	5/1/2007	59.4	41.8	0.006	216.8	5.9
Wednesday	5/2/2007	57.9	62.8	0.004	185.5	7.5
Thursday	5/3/2007	59.6	34.1	-	301.0	5.0
Friday	5/4/2007	59.8	33.0	-	279.5	5.8
Saturday	5/5/2007	60.0	37.6	-	287.8	5.6
Sunday	5/6/2007	52.4	45.4	-	243.6	12.6
Monday	5/7/2007	52.4	54.7	-	289.0	5.6
Tuesday	5/8/2007	57.0	56.6	-	300.0	6.9
Wednesday	5/9/2007	66.8	73.0	-	270.0	7.9
Thursday	5/10/2007	68.2	80.6	-	169.5	6.9
Friday	5/11/2007	67.1	80.9	0.006	165.6	5.3
Saturday	5/12/2007	63.8	68.1	0.003	256.8	7.9
Sunday	5/13/2007	59.7	40.3	0.106	318.7	9.7

Monday	5/14/2007	61.3	37.0	-	410.7	8.8
Tuesday	5/15/2007	69.3	50.4	-	279.7	13.8
Wednesday	5/16/2007	70.4	16.7	0.021	0.0	21.1
Thursday	5/17/2007	61.1	64.2	-	347.8	7.1
Friday	5/18/2007	52.4	67.9	-	194.4	10.4
Saturday	5/19/2007	53.5	68.0	0.003	171.2	8.1
Sunday	5/20/2007	63.9	57.4	0.001	308.7	9.0
Monday	5/21/2007	62.5	43.8	-	493.7	8.2

* No precipitation observed.

III-2. Ground level NO_x-O₃ concentration data (ppm).

Date	NO	NO₂	NO_x	O₃
2/22/2007	92.73	48.41	141.14	7.42
2/23/2007	2.14	7.43	9.57	31.63
2/24/2007	1.42	6.27	7.69	33.94
2/25/2007	13.64	26.60	40.23	16.45
2/26/2007	13.91	36.20	50.11	6.74
2/27/2007	53.03	37.65	90.68	3.92
2/28/2007	2.68	17.68	20.36	26.04
3/1/2007	28.91	47.36	76.27	6.88
3/2/2007	21.07	34.60	55.68	18.46
3/3/2007	91.32	40.20	131.52	20.05
3/4/2007	0.45	6.47	6.91	33.81
3/5/2007	1.10	7.66	8.76	34.20
3/6/2007	1.46	5.79	7.25	33.20
3/7/2007	8.24	25.65	33.89	17.96
3/8/2007	3.98	17.00	20.98	28.47
3/9/2007	19.34	34.69	54.03	14.48
3/10/2007	62.39	53.14	115.53	7.36
3/12/2007	52.12	48.24	100.36	7.97
3/13/2007	56.50	55.00	111.50	3.13
3/14/2007	90.65	64.66	155.31	8.65
3/15/2007	39.64	35.23	74.87	17.93
3/16/2007	4.61	17.19	21.80	20.99
3/18/2007	0.74	7.16	7.91	37.89
3/19/2007	7.46	32.11	39.57	19.73
3/20/2007	7.68	18.98	26.66	27.68
3/21/2007	7.62	20.51	28.13	25.73
3/22/2007	13.54	30.82	44.36	17.05
3/23/2007	4.36	25.37	29.73	15.63
3/24/2007	8.70	31.24	39.94	15.16
3/25/2007	3.83	21.36	25.19	21.69
3/26/2007	14.00	31.46	45.46	15.30
3/27/2007	54.37	29.01	83.38	23.86
3/28/2007	4.95	15.06	20.00	29.55
3/29/2007	2.04	9.52	11.57	36.51

3/30/2007	7.23	17.59	24.82	29.87
3/31/2007	4.06	20.45	24.50	27.80
4/1/2007	9.95	30.86	40.80	19.48
4/2/2007	30.13	41.35	71.48	8.98
4/3/2007	9.91	33.17	43.08	14.48
4/4/2007	5.59	26.91	32.49	18.57
4/5/2007	2.20	8.53	10.73	21.77
4/6/2007	1.64	9.45	11.09	28.47
4/7/2007	2.15	11.00	13.15	27.93
4/8/2007	0.78	5.94	6.72	23.54
4/9/2007	1.82	8.97	10.79	29.85
4/10/2007	13.55	14.61	28.16	26.02
4/11/2007	1.52	15.99	17.52	36.50
4/12/2007	2.61	21.53	24.13	25.78
4/13/2007	0.78	7.43	8.21	28.71
4/14/2007	2.10	10.24	12.34	38.24
4/15/2007	1.75	15.91	17.67	32.42
4/16/2007	0.73	7.64	8.36	33.29
4/17/2007	1.30	7.16	8.46	34.93
4/18/2007	1.97	9.39	11.35	29.87
4/19/2007	3.53	16.57	20.10	25.58
4/20/2007	9.83	23.38	33.21	25.20
4/21/2007	18.55	27.20	45.75	22.23
4/22/2007	16.81	29.96	46.77	25.70
4/23/2007	34.37	35.74	70.11	34.78
4/24/2007	0.63	7.06	7.68	46.81
4/25/2007	3.55	17.30	20.85	28.06
4/26/2007	5.37	18.50	23.87	25.72
4/27/2007	54.24	42.36	96.60	5.17
4/28/2007	8.97	13.39	22.36	25.40
4/29/2007	0.52	7.14	7.66	27.96
4/30/2007	7.69	16.69	24.38	34.46
5/1/2007	3.34	17.39	20.74	27.63
5/2/2007	3.99	16.69	20.68	27.38
5/3/2007	6.70	19.49	26.18	25.89
5/4/2007	13.14	20.75	33.89	22.82
5/5/2007	9.18	23.07	32.26	26.36

5/6/2007	0.94	6.14	7.08	34.27
5/7/2007	8.31	22.03	30.34	17.86
5/8/2007	19.40	28.61	48.02	12.90
5/9/2007	16.88	26.87	43.75	6.14
5/10/2007	8.00	17.37	25.37	12.16
5/11/2007	18.81	29.76	48.57	9.08
5/12/2007	4.05	14.73	18.77	20.49
5/13/2007	1.15	7.93	9.08	32.59
5/14/2007	7.21	17.83	25.04	26.91
5/15/2007	1.57	12.00	13.57	54.84
5/16/2007	0.72	11.78	12.50	48.15
5/17/2007	1.20	10.10	11.30	27.34
5/18/2007	2.81	11.24	14.05	18.44
5/19/2007	0.50	7.68	8.18	21.89
5/20/2007	0.21	4.94	5.15	38.11
5/21/2007	0.64	5.82	6.47	30.82

Curriculum Vitae

Fei Song

Department of Earth & Environmental Sciences, Rutgers Newark
101 Warren Street, Smith Hall, Newark, NJ 07102

Education

- *Ph.D* Atmospheric Environment, Rutgers-Newark, Expected May 2011.
- *M.S.* Applied Mathematics, Rutgers- New Brunswick, May 2010
- *M.S.* Environmental Science, Chinese Academy of Science, China, 2006.
- *B.S.* Chemistry, Ocean University of China, China, 2003.

Experience

Quantitative Analyst, BGC (Cantor Fitzgerald), NYC, New York Nov. 2009 – Present

- Fix income derivative pricing modeling and interest rate models research
- GUI (C#) and Spreadsheets (VBA) applications development, numerical library maintenance and upgrading.

Quantitative Analyst, Frontier, NYC, New York Aug. 2009 –Nov. 2009

- Quantitative analysis of equity trading strategies, trading technical support.
- Built several applications/platforms including GIPS reporting system, portfolio management system in VBA.

Data Engineer and Modeler, DRBC Ewing, New Jersey May 2009-Aug. 2009

- Data mining and Statistical analysis of big volume pre-modeling data in SAS, VBA and MatLab
- Model calibration and conditional factors optimization, input files generation application.
- Relative environmental research, reporting and presentations.

Teaching/Research Assistant, Rutgers University, Newark, NJ. Sep. 2006- May, 2009.

- Taught undergraduate students each semester in environmental geology
- Urban air pollution research.

Project Manager, Chinese Academy of Science, Qingdao, China. 2005-2006

- Planed and leaded the 1st and 2nd “source-to-sink” nitrogen pollution investigation on Yangtze River independently.

Honors and Awards

- Graduate Assistantship, Rutgers University, 2006-2009.
- Graduate School Scholarship, Chinese Academy of Sciences, 2003-2006.
- Undergraduate Scholarships. Ocean University of China, 1999-2003.
- Member of the "National Class" for Excellent Students. Ocean University of China, 1999– 2003.

Publications

Journals

- **Song, F.**, and Y. Gao, Size Distributions of Trace Elements Associated with Ambient Particulate Matter in the Affinity of Highways in the New Jersey-New York Metropolitan Area on the US East Coast, in review.
- **Song, F.**, J. Shin, Y. Gao, Relationships among the Springtime Ground-level NO_x, O₃ and NO₃ in the Vicinity of Highways in the US East Coast, Atmospheric Pollution Research, accepted (scheduled to be published in the third issue of 2011).
- **Song, F.**, and Y. Gao, Chemical characteristics of precipitation at metropolitan Newark in the US East Coast, Atmospheric Environment, 43, 4903-4913, 2009.
- **Song, F.**, Song, X., Yu, Z., 2007. The distribution of $\delta^{15}\text{N}$ in particulate organic matter in surface water of the Changjiang river estuary. Oceanologia et Limnologia Sinica 38, 521-528.
- Zhang, S., Yu, Z., Song, X., **Song, F.**, Wang Y., 2005. Competition about nutrients between *Gracilaria lemaneiformis* and *Prorocentrum donghaiense*. Acta Ecologica Sinica 25, 2676-2680.

Conferences

- **Song, F.**, Xia, L., Jusino-Atresino, R., Thuman, C., Gao, Y., 2008. Particle-size distributions and elemental composition of particulate matter observed in the vicinity of highways in the US East Coast. AGU Fall meeting (A27).
- Gao, Y., Shin, J. Y., **Song, F.**, Artigas, F., 2007. Springtime Atmospheric Nitrogen Over The Meadowlands. Meadowlands Symposium II: Featuring Sessions on Renewable Energy and Urban Wetlands.
- Jusino-Atresino, R., **Song, F.**, Xia, L., Gao, Y., 2008. Aerosol Chemical and Physical Properties Observed over Puerto Rico in the Tropical North Atlantic Ocean. AGU Fall meeting (OS05).
- Xia, L., **Song, F.**, Jusino-Atresino, R., Thuman, C., Gao, Y., 2008. Quantifying the Input of Aeolian Soluble Iron to the Ocean Using Integrated Approaches of In-situ Observations, Laboratory Experiments and Modeling, NASA carbon cycle and ecosystems joint science workshop (Adelphi, MD)
- Xia, L., **Song, F.**, Jusino-Atresino, R., Thuman, C., Gao, Y., 2008. Chemical Compositions and Size Distributions of Coastal Aerosols Observed in Southern New Jersey in the U.S. East Coast. AGU Fall Meeting (OS05).